

HENRI RUOTSALAINEN

Interactive Multiobjective Optimization in Model-based Decision Making with Applications

Doctoral dissertation

To be presented by permission of the Faculty of Natural and Environmental Sciences
of the University of Kuopio for public examination in Auditorium L21, Snellmania building,
University of Kuopio, on Saturday 16th January 2010, at 12 noon

Department of Physics
University of Kuopio



KUOPION YLIOPISTO

KUOPIO 2009

Distributor: Kuopio University Library
P.O. Box 1627
FI-70211 KUOPIO
FINLAND
Tel. +358 40 355 3430
Fax +358 17 163 410
<http://www.uku.fi/kirjasto/julkaisutoiminta/julkmyyn.shtml>

Series Editor: Professor Pertti Pasanen, Ph.D.
Department of Environmental Science

Author's address: Department of Physics, University of Kuopio
P.O. Box 1627
FI-70211 KUOPIO, FINLAND
Tel. +358 40 757 8538
Email: Henri.Ruotsalainen@uku.fi

Supervisors: Professor Jari Hämäläinen, Ph.D.
Department of Physics, University of Kuopio

Professor Kaisa Miettinen, Ph.D.
Department of Mathematical Information Technology,
University of Jyväskylä

Doctor Elina Madetoja, Ph.D.
Department of Physics, University of Kuopio

Reviewers: Associate Professor Francisco Ruiz, Ph.D.
Department of Applied Economics (Mathematics),
University of Málaga

Associate Professor Eva K. Lee, Ph.D.
Center for Operations Research in Medicine and HealthCare,
School of Industrial and Systems Engineering,
Georgia Institute of Technology

Opponent: Associate Professor Matthias Ehr Gott, Ph.D., Dr. habil.
Department of Engineering Science
University of Auckland

ISBN 978-951-27-1407-0
ISBN 978-951-27-1462-9 (PDF)
ISSN 1235-0486

Kopijyvä
Kuopio 2009
Finland

Ruotsalainen, Henri. Interactive Multiobjective Optimization in Model-based Decision Making with Applications. Kuopio University Publications C. Natural and Environmental Sciences 269. 2009. 127 p.

ISBN 978-951-27-1407-0

ISBN 978-951-27-1462-9 (PDF)

ISSN 1235-0486

ABSTRACT

In this thesis, model-based multiple criteria decision making (MCDM) is investigated with the focus being on improving and applying approaches based on interactive multiobjective optimization methods. These approaches are applied in real world situations in which there are multiple conflicting objectives: intensity modulated radiotherapy (IMRT) and brachytherapy (and papermaking in the appendix).

The novel ideas for supporting model-based MCDM and interactive multiobjective optimization devised in this thesis include efficient use of trade-off information as a part of the decision making process, and making approximations of Pareto optimal solution spaces in order to reduce the number of solutions needed to be computed. In addition, a new way is introduced of visualizing the Pareto optimal solutions obtained with virtual reality facilities as a part of the decision making process. All these ideas are designed to make it easier for the decision maker to obtain a more in-depth understanding of the problem under consideration. Processes of many application areas can be made more efficient with new tools supporting the decision making.

In addition to the methodological aspects, there has been a focus on applying the interactive multiobjective optimization and the developed ideas to IMRT, and brachytherapy (and papermaking in the appendix). The application areas considered in this thesis contain very complex processes and conflicting targets which have gathered increasing interest of modeling and optimization during the years. However, these research areas are still novel, and the problems involved are not totally understood. Hence, this thesis is one of the first attempts to extend the research into interactive multiobjective optimization methods applied to radiotherapy treatment planning.

AMS (MOS) Classification: 58E17, 68U35, 90B50, 90C29, 90C90

Universal Decimal Classification: 004.946, 005.53, 005.591.1, 005.642.4, 519.863

INSPEC Thesaurus: optimisation; decision making; decision support systems; Pareto analysis; virtual reality; data visualisation; simulation; radiation therapy; brachytherapy; patient treatment; planning; paper making

To my parents

Matti and Marja-Leena Ruotsalainen

who provided me with a better opportunity
to study than was available to themselves

Acknowledgments

This work was done at the Department of Physics, University of Kuopio during the years 2005 - 2009 in collaboration with Prof. Jari Hämäläinen, Dr. Elina Madetoja, Prof. Kaisa Miettinen, Designer Veli-Matti Mönkkönen and Prof. Kalyanmoy Deb. I want to thank my supervisors Prof. Hämäläinen for giving me a great opportunity to undertake this thesis, and Dr. Madetoja for giving me everyday support during the research. Especially I want to say thank you to Prof. Miettinen for her support in writing this thesis and supervising me despite the fact that we are not even working in the same university. Discussions also with Petri Eskelinen, Ph.D., Jussi Hakanen, Ph.D., and Vesa Ojalehto, M.Sc., were helpful and, thus, acknowledged. In addition, constructive comments given by pre-examiners Prof. Francisco Ruiz and Prof. Eva K. Lee were valuable when finishing this thesis.

In application areas, collaboration with radiotherapy experts such as Eeva Boman, Ph.D., Jouko Tervo, Ph.D., Jan-Erik Palmgren, Ph.Lic., Tapani Lahtinen, Ph.D., Fredrik Carlsson, Ph.D., and Joakim Pyyry, M.Sc.(Tech.), have been very fruitful. In addition, I wish to thank also papermaking expert Petter Honkalampi, Ph.Lic., for useful tips and his expertise in papermaking.

This work was financially supported by Tekes (Finnish Funding Agency for Technology and Innovation) MASI technology programme.

Moreover, I want to say thank you to the pleasant working community and also to those a few mates I have been working with since my university studies started. Finally, the biggest thanks goes to my family and fiancée for all the support they have given to me.

Kuopio, 9th December 2009

Henri Ruotsalainen

Abbreviations

2D	two dimensional
3D	three dimensional
BTE	Boltzmann transport equation
CAD	computer aided design
CFD	computational fluid dynamics
CPU	central processing unit
CRT	cathode ray tube
CT	computed tomography
DCC	digital content & creation
DIN	Deutsches Institut für Normung
DTLZ	Deb, Thiele, Laumanns, Zitzler: scalable multiobjective optimization test problems
DSS	decision support system
EA	evolutionary algorithm
ESTRO	European Society for Therapeutic Radiology and Oncology
FEM	finite element method
GPU	graphics processing unit
GUESS	interactive method related to the reference point method (a naïve method)
Gy	Gray, absorbed dose
HDR	high dose rate
Hz	Hertz
IND-NIMBUS	implementation of the interactive NIMBUS method for multiobjective optimization for industrial purposes
IMRT	intensity modulated radiotherapy
KKT	Karush-Kuhn-Tucker
LCD	liquid crystal display
MCDA	multiple criteria decision analysis
MCDM	multiple criteria decision making
MIRA	multicriteria interactive radiotherapy assistant
MOEA	multiobjective evolutionary algorithm
MRI	magnetic resonance imaging
NAUTILUS	interactive technique in multiobjective optimization based on the nadir point
NIMBUS	interactive classification-based method for multiobjective optimization
NSGA-II	elitist non-dominated sorting genetic algorithm version II
PC	personal computer
STOM	satisficing trade-off method
SVD	singular value decomposition
VR	virtual reality

Nomenclature

AP_i	approximated Pareto optimal set i
C	critical organ region
\mathbf{d}	direction
d_{ij}	kernel value
D_i	dose in dose point i
E	energy domain
E_{PO}	Pareto optimal set in decision space
\mathbf{f}	vector of objectives
f_i	(single) i th objective function
g	radial dose function
\mathbf{h}	step length
I_i	finite set in i
J_f	Jacobian matrix
M_i	source node i
M_{PO}	trade-off rate matrix
N	normal tissue region
N_i	node point i
P	Taylor's polynomial
PP	subset of Pareto optimal set E_{PO}
r_{ij}	distance between dwell position j and dose calculation point i
\mathbf{R}^k	objective space
\mathbf{R}^n	decision space
S	feasible set
\mathbf{S}	vector of BTE model parameters
S_l	radiation field
S_k	air kerma strength
t_{ij}	trade-off rate
t_j, t	dwell time (decision variables in brachytherapy case)
T	target region
T_{ij}	ratio of change
u_l	radiation flux
V	patient region
w_i	objective weight i.e. weighting coefficient
\vec{x}	point in the patient domain (in radiotherapy cases)
\mathbf{x}	vector of decision variables
\mathbf{z}	objective vector
\bar{z}_i	i th aspiration level (for f_i)
$\bar{\mathbf{z}}$	reference point (vector of aspiration levels)
\mathbf{z}^*	Pareto optimal objective vector
\mathbf{z}^*	ideal objective vector
\mathbf{z}^{**}	utopian objective vector
\mathbf{z}^{nad}	nadir objective vector

Nomenclature

Z	image of feasible set
∇f_i	gradient of f_i
$\nabla^2 f_i$	Hessian matrix of f_i
∂f_i	partial derivative of f_i
γ	vector of BTE model parameters (decision variables in IMRT case)
θ	angular domain
κ	artificial stopping power
Λ	dose-rate constant
Φ_{an}	anisotropy function

1	Introduction	11
1.1	Background	11
1.2	Objectives of the thesis	13
1.3	Outline of the thesis	15
1.4	Author's contribution	16
2	The multiple criteria problem	18
2.1	Multiple criteria decision making	18
2.1.1	Problem identification and structuring	18
2.1.2	Model building and use	19
2.1.3	Action plans	20
2.2	Implementing and applying MCDM	20
2.2.1	Decision support systems	20
2.2.2	Supporting MCDM in real world problems	22
2.3	Concluding comments	23
3	Multiobjective optimization	25
3.1	Multiobjective optimization problem	25
3.1.1	Basic concepts	25
3.1.2	Pareto optimality	27
3.1.3	Decision making	28
3.2	Multiobjective optimization methods	30
3.2.1	Interactive multiobjective optimization methods	31
3.2.2	Weighting method as an a priori method	34
3.2.3	Multiobjective evolutionary algorithms	36
4	New approaches for supporting MCDM	38
4.1	Navigation on a Pareto optimal front utilizing gradient information	38
4.1.1	Approximating Pareto optimal fronts	39
4.1.2	Utilizing trade-off information	43
4.1.3	Example	46
4.2	Novel visualization technique: virtual reality	49
4.2.1	Virtual Reality	50

4.2.2	Integration of multiobjective optimization and virtual reality	50
4.2.3	Example	52
4.2.4	Future extensions	55
5	Interactive multiobjective optimization of IMRT	59
5.1	Introduction to IMRT	59
5.2	Dose calculation using finite element model	61
5.3	Objective function formulation	61
5.3.1	Acceptable solution for radiotherapy treatment planning . .	62
5.3.2	Objective functions	63
5.4	IMRT examples	66
5.4.1	Interactive treatment planning optimization	66
5.4.2	Utilizing gradient information	76
5.4.3	Utilizing virtual reality	79
5.5	Concluding comments	79
6	Interactive multiobjective optimization of b-therapy	82
6.1	Introduction to brachytherapy	82
6.2	Dose calculation	84
6.3	Objective function formulation	85
6.4	Brachytherapy examples	86
6.4.1	Problem settings	86
6.4.2	Example 1: Fletcher-Suit applicator	87
6.4.3	Example 2: Ring applicator	93
6.5	Concluding comments	94
7	Conclusions and topics for further research	97
	References	102
A	Dose calculation using finite element model	116
B	Case study: papermaking	121

1.1 Background

Almost every real-world optimization problem involves simultaneous optimization of several incommensurable and often competing objectives. For example, consider the design of a complex system containing hardware and software such as that found in mobile phones, cars, aeroplanes, etc. Often the cost of such a system needs to be minimized, but nonetheless maximum performance is desired. Depending on the application, further objectives may be important such as reliability and energy consumption. These are only examples, but as can be seen, decision making with multiple conflicting objectives in every day operations can be difficult. Moreover, an unfavorable decision can be financially expensive or even hazardous in some situations. Thus, there exists a need to develop different ways to support multiple criteria decision making (MCDM) processes.

This thesis begins with a description and definition of *multiple criteria decision making* [4, 11, 55, 95, 132, 133, 153, 158], starting with decision making. *Decision making* can be understood as an outcome of mental processes leading to the selection of a course of action after weighting the alternatives [4]. In the decision making context, *criterion* can be interpreted as a standard by which one particular choice or course of action could be judged to be more satisfying than some other. When we are considering several, i.e. *multiple*, different choices or courses of actions which are in conflict, it becomes a *multiple criteria decision making* problem. For example, selecting a new car is a MCDM problem which typically involves consideration of many criteria such as price, comfort, performance, and safety, see Figure 1.1. In the figure, there are two cars having totally different characteristics: one is a high-priced luxury model and another one is a cheap and humble basic model. Nevertheless, both of these cars can be optimal solutions to a MCDM problem.

In fact, almost every decision we ever make requires MCDM – the consideration of multiple factors, i.e. criteria. It is such an ordinary action that we sometimes make these decisions without any conscious thought. For example, when you

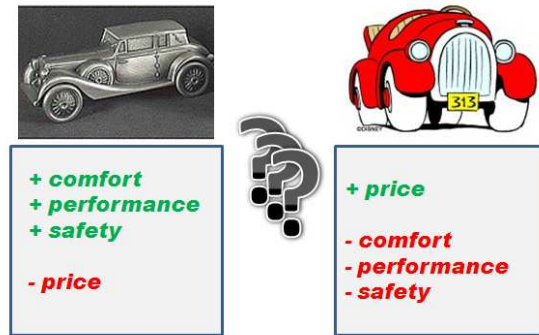


Figure 1.1: A simplified example of multiple criteria decision making.

consider what to buy in a food shop you automatically pay attention to what you will be cooking that night, what ingredients you already have in your fridge, do you or one of the diners have any allergies, or simply how much money do you have to spend. However, not many individuals build a more formal model for his/her decision making problems, and probably very few have analyzed their decisions. That is maybe because it is too complex, the issue is not worth it, or it is easy to take into account the factors in one's head with satisfying accuracy. In a nutshell, in everyday life some decisions do not matter that much. However, when we are studying MCDM, or applying it to the engineering sciences or health care, all decisions are important – in other words decisive.

In the engineering sciences or health care, the corollaries of decisions, whether they affect for example management decisions or clinical treatment plans, are more substantial. The impacts of the decisions are more long-lasting, more expensive, and may affect many people. In addition, mistakes might not be easily fixed. In these circumstances, the tools and methods presented in this thesis are useful, since it is known that the human brain can only cope with a limited amount of information simultaneously [76].

The fundamental nature of the MCDM problem is that it is characterized by complex and conflicting information. This information can reflect different viewpoints or it can change as a function of time. One goal of the MCDM is to help decision makers (who are experts on the application being considered and who will have to make the final decision) to organize all the information to be considered in such a way that it helps them in making their final decision, it provides confidence in making a decision, and minimizes the risk of making costly errors. That is why MCDM or multicriteria decision analysis (MCDA) can be understood as an umbrella term [4] describing a collection of approaches which can be used in helping individuals or groups exploring decisions in multiple criteria problems, whether they are used in personal decisions (buying a car, for example), or in high level management decisions in public or private sectors (often

integer problems), or in model-based decision support in engineering and health care problems (often continuous problems) such as those examined in this thesis.

Here the focus is on utilizing interactive multiobjective optimization [95, 138] in model-based multiple criteria decision support with applications. In interactive multiobjective optimization, the optimization process is iterative and the decision maker directs the solution process during the optimization to the most preferred direction. The model-based decision support [153] based on interactive multiobjective optimization belongs to the field of MCDM. In the literature, different MCDM techniques are utilized for example in sorting problems, ranking problems, description problems, design problems, and, as in this thesis also in engineering problems and health care problems (see [9, 28, 134, 135, 162], for examples). The diversity of approaches makes it possible for many kinds of users, i.e. decision makers, to utilize MCDM tools for different applications and goals.

1.2 Objectives of the thesis

In this thesis, the focus is on improving and applying approaches based on interactive multiobjective optimization methods. The approaches studied are applied to model-based real world applications: intensity modulated radiotherapy (IMRT) and brachytherapy, and papermaking (in the appendix).

Multiobjective optimization methods are selected for model-based decision support because they are capable of handling multiple conflicting objectives at the same time [12, 20, 95]. Solutions of the multiobjective optimization problem form a Pareto optimal front, i.e. a set of compromised trade-off solutions from which the best possible compromise solution can be selected. However, even when different Pareto optimal solutions are found, choosing a particular optimal compromise solution is not a trivial task, especially when the number of objectives is larger than two. Furthermore, the objectives in a multiobjective optimization task do not need to be commensurable.

In view of the above stated reasoning, one goal of this thesis is to introduce new ideas for supporting MCDM and interactive multiobjective optimization based decision support. These involve efficient use of gradient and trade-off information, and making approximations of Pareto optimal solutions and fronts in order to reduce the number of solutions needed to be computed. In addition, it is appreciated that new ways of visualizing the Pareto optimal solutions as a part of decision making process are needed [62, 86, 95]. In multiobjective decision making, Pareto optimal fronts are often visualized because in this way a comparison between solutions becomes easier. A Pareto optimal front is easy to visualize when there are only two objective functions, but visualizing more than two objective functions is problematic. This thesis examines the integration of multiobjective optimization with the three dimensional virtual reality environment in order to study the Pareto optimal solutions and approximated Pareto optimal fronts. This is done in order to help in making a better decision when choosing the final solution. Many kinds of innovative tools are designed to make it easier to obtain a deeper understanding of the MCDM problem.

In this thesis radiotherapy and papermaking can be considered to represent very complex processes which have obtained increasing interest of modeling, simulation and optimization over the years. However, these research areas are still novel, and the problems involved are not very well known [5, 87]. At the time when this research started (end of the year 2005), there were no interactive multiobjective optimization methods which had been applied to radiotherapy treatment planning while many other kinds of interactive approaches are used even in the clinics. Thus, this work is the first attempt to extend research into that area (as interactive multiobjective optimization methods are defined e.g. in [95]).

In radiotherapy (IMRT [37, 66, 128] or brachytherapy [69, 79, 105]), the goal is to irradiate the tumor without affecting the surrounding healthy tissue and critical organs. These targets are competing because in many cases the radiation dose must be delivered through healthy tissue. Though there are several studies where the idea of supporting the decision making process and comparing solutions has been discussed [15, 16, 17, 31, 41, 50, 65, 66, 93, 106, 145], not all the clinics are using decision support systems actively, i.e. the treatment planning is done at least partially by using a trial-and-error approach with planning parameters being adjusted manually by the treatment planner. Thus, easy-to-use and intuitive tools would be very welcome in the clinics. For some reason, interactive multiobjective optimization methods, i.e. the optimization process is iterative, have not been studied in the field of radiotherapy optimization before. The drawbacks of methods used in the literature are that it can be difficult for the decision maker to specify preferences (e.g. target weights or penalties) before the solution process has started and, on the other hand, generating many Pareto optimal solutions for the decision maker to compare can be computationally costly. It is also problematic to compare many solutions without imposing an excessive cognitive load on the decision maker [76]. Thus, it is our belief that an interactive multiobjective optimization method would be ideal for radiotherapy optimization. They assist the decision maker in controlling the solution process iteratively and thus he/she can learn about the conflicting radiotherapy targets during the optimization procedure. An interactive approach may also involve shorter computing times, because the decision maker directs the solution process and only solutions are generated in which he/she is interested. In this way, trial-and-error planning can be avoided.

As this thesis shows, the same multiobjective optimization approaches and decision making aids can be applied in different applications. In papermaking [43, 44, 46, 49, 52, 88], the goal is to produce as much paper as possible with minimal costs. Moreover, there are several paper quality properties which need to be fulfilled at the same time. As can be easily understood, these objectives are conflicting and thus MCDM approaches are welcome. The processes used in many different application areas can be made more efficient with optimization and the introduction of new tools to support the decision making.

1.3 Outline of the thesis

Outline of this thesis is as follows. After the Introduction, the basic concepts of MCDM and multiobjective optimization are considered. They are introduced in Chapters 2 and 3, respectively, as they are presented in the original works [4, 95, 158]. Chapter 2 will consider the nature of MCDM problems and present the usual MCDM process: it is divided into different phases and the characteristics of these phases are discussed. Also implementation and usability of MCDM approaches are discussed from the applications point of view, and the roles of interfaces, and simulation and optimization softwares are also examined. Chapter 3 is dedicated to multiobjective optimization which is the cornerstone of this work. This work is mostly based on interactive multiobjective optimization which can be used in finding Pareto optimal solutions and, thus, supporting decision making which is why it belongs to the subordination of the MCDM. In Chapter 3, concepts and different methods for multiobjective optimization are presented. However, only those methods which have been used in this thesis are described.

Chapter 4 constitutes the new theoretical ideas suggested to support model-based MCDM. This chapter includes new approaches for navigating on a Pareto optimal front utilizing trade-off information, and making approximations of the Pareto optimal front in order to reduce the number of solutions needed to be computed. With these approaches, the behavior of the Pareto optimal front can be predicted in a certain area and the decision maker can predict the most profitable direction in which to guide the optimization process between the conflicting targets. In addition, a novel visualization tool based on a virtual reality environment for visualizing Pareto optimal solutions and thus supporting the decision maker in decision making is presented in this chapter. Virtual reality offers new and interesting opportunities to support MCDM by providing versatile visualizing abilities which can be used in studying and analyzing the Pareto optimal solution.

In Chapters 5 and 6, radiotherapy treatment planning is studied and the presented tools are applied to radiotherapy treatment planning. Academic examples of treatment planning of IMRT are presented and optimized in Chapter 5, and clinical examples of patient treatment plans of brachytherapy are presented in Chapter 6.

Finally, Chapter 7 is devoted to the conclusions and future prospects of how these ideas and methods can be improved, utilized, and made more applicable to real world situations.

After these chapters, there are appendices containing a dose calculation model and a case study. In Appendix A, a dose calculation model-based on the Boltzmann transport equation is presented. It is presented in the appendix because it is based on work done by Boman, Tervo and Vauhkonen [5, 144] but it is still an important piece of this work. In Appendix B, a case study of the interactive multiobjective optimization of the papermaking process is discussed with examples.

1.4 Author's contribution

Although this thesis is a monograph, some of the ideas and research results of this thesis have been published elsewhere or have been presented in conferences. The new theoretical ideas suggested for MCDM have been discussed also in:

- a paper *Navigation on a Pareto-optimal front utilizing gradient information in interactive multiobjective optimization* [122] published in a conference proceedings
- a paper *Supporting multiobjective decision making with 3D virtual reality: preliminary results and future extensions* [123] submitted to a journal
- a paper *Visualizing multi-dimensional Pareto-optimal fronts with a 3D virtual reality system* [90] published in a refereed conference proceedings
- a journal paper *Approach for visualizing multi-dimensional Pareto-optimal fronts using a 3D VR system* [91].

The first study has been conducted with Prof. Jari Hämäläinen and Dr. Elina Madetoja, and the author's role was to execute the research after the idea was conceived by the co-authors. The three other research papers consider the new visualization approach with the virtual reality environment. The author's role in these papers was to conceive and execute how the VR environment could be used in supporting model-based decision making, mostly with the help of Dr. Madetoja. The collaboration of Mr. Veli-Matti Mönkkönen (technical realization), Prof. Jari Hämäläinen and Prof. Kalyanmoy Deb was also helpful during the research, and some of the ideas have been devised by these individuals.

The results considering radiotherapy treatment planning have been published or have been submitted for publication as follows:

- a working paper *Interactive multiobjective optimization for IMRT* [120]
- a journal paper *Nonlinear interactive multiobjective optimization method for radiotherapy treatment planning with Boltzmann transport equation* [121]
- a working paper *Interactive multiobjective optimization for HDR brachytherapy* [125]
- a paper *Interactive multiobjective optimization for 3D HDR brachytherapy applying IND-NIMBUS* [124] accepted for publication in a refereed conference proceedings.

The research considering interactive multiobjective optimization of radiotherapy treatment planning has been executed by the author utilizing also ideas from the co-authors. The expertise and support of Prof. Kaisa Miettinen is acknowledged in the multiobjective optimization side, and the knowledge of radiotherapy experts Dr. Eeva Boman, Dr. Jouko Tervo, Mr. Jan-Erik Palmgren, Ph.Lic., and Dr. Tapani Lahtinen was most helpful when the research was being implemented.

The results considering papermaking are discussed also in the following works:

- a book chapter *CFD-based optimization for a complete industrial process: papermaking* [44]
- a paper *Simulation-based optimization and decision support for papermaking* [45] published in a conference proceedings
- a paper *New visualization aspects related to intelligent solution procedure in papermaking optimization* [89] published in a conference proceedings.

The author's role in these works concentrated mainly on optimization and aspects involved in the decision support, and thus these studies are not the focus of this thesis. These papers were mainly conceived and written by Prof. Hämäläinen and Dr. Madetoja.

The multiple criteria problem

2.1 Multiple criteria decision making

To begin with, let us discuss the process of MCDM. Before going into details, one must consider some important features of MCDM. The goal of MCDM is to lead to better considered, justified and explained decisions. MCDM will not give the "right" answer or provide an "objective" analysis which will replace decision makers of making difficult judgments. The MCDM process helps to structure the problem, and it seeks to pay reasonable attention to multiple and conflicting criteria. Therefore it makes it easier for the decision makers to learn about the problem being considered, and about their own and others' values and judgments. The final outcome of a MCDM process should provide decision makers with information to help to identify the most preferred solution or course of action. Extensive discussion belongs to the nature of a MCDM process. The concepts of MCDM are presented and discussed mostly based on the book by Belton and Stewart [4].

In the following section, each of the three key phases [4]: problem identification and structuring, model building and use, and the development of action plans of the MCDM problem are discussed more thoroughly. The phases are illustrated also in Figure 2.1.

2.1.1 Problem identification and structuring

"A problem well structured is a problem half solved"

is an old Finnish proverb. Problem identification and structuring is also the first and very important step of MCDM since no analysis can be done before an adequate understanding of the problem is obtained. At the very onset, initial problem structuring means a focused way of thinking: opening up the issue, defining the complexity, and trying to understand and manage the problem. In this phase, those factors which constitute the agenda for further analysis need to be identified and considered, such as goals, values, constraints, and uncertainties. A mismatch

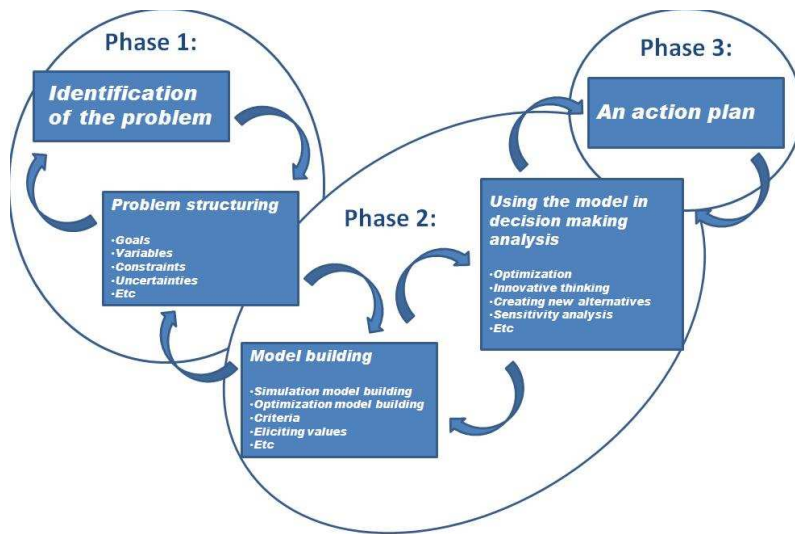


Figure 2.1: The process of MCDM

between the problem and model used is the most common reason for the failure in the MCDM analysis [147].

When applying MCDM to real world problems, goals, limitations and variables are examples of aspects to be realized which arise from the application area under consideration and, thus, they are very application specific. In other words, there is no problem structure which stands for all issues but innovative thinking is needed in problem structuring.

2.1.2 Model building and use

At some stage, the problem structuring changes to model building. As in the whole MCDM process, model building must be a very dynamic process interacting with a problem structuring process and model use. It can involve iteration, searching for new solutions and criteria, and rejecting old ones. Model building can be understood as a convergent way of thinking and trying to identify the essences of the complex phenomena. This is the case especially in the model-based decision support, where the models to be built are very complex, including physical and mathematical modeling which can be computationally very challenging. Thus, model building can be divided into two parts: simulation model building and optimization model building.

Since some MCDM problems arise from engineering sciences (such as in the applications presented this thesis) in which large processes need to be modeled, the simulation model building can be really extensive including different kinds of modeling techniques. In addition, also computational aspects, numerical issues, and discretization of the simulation model need to be considered.

In optimization model building, the goal is to choose the objectives and variables, and to develop formal models to model the goals (i.e. objectives functions), values, and preferences so that the alternative actions under consideration can be compared to each other in a systematic and transparent manner. Depending on the application, also these models can be very dissimilar. Multiple criteria models can sometimes appear very simple, but a simple model does not necessarily mean that there will not be complexity inherent in the problem.

After the models have been built, they can be used in supporting the decision making. In this thesis, an interactive multiobjective optimization will be used to solve the devised mathematical optimization models. In that way, all the information given by the models can be taken into account efficiently in decision making.

2.1.3 Action plans

Model building and use cannot solve the decision making problem. An important aspect is to implement the results into specific plans of action. MCDM is not only technical modeling of the application concerned, it is more about the support and insight given to implementation.

Action plans are often obtained after moving from one phase back to another several times. That is why iterative and interactive multiobjective optimization methods suit well for MCDM, and they are used also in this thesis. As a result of this MCDM process, the decision maker should have the best possible understanding of the problem considered and he/she should be able to make the best possible decision. In other words, he/she will now be able to choose the best solution or course of action to be the final one which then can be executed.

2.2 Implementing and applying MCDM

In the following section, the implementation and utilization of the MCDM techniques in application fields is discussed. In general, implementation is interpreted as the realization of an application, or execution of a plan, idea, model, or algorithm. In computer sciences, an implementation means a realization of a technical specification or algorithm as a program, software component, or other computer system. The development of computers and computing capacity have made it possible to produce more sophisticated software for solving multiobjective optimization problems and to implement many kinds of algorithms and computer softwares for MCDM problems. At the same time, these implementations are being applied to many more varied applications as is done also in this thesis. These kinds of software packages for MCDM and multiobjective optimization problems are termed multiobjective *decision support systems* [4, 95].

2.2.1 Decision support systems

Decision support systems (DSSs) are usually depicted as a specific class of computerized information systems that are designed for supporting business and organizational decision making activities [95]. A DSS is a software based system

intended to help decision makers, for example, in compiling useful information from raw data, documents, personal knowledge, and/or models to identify and solve problems and, more importantly, make decisions.

A typical decision support system might gather and present information such as:

- An inventory of all of your current information assets
- Comparative graphs, figures and tables between solutions
- Consequences of different decision alternatives.

This thesis will consider so-called model-based or model-driven decision support systems [114] which are usually based on statistical data, a simulation model, and/or optimization. Model-based DSSs use data and parameters provided by an individual called an analyst to assist decision makers in analyzing a situation and coming to a decision.

By an *analyst* we mean an individual (or in some cases a computer program) responsible for the mathematical side of the solution process [95]. He/she is an expert in using this kind of software, and sometimes he/she is responsible also for implementation and programming. In addition to the decision maker who has responsibility for the decision, an analyst is on hand to guide and assist the decision maker in reaching a desired decision. The analyst works in co-operation with the decision maker: he/she generates information for the decision maker to consider, and then the final solution is selected by the decision maker.

It has been demonstrated that DSSs increase the understanding of the problem, they contribute to progress in solution process, and thus, reduce frustration in problem solving [114]. In general, DSSs should be easy to use and they should follow the decision maker's thinking. Moreover, they should be able to support different decision styles, problem structures, and applications [151].

Software specifically implementing MCDM methodology can be divided into three groups [151]:

- Commercially available software packages
- Software packages developed primarily for research purposes
- Programs written for experimental implementation and testing of new MCDM techniques.

Commercially available softwares can be true application oriented simulators which are designed for supporting decision making in some certain application or problem (e.g. MIRA [145] which is however an open source program). Simultaneously, some of those software packages are very generic systems which can be implemented to solve almost any problem which have been modeled in a reliable enough manner (e.g. modeFRONTIER [36] or NIMBUS [97, 99]). Most of the implementations are designed for research and testing purposes.

A list of some software products designed for supporting MCDM can be found on www.mcdmsociety.org/soft.html which is the webpage of the International Society on MCDM. Many kind of macros can be used in supporting MCDM. Thus, the above list does not claim to be complete.

2.2.2 Supporting MCDM in real world problems

In order to support MCDM in solving of a real world problem, the following steps are considered in a model-based DSS in this thesis:

- Simulation model
- Optimization tool (or optimizer, solver)
- Interface between the model, the optimizer, and the user (decision maker or in some case analyst).

Here, the interface refers to input, output and exchange of information, and presentation of results for the decision maker. The cooperation of simulation model, optimization tool, interface and user is clarified also in Figure 2.2.

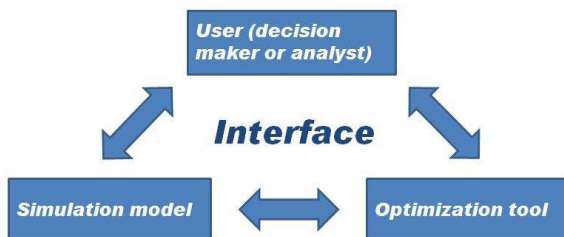


Figure 2.2: An illustration of model-based decision support system.

SIMULATION MODEL

The role of simulation (and optimization) model building was already discussed in Section 2.1.2. A simulation model forms the cornerstone of model-driven DSSs, because it is the way the system acquires information and data about the system considered. Thus, if the simulation model is unreliable, then the information given by the DSS is unreliable. Optimization models to be solved are built up by using simulation models.

OPTIMIZATION TOOL

Model-based DSSs are usually constructed in such a way that many optimization tools or optimizers can be used to solve the optimization model or problem in

question. The selection of the optimizer depends mostly on the problem structure: problems can be continuous or integer-valued, linear or nonlinear, convex or non-convex, differentiable or non-differentiable, or problem can be single or multiobjective optimization problem. There are different methods suitable for different kinds of problems, and choosing the appropriate optimizer case-specifically is important for maintaining the efficiency of the DSS.

INTERFACE

It is important to highlight the role of the interface. In many cases, a great effort has been spent in developing the methodological and computational aspects of the system (i.e. modeling work and developing the optimizer), but the interface between the model, the optimizer, and the user is not so well clarified [4]. This can cause problems, since no matter how exact is the model used or how efficient is the optimizer it will fail if the interface between those features and the user does not work as expected. Graphical user interfaces with illustrative visualizations, graphs and figures play an essential role in DSSs nowadays [62, 95].

In a nutshell, examples of the requirements for computer implementation of a DSS can be listed as follows:

- Simulation model must be validated
- Flexible to test and analyze different model parameters and set-ups
- Possibility to add models to the system
- Proper optimizer and possibility to modify optimization problem solved
- Possibility to add optimizers to the system
- Appropriate interface
- Fast enough results.

2.3 Concluding comments

So far, the problems involved in MCDM have been introduced with simple examples taken from everyday life. Here, the main concepts of MCDM were discussed shortly. Only the main works were cited here which does not pay full respects to the rich literature of MCDM. Thus, readers are recommended to familiarize themselves with the references listed in [4, 11, 55, 95, 134, 158], for example.

In the following section, some concepts of multiobjective optimization will be described and then the focus will switch to new ideas developed for interactive multiobjective optimization and MCDM. As already stated, multiobjective optimization is one part of the MCDM umbrella term since it is used here to help decision makers in making decision in multiple criteria problems.

After the theoretical and methodological part of the thesis, we apply the introduced and developed approaches to the real world applications IMRT, and

brachytherapy (and papermaking in the case depicted in the appendix). As can be understood from the diversity of the applications, model-based MCDM approaches and DSSs can be implemented in many areas in order to support decision makers.

Multiobjective optimization

3.1 Multiobjective optimization problem

3.1.1 Basic concepts

In this chapter, the principles of multiobjective optimization are outlined and basic concepts are formally defined following the notation presented by Miettinen in her book [95]. A multiobjective optimization problem can be defined as follows [95]

$$\begin{aligned} \min \quad & \{f_1(\mathbf{x}), f_2(\mathbf{x}), \dots, f_k(\mathbf{x})\} \\ \text{subject to} \quad & \mathbf{x} \in S, \end{aligned} \tag{3.1}$$

where \mathbf{x} is a vector of continuous decision variables from the feasible set $S \subset \mathbb{R}^n$ defined by linear, nonlinear and/or box constraints ($k \geq 2$). We can denote an objective vector by $\mathbf{f}(\mathbf{x}) = (f_1(\mathbf{x}), f_2(\mathbf{x}), \dots, f_k(\mathbf{x}))^T$. Furthermore, we denote the image of the feasible set by $\mathbf{f}(S) = Z$ and call it a feasible objective set. It is a subset of the objective space \mathbb{R}^k . As stated, the elements of Z are called objective vectors and denoted by $\mathbf{f}(\mathbf{x})$ or $\mathbf{z} = (z_1, z_2, \dots, z_k)^T$, where $z_i = f_i(\mathbf{x})$ for all $i = 1, \dots, k$ are objective function values.

The word "min" means "minimize" and it is intended to minimize all the objective functions at the same time. If an objective function f_i is to be maximized, this is equivalent to considering minimization of $-f_i$. If there is no conflict between the objective functions, then a solution can be found where every the objective function attains its optimum (i.e. minimum or maximum). In such a case, no special multiobjective optimization methods are needed. Here, we assume that there does not exist a single solution that is optimal with respect to every objective function. This means that the objective functions are conflicting (at least partly).

Before defining optimality in multiobjective optimization, let us define some of the basic concept of multiobjective optimization used in this thesis.

Definition 3.1.1 The multiobjective optimization problem is *linear* if all the objective functions and constraint functions are linear.

We have a nonlinear multiobjective optimization problem if any of the objective or constraint functions are nonlinear.

Definition 3.1.2 A function $f_i : \mathbb{R}^n \rightarrow \mathbb{R}$ is *convex* if for all $\mathbf{x}^1, \mathbf{x}^2 \in \mathbb{R}^n$ is valid that $f_i(\beta\mathbf{x}^1 + (1 - \beta)\mathbf{x}^2) \leq \beta f_i(\mathbf{x}^1) + (1 - \beta)f_i(\mathbf{x}^2)$ for all $0 \leq \beta \leq 1$.

The definition of convex functions can be modified for *concave* functions by replacing " \leq " by " \geq ". A set $S \subset \mathbb{R}^n$ is convex if $\mathbf{x}^1, \mathbf{x}^2 \in S$ implies that $\beta\mathbf{x}^1 + (1 - \beta)\mathbf{x}^2 \in S$ for all $0 \leq \beta \leq 1$.

Definition 3.1.3 If all the objective functions and the feasible region are convex, the multiobjective optimization problem is convex.

Definition 3.1.4 A function $f_i : \mathbb{R}^n \rightarrow \mathbb{R}$ is *differentiable* at \mathbf{x}^* if $f_i(\mathbf{x}^* + \mathbf{d}) - f_i(\mathbf{x}^*) = \nabla f_i(\mathbf{x}^*)^T \mathbf{d} + \|\mathbf{d}\| \epsilon(\mathbf{x}^*, \mathbf{d})$, where $\nabla f_i(\mathbf{x}^*)$ is the gradient of f_i at \mathbf{x}^* , $\mathbf{d} \in \mathbb{R}^n$ is a feasible direction emanating from $\mathbf{x} \in S$, and $\epsilon(\mathbf{x}^*, \mathbf{d}) \rightarrow 0$ as $\|\mathbf{d}\| \rightarrow 0$.

In addition, f_i is *continuously differentiable* at \mathbf{x}^* if all of its *partial derivatives* $\frac{\partial f_i(\mathbf{x}^*)}{\partial x_j}$ ($j = 1, \dots, n$), i.e. all the components of the gradient, are continuous at \mathbf{x}^* .

Definition 3.1.5 If at least one of the objective functions or the constraint functions forming the feasible region is nondifferentiable, the multiobjective optimization problem is *nondifferentiable*.

Definition 3.1.6 A function $f_i : \mathbb{R}^n \rightarrow \mathbb{R}$ is *twice-differentiable* at \mathbf{x}^* if $f_i(\mathbf{x}^* + \mathbf{d}) - f_i(\mathbf{x}^*) = \nabla f_i(\mathbf{x}^*)^T \mathbf{d} + \frac{1}{2} \mathbf{d}^T \nabla^2 f_i(\mathbf{x}^*) \mathbf{d} + \|\mathbf{d}\| \epsilon(\mathbf{x}^*, \mathbf{d})$, where $\nabla f_i(\mathbf{x}^*)$ is the gradient, the symmetric $n \times n$ matrix $\nabla^2 f_i(\mathbf{x}^*)$ is a *Hessian matrix* of f_i at \mathbf{x}^* and $\epsilon(\mathbf{x}^*, \mathbf{d}) \rightarrow 0$ as $\|\mathbf{d}\| \rightarrow 0$. The Hessian matrix of a twice-differentiable function consists of *second-order partial derivatives* $\frac{\partial^2 f_i(\mathbf{x}^*)}{\partial x_j \partial x_l}$, $j, l = 1, \dots, n$. In other words

$$\nabla^2 f_i(\mathbf{x}^*) = \begin{bmatrix} \frac{\partial^2 f_i(\mathbf{x}^*)}{\partial x_1^2} & \cdots & \frac{\partial^2 f_i(\mathbf{x}^*)}{\partial x_1 \partial x_n} \\ \vdots & \ddots & \vdots \\ \frac{\partial^2 f_i(\mathbf{x}^*)}{\partial x_n \partial x_1} & \cdots & \frac{\partial^2 f_i(\mathbf{x}^*)}{\partial x_n^2} \end{bmatrix}.$$

In addition, f_i is *twice continuously differentiable* at \mathbf{x}^* if all of its second-order partial derivatives are continuous at \mathbf{x}^* .

Definition 3.1.7 A function $f_i : \mathbb{R}^n \rightarrow \mathbb{R}$ is *increasing* if for \mathbf{x}^1 and $\mathbf{x}^2 \in \mathbb{R}^n$ holds that $x_j^1 \leq x_j^2$ for all $j = 1, \dots, n$ imply $f_i(\mathbf{x}^1) \leq f_i(\mathbf{x}^2)$.

Correspondingly the function f_i is *decreasing* if $f_i(\mathbf{x}^1) \geq f_i(\mathbf{x}^2)$. Moreover, a function is *monotonic* if it is either decreasing or increasing.

3.1.2 Pareto optimality

Due to the conflicting objectives and possible incommensurability of the objective functions it is not possible to find a single solution that would be optimal for all the objectives at the same time. In multiobjective optimization, optimality is often understood in the sense of Pareto optimality [95]. The existence of Pareto optimal solutions has been discussed in [95, 126], for example. Pareto optimality is named after Vilfredo Pareto [111, 112].

Definition 3.1.8 A decision vector $\mathbf{x}^* \in S$ is *Pareto optimal* if there does not exist another decision vector $\mathbf{x} \in S$ such that $f_i(\mathbf{x}) \leq f_i(\mathbf{x}^*)$ for all $i = 1, \dots, k$ and $f_j(\mathbf{x}) < f_j(\mathbf{x}^*)$ for at least one index j .

Definition 3.1.8 introduces also *global Pareto optimality*.

Definition 3.1.9 An objective vector $\mathbf{z}^* \in Z$ is *Pareto optimal* if there does not exist another objective vector $\mathbf{z} \in Z$ such that $z_i \leq z_i^*$ for all $i = 1, \dots, k$ and $z_j < z_j^*$ for at least one index j .

Equivalently, \mathbf{z}^* is Pareto optimal if the decision vector corresponding to it is Pareto optimal.

These Pareto optimal solutions form a Pareto optimal set (or front) (bold line in Figure 3.1). This figure illustrates a feasible set $S \subset \mathbb{R}^3$ and its image, a feasible objective set $Z \subset \mathbb{R}^2$. Usually, for continuous problems there is an infinite number of Pareto optimal solutions. The Pareto optimal set can be nonconvex and disconnected.

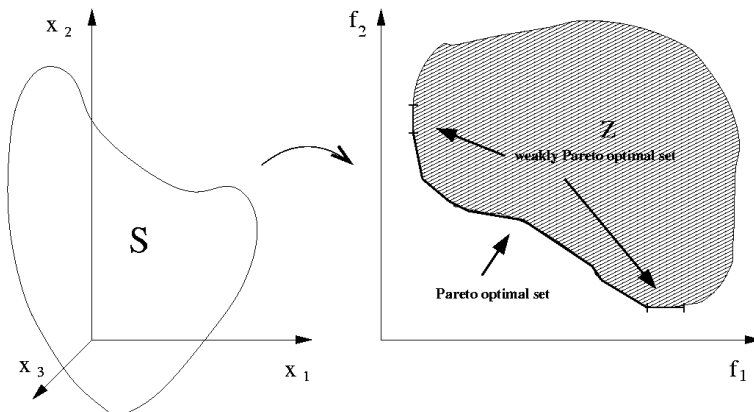


Figure 3.1: An example of the sets S and Z and the Pareto optimal set.

Definition 3.1.10 A decision vector $\mathbf{x}^* \in S$ is *locally Pareto optimal* if there exists $\delta > 0$ such that \mathbf{x}^* is Pareto optimal in $S \cap B(\mathbf{x}^*, \delta)$.

Naturally, any globally Pareto optimal solution is locally Pareto optimal. In addition, any locally Pareto optimal solution is globally Pareto optimal in convex multiobjective optimization problems [95].

Definition 3.1.11 A decision vector $\mathbf{x}^* \in S$ is *weakly Pareto optimal* if there does not exist another decision vector $\mathbf{x} \in S$ such that $f_i(\mathbf{x}) < f_i(\mathbf{x}^*)$ for all $i = 1, \dots, k$.

Definition 3.1.12 An objective vector $\mathbf{z}^* \in Z$ is *weakly Pareto optimal* if there does not exist another objective vector $\mathbf{z} \in Z$ such that $z_i < z_i^*$ for all $i = 1, \dots, k$.

The weakly Pareto optimal set is also denoted in Figure 3.1. The Pareto optimal set is a subset of the weakly Pareto optimal set which can be seen also from the figure.

In the Pareto optimal set, an *ideal objective vector* $\mathbf{z}^* \in \mathbb{R}^k$ gives lower bounds for the objective functions, and it is obtained by minimizing each objective function individually subject to the constraints. A vector strictly better than \mathbf{z}^* can be called a *utopian objective vector* \mathbf{z}^{**} , that is, we set $z_i^{**} = z_i^* - \epsilon$ for $i = 1, \dots, k$, where ϵ is a small positive scalar. A *nadir objective vector* \mathbf{z}^{nad} giving upper bounds of objective function values in the Pareto optimal set is usually difficult to calculate, and, thus, its values are usually only approximated e.g. by using pay-off tables, see, for example [23, 95]. The ideal and nadir objective vectors are illustrated in Figure 3.2.

In the multiobjective optimization context, we are usually interested in the objective space \mathbb{R}^k whereas in single objective optimization the main focus is often on the decision variable space \mathbb{R}^n . That is because in multiobjective optimization, we usually have less objectives than variables and the objectives describe the trade-offs in the problem but also the variables are important. Typically, only Pareto optimal solutions are interesting, not the other feasible solutions in Z . If the optimization model is badly defined or it does not describe the real goals of the problem, some other feasible solutions can be better than Pareto optimal ones. Since all the Pareto optimal solutions are equally good from a mathematical point of view, they can be regarded as equally valid compromise solutions of the problem. Thus, there exists no trivial mathematical tool in order to find the best solution in the Pareto optimal set because vectors cannot be ordered completely. For this reason some additional information is needed in decision making.

3.1.3 Decision making

When are needs to solve a multiobjective optimization problem, two separate phases can be identified: multiobjective optimization and decision making [53] (compare to the phases two and three of the MCDM problem [4]). The first phase refers to the optimization process in which the feasible set is sampled for Pareto optimal solutions without committing any information about what represents a

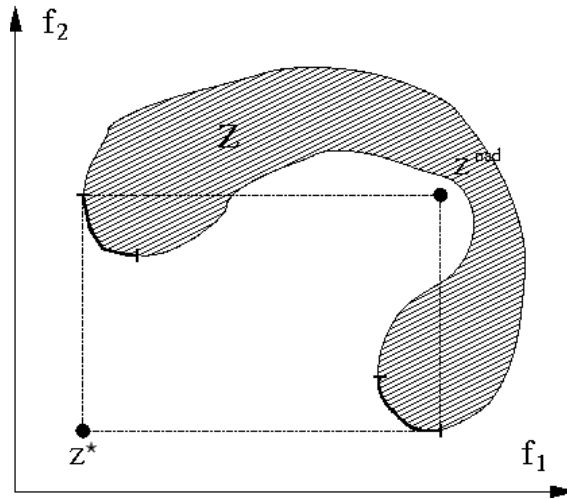


Figure 3.2: An example of an ideal objective vector and a nadir objective vector.

suitable compromise solution. The second phase addresses the problem of selecting a suitable compromise solution from the Pareto optimal set (in some cases, decision making process can happen before the multiobjective optimization or during the multiobjective optimization process). Thus, usually a human decision maker is necessary to make the often difficult trade-offs between conflicting objectives. In other words, when one speaks of solving a multiobjective optimization problem, what is meant is finding a feasible Pareto optimal decision vector that also satisfies the requirements set to the solution.

Typically a *decision maker* (or a group of decision makers), i.e. an expert of the problem, is needed in order to find the best or most satisfying solution to be called the *final solution*, see [95] and references therein. It is assumed that the decision maker has a better insight into the problem, and he/she can express preference relations between different solutions. Thus, for example it can be useful for the decision maker to know the ranges of the objective function values (ideal and nadir points) in the Pareto optimal set. The decision maker can participate in the solution process, and, in some way, determine which of the obtained Pareto optimal solutions is the most satisfying to be considered as the final solution.

One example of ways how the decision maker can specify preference information when looking for the best possible compromise, is that he/she can define aspiration levels (forming a reference point) [152].

Definition 3.1.13 Objective function values that are desirable to the decision maker are called *aspiration levels* and denoted by \bar{z}_i , $i = 1, \dots, k$.

Definition 3.1.14 The vector $\bar{\mathbf{z}} \in \mathbb{R}^k$ (consisting of aspiration levels) is called a *reference point*.

3.2 Multiobjective optimization methods

Multiobjective optimization problems are often solved by scalarization. Well-known exceptions are linear multiobjective optimization problems (some simplex-based solution methods can find Pareto optimal extreme points) [94], multiobjective proximal bundle method for nondifferentiable problems (though this is not based on scalarization in the traditional sense) [94, 95], and multiobjective evolutionary algorithms [20]. In scalarization, objectives are aggregated into a single, scalarized objective function before the optimization search. Three requirements are set for a scalarizing function [126]:

1. It can cover any Pareto optimal solution
2. Every solution it finds is a Pareto optimal
3. Its solution is satisficing (i.e. it satisfies all the aspirations of the decision maker) if the aspiration levels used are feasible (only if the scalarizing function is based on aspiration levels)

Unfortunately, not any scalarizing function is satisfying all three requirements.

The scalarization function may contain preference information set by the decision maker as its parameters. Several optimization runs with different parameters may be performed in order to achieve a set of solutions which approximates to the Pareto optimal set, or only one scalarizing function is used if only one Pareto optimal solution is generated at a time. Basically, this procedure is independent of the underlying optimization algorithm which is used to solve the scalarized objective function. In the literature, difficulties of using scalarizing functions are mentioned: e.g. some of the techniques can be sensitive to the shape of the Pareto optimal front, or knowledge of the problem can be required which may not be available [163].

Recently, multiobjective evolutionary algorithms [12, 20] have become popular alternatives for solving multiobjective optimization problems in addition to scalarizing-based methods. The advantages of using evolutionary algorithms are that large search spaces as well as nondifferentiable and nonconvex problems can be handled, and multiple alternative trade-offs can be generated in a single optimization run, see e.g. [163]. In contrast, the drawbacks of evolutionary algorithms are that generating many Pareto optimal solutions for the decision maker to compare can also be computationally costly, it is problematic to compare many solutions without imposing too great a cognitive load on the decision maker, and comparing the solutions is difficult when $k > 3$.

Methods developed for multiobjective optimization can be divided into four classes according to role of the decision maker [95]. Those classes are:

- Methods where a decision maker is not used
- A priori methods
- A posteriori methods
- Interactive methods

In those methods where no decision maker is available, the final solution is some neutral compromise solution [95]. In the three other classes, the decision maker participates before the solution process has started, after it or iteratively, and they are called a priori, a posteriori and interactive methods, respectively. In the following section, the multiobjective optimization methods (several interactive methods, a priori weighting method and a posteriori multiobjective evolutionary algorithms) used in this thesis are shortly presented.

Interactive methods were selected in this thesis because they are applied successfully for different applications [40, 46, 47, 101], and the implementations of those were available. The weighting method was selected because it has been used considerably in the literature. Thus, it is used for comparison in this thesis. Multiobjective evolutionary algorithms were used since they are convenient when generating a large number of Pareto optimal solutions, and they are used also extensively in the literature.

3.2.1 Interactive multiobjective optimization methods

In interactive multiobjective optimization methods, the decision maker works together with an analyst or an interactive computer program. A solution pattern is formed and repeated several times, and after every iteration, information is given to the decision maker and he/she is asked to provide some other type of information. The information given to and asked from the decision maker must be readily understandable. Finally, he/she decides, which one of the obtained Pareto optimal solutions is the most desired.

In this thesis, we use the so-called synchronous NIMBUS method [95, 97, 99]. The NIMBUS method is based on the idea of classification of objective functions. It is known that the classification can be considered as an acceptable task for human decision makers from a cognitive point of view [76]. During the solution process, the decision maker classifies objective functions at the current Pareto optimal point into up to five classes. The classes are the following:

- $I^<$ functions whose values should be improved,
- I^{\leq} functions whose values should be improved until a desired aspiration level \hat{z}_i ,
- $I^=$ functions whose values are satisfactory,
- I^{\geq} functions whose values can be impaired until a given bound ϵ_i ,
- $I^>$ functions whose values can change freely.

Since all the solutions considered are Pareto optimal, the decision maker can not make a classification where all the objective function values need to be improved without allowing at least one of the objective functions to be impaired. The aspiration levels and the bounds are asked from the decision maker during the classification procedure if they are needed. Based on preference information about how the current solution should be improved (given by the decision maker by classifying the objective functions), a scalarized single objective optimization problem, a subproblem, as we call it, can be formed.

In the synchronous NIMBUS method [99], there are four different subproblems available, and thus, the decision maker can choose if he/she wants to see one to four new solutions after each classification. Each subproblem uses a different scalarization, and thus generates a new Pareto optimal solution that satisfies the preferences given in the classification as well as possible, but the preferences are taken into account in slightly different ways [98]. As stated, subproblems formed are solved with an appropriate single objective optimizer.

When using the synchronous NIMBUS, the decision maker can use any solution obtained at that point as a starting point for a new classification. Alternatively, the decision maker can generate a desired number of intermediate Pareto optimal solutions between any two Pareto optimal solutions. He/she can also save interesting solutions in a database to allow him/her to return later to these solutions and continue the solution process from any of them. The NIMBUS flowchart is presented in Figure 3.3. For further details, see [99].

Interactive multiobjective optimization approaches may provide shorter computing times compared to other methods because the decision maker directs the solution process in the way he/she desires and only such solutions are generated in which he/she is interested. In this way, trial-and-error optimization, i.e. varying objective weights and/or other optimization parameters, can be avoided.

SCALARIZING FUNCTIONS AND SUBPROBLEMS

Scalarizing functions used in subproblems play a vital role in solving multiobjective optimization problems. In the literature, many different scalarizing functions have been presented but this thesis will concentrate on classification and reference-point based functions which are available in the synchronous NIMBUS (selected the comparisons reported in [98]).

In the NIMBUS method [95, 97], a subproblem is formed based on the classification and the corresponding aspiration levels and upper bounds. Different formulations have been used in different NIMBUS versions. The subproblem used in the synchronous NIMBUS [99] is

$$\begin{aligned}
 \min \quad & \max_{i \in I^<, j \in I^{\leq}} \left[\frac{f_i(\mathbf{x}) - z_i^*}{z_i^{nad} - z_i^{**}}, \frac{f_j(\mathbf{x}) - \bar{z}_j}{z_j^{nad} - z_j^{**}} \right] + \rho \sum_{i=1}^k \frac{f_i(\mathbf{x})}{z_i^{nad} - z_i^{**}} \\
 \text{subject to} \quad & f_i(\mathbf{x}) \leq f_i(\mathbf{x}^c) \quad \text{for all } i \in I^< \cup I^{\leq} \cup I^= \\
 & f_i(\mathbf{x}) \leq \epsilon_i \quad \text{for all } i \in I^{\geq} \\
 & \mathbf{x} \in S,
 \end{aligned} \tag{3.2}$$

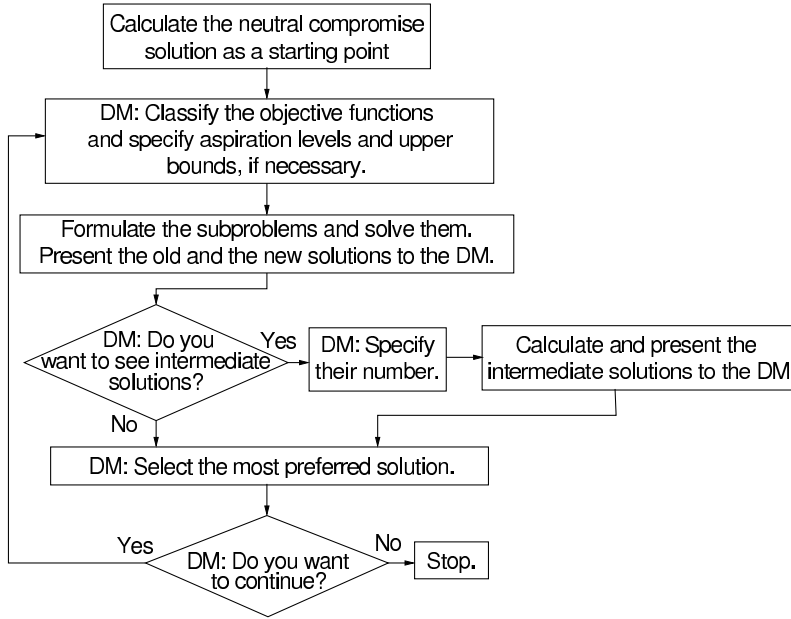


Figure 3.3: The NIMBUS flowchart [102].

where a so-called augmentation coefficient $\rho > 0$ is a relatively small scalar, and $\mathbf{x}^c \in S$ the current Pareto optimal decision vector. Aspiration level \bar{z}_j and bound ϵ_i are given by the decision maker by classifying the objectives [95]. The scaling factors $(1/(z_j^{nad} - z_j^{**}))$ are used because they increase computational efficiency and better enable capturing the decision maker's preferences [100].

The other subproblems available in the synchronous NIMBUS originate from reference point based methods. For a description on how a reference point is obtained from classification information, see [98, 99]. The second subproblem emerges from the satisficing trade-off method (STOM) [109]. The subproblem is of the form

$$\begin{aligned} \min \quad & \max_{i=1, \dots, k} \left[\frac{f_i(\mathbf{x}) - z_i^{**}}{\bar{z}_i - z_i^{**}} \right] + \rho \sum_{i=1}^k \frac{f_i(\mathbf{x})}{\bar{z}_i - z_i^{**}} \\ \text{subject to} \quad & \mathbf{x} \in S, \end{aligned} \quad (3.3)$$

where \bar{z}_i must be strictly higher than the corresponding component of z_i^{**} .

Thirdly, there is the achievement scalarizing function which has been presented in [152], for example. In NIMBUS, we use the formulation

$$\begin{aligned} \min \quad & \max_{i=1, \dots, k} \left[\frac{f_i(\mathbf{x}) - \bar{z}_i}{z_i^{nad} - z_i^{**}} \right] + \rho \sum_{i=1}^k \frac{f_i(\mathbf{x})}{z_i^{nad} - z_i^{**}} \\ \text{subject to} \quad & \mathbf{x} \in S. \end{aligned} \quad (3.4)$$

The fourth subproblem used is related to that used in the GUESS method [8]

$$\begin{aligned} \min \quad & \max_{i=1,\dots,k} \left[\frac{f_i(\mathbf{x}) - z_i^{nad}}{z_i^{nad} - \bar{z}_i} \right] + \rho \sum_{i=1}^k \frac{f_i(\mathbf{x})}{z_i^{nad} - \bar{z}_i} \\ \text{subject to} \quad & \mathbf{x} \in S. \end{aligned} \quad (3.5)$$

In conclusion, each of these subproblems generates a solution taking the classification information into account in a slightly different way. In addition, the solutions generated are Pareto optimal and any Pareto optimal solution can be found [99].

Remark Only the NIMBUS method includes other constraints than box constraints for decision variables. In three other subproblems, aspiration level \hat{z}_i and bound ϵ_i are handled as a soft constraint which can be violated [99].

Instead of an interactive method, one can use an a priori method and generate a Pareto optimal solution after having asked the decision maker to specify his/her preferences. One of the simplest methods is the weighting method.

3.2.2 Weighting method as an a priori method

In the weighting method, the idea is to equip each objective function with a weighting factor and minimize the weighted sum of the objectives. In this way, the multiple objective functions are transformed (scalarized) into a single objective function. Weighting coefficients w_i are real numbers such that $w_i \geq 0$ for all $i = 1, \dots, k$. In addition, weights are often normalized, that is, $\sum_{i=1}^k w_i = 1$. Now, the multiobjective optimization problem can be formulated as

$$\begin{aligned} \min \quad & \sum_{i=1}^k w_i f_i(\mathbf{x}) \\ \text{subject to} \quad & \mathbf{x} \in S, \\ & w_i \geq 0 \text{ for all } i = 1, \dots, k, \text{ and} \\ & \sum_{i=1}^k w_i = 1. \end{aligned} \quad (3.6)$$

Theorem 3.2.1 The solution of the weighting method is Pareto optimal if the weighting coefficients are all positive, i.e. $w_i > 0$, for all $i = 1, \dots, k$. See [95] for proof.

Theorem 3.2.2 The solution of the weighting method is Pareto optimal if the solution is unique. See [95] for proof.

The weakness of the weighting method is that all of the Pareto optimal solutions cannot be found unless the problem is convex. This is illustrated in Figure 3.4. As can be seen from the figure, Pareto optimal solutions located in the middle part of the front cannot be obtained because the $w_1 f_1 + w_2 f_2$ is linear. More formally, we have the following theorem.

Theorem 3.2.3 If $\mathbf{x}^* \in S$ is a Pareto optimal solution of a convex multiobjective optimization problem, then there exists a weighting vector $\mathbf{w} ((w_1, \dots, w_k)^T)$ such

that \mathbf{x}^* is the solution of the weighting problem (3.6). See [95] for proof.

Furthermore, all the solutions of a multiobjective linear programming problem can be hard to find by the weighting method. That is because the single objective optimization routines for linear problems usually find only extreme point solutions. Thus, if some facet of the feasible region is Pareto optimal, it can remain unidentified [95].

Furthermore, the weighting vector that produces a certain Pareto optimal solution is not necessarily unique. This is true especially for linear problems [95].

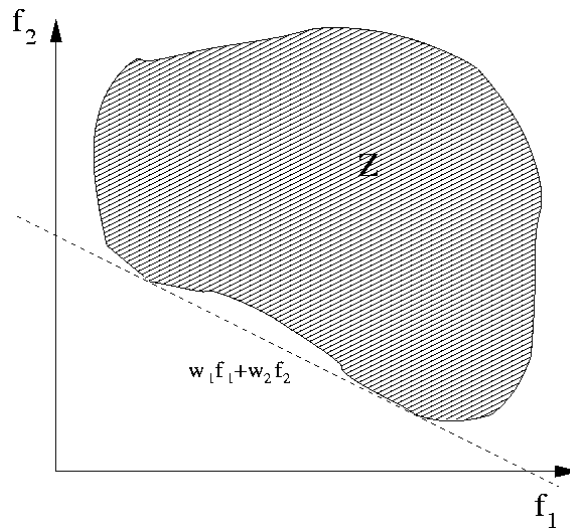


Figure 3.4: An example of weighting method with a nonconvex problem.

In the weighting method, the decision maker specifies a weighting coefficients representing her/his preference information beforehand (an a priori method). The weighting method can be used also as an a posteriori method where the decision maker selects the most preferred solution out of all the generated alternatives. Here, we use it as an a priori method, and thus, we minimize the weighted sum of the objectives obtaining only one solution to be the final version. This method can also be extended into an interactive form by letting the decision maker modify the weighting coefficients after each iteration. The drawback is that weights are not so intuitive and they can be even misleading. Thus, it can be time consuming and difficult to obtain a satisfying solution. A notable point is that the objective functions should be normalized or scaled so that their objective values are approximately of the same magnitude. This is done in order to produce solutions which have desirable ranges of the objective functions [95].

3.2.3 Multiobjective evolutionary algorithms

The term evolutionary algorithm (EA) stands for a class of stochastic optimization methods that simulate the process of natural evolution. Multiobjective evolutionary algorithms (MOEA) are often well-suited for demanding optimization problems involving conflicting objectives because they can handle nonconvex and nondifferentiable problems [12, 20, 163]. An EA is a generic population-based meta-heuristic global optimization algorithm, and its principle is described in Figure 3.5. An EA uses several mechanisms inspired by biological evolution: reproduction, mutation, recombination, and natural selection. Solution candidates of the optimization problem play the role of individuals in a population, and the fitness function determines the way in which the goodness of the solutions are evaluated. In MOEAs, a typical fitness function assignment strategy is based on Pareto dominance, see for example [20]. It is common that MOEAs generate a large set of solutions approximating to Pareto optimal solutions for many types of problems because they do not make any assumption about the underlying fitness landscape: this generality is shown by their successes in fields as diverse as engineering, biology, physics and operations research, see for example [12]. Genetic algorithms are a particular class of evolutionary algorithms.

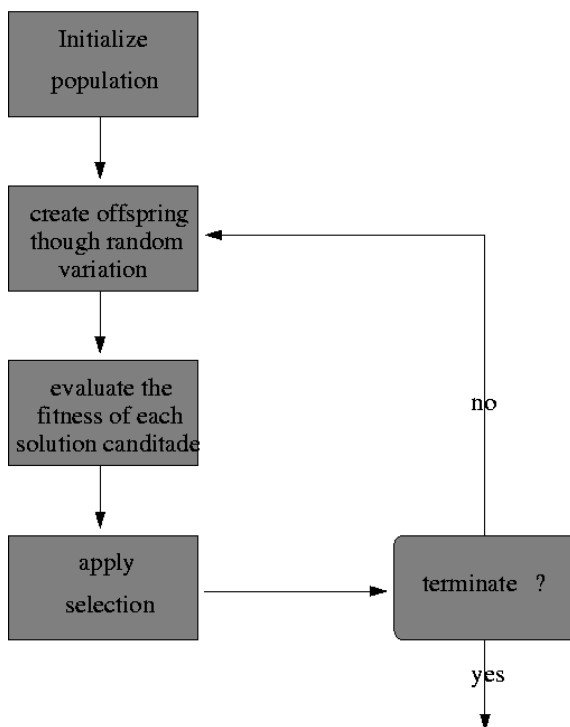


Figure 3.5: Principle of evolutionary algorithms.

From the decision making point of view, MOEAs belong to the class of a posteriori methods. In other words, a large set of solutions approximating to Pareto optimal solutions are calculated beforehand, and the decision making process is executed subsequently. However, Pareto optimality of the solutions obtained cannot be guaranteed. Since one may have a large set of solutions approximating to a Pareto optimal front, it is sometimes difficult to compare and visualize the solutions obtained with a MOEA. This is an issue especially when there are more than two objectives in the problem. Generating many solutions for the decision maker to compare can also be computationally costly.

In this thesis, no particular MOEA is introduced because they are used as black-box solvers solving the multiobjective optimization problems formed. In other words, any MOEA could be used in the examples presented in this thesis.

After presenting the necessary basic concepts of MCDM and multiobjective optimization, the next chapter will describe some new ideas for supporting MCDM and interactive multiobjective optimization.

New approaches for supporting MCDM

In this chapter, some new ideas for MCDM and multiobjective optimization are suggested. Section 4.1 includes new ideas for navigating on a Pareto optimal front, and Section 4.2 involves a novel visualization tool for viewing multiple dimensional Pareto optimal solutions and thus supporting the decision maker in decision making.

4.1 Navigation on a Pareto optimal front utilizing gradient information

This section provides some preliminary ideas on how gradient (i.e. derivative) information can be used to assist solution processes and navigation through a Pareto optimal front in multiobjective optimization in different ways. First, a computationally efficient meta-model for approximating a Pareto optimal front can be produced using the gradient information. With the approximated Pareto optimal front, behavior of the Pareto optimal solutions can be predicted in a certain area, which can be useful information in decision making. This kind of meta-modeling is computationally light since in many cases it is essential that gradients are calculated (e.g. in gradient-based optimization solvers). Here, we utilize the existing gradient information more thoroughly to assist the decision making process, and thus these kinds of ideas are welcome. Similar ideas of approximating Pareto optimal fronts have been presented also in the literature [60, 139, 140, 141].

Second, gradient information can be employed during an interactive solution process to generate so-called trade-off information. Here, a decision maker utilizes the trade-off information to predict the most profitable direction in which to seek the best Pareto optimal solution. In other words, when one target is being improved, how can one maintain reasonable levels as the other targets. The concept of the trade-off is used in the context of multiobjective optimization because the Pareto optimal solutions of the conflicting targets are mathematically incomparable and one has to make a sacrifice in some objective in order to gain in some other objective, and this is called trading-off [11]. In other words, this kind of

trade-off information describes interdependencies between objective functions and how their values change locally with respect to the other functions. Furthermore, we want to present the trade-off information to the decision maker as clearly as possible so that interpreting and utilizing this data becomes easier and the desired solution is straightforward to choose. The concept of trade-off has been widely discussed in the literature, see e.g. [32, 33, 34, 38, 48, 57, 58, 67, 108, 155, 156], but here the emphasis is placed on the decision making process with the trade-off information such as in [39].

The support provided by gradient information is extremely useful especially when the evaluation of objectives requires solving of computationally costly mathematical models (assuming that the gradients can be calculated in a reliable way by using finite differences or analytically). That is the case in engineering problems, see e.g. [44], in which it is important to reduce the number of trial-and-error computations to be made.

4.1.1 Approximating Pareto optimal fronts

Here, we produce a meta-model for approximating a Pareto optimal front using the gradient information, and, with this approximation, the behavior of the Pareto optimal solutions can be predicted in the neighborhood of Pareto optimal points.

In this thesis, Taylor's formula has been utilized to find a successive approximation to a Pareto optimal front. Taylor's formula expresses a function as an infinite sum of terms calculated from the values of its derivatives at a single point.

Definition 4.1.1 Taylor's formula in the neighborhood of \mathbf{x} (a polynomial approximation and an error (remainder) term) can be written as

$$\mathbf{f}(\mathbf{x} + \mathbf{h}) = \sum_{l=0}^p \frac{1}{l!} \frac{\partial^l \mathbf{f}(\mathbf{x})}{\partial \mathbf{x}^l} \mathbf{h}^l + \frac{1}{(p+1)!} \frac{\partial^{p+1} \mathbf{f}(\xi)}{\partial \mathbf{x}^{p+1}} \mathbf{h}^{p+1},$$

where $p \in \mathbb{N}$ and $\frac{\partial^l \mathbf{f}}{\partial \mathbf{x}^l}$ denotes l order of derivatives, \mathbf{h} describes a small step from point \mathbf{x} , and ξ is a point in the neighborhood of \mathbf{x} [115].

In Taylor's formula, the first term (expressed as a sum) gives a polynomial approximation of function \mathbf{f} in the neighborhood of point \mathbf{x} , and its accuracy can be estimated with the second term even if the point ξ is unknown.

Using Taylor's formula, a polynomial approximation of function \mathbf{f}

$$\mathbf{P}(\mathbf{x} + \mathbf{h}) = \sum_{l=0}^p \frac{1}{l!} \frac{\partial^l \mathbf{f}(\mathbf{x})}{\partial \mathbf{x}^l} \mathbf{h}^l, \quad (4.1)$$

is a Taylor's polynomial of a function \mathbf{f} in point $\mathbf{x} + \mathbf{h} \in \mathbb{R}^n$. Using Equation (4.1), an approximation of a Pareto optimal front can be formed (see, e.g. Figure 4.1). In the Figure 4.1, different order ($p = 0, \dots, 3$) polynomial approximations of a Pareto optimal front based on Taylor's polynomial are presented. Polynomial

$\mathbf{P}(\mathbf{x} + \mathbf{h})$ of degree p describes a Pareto optimal front better than any other polynomial of degree p . In addition, the approximation is more exact when p becomes larger.

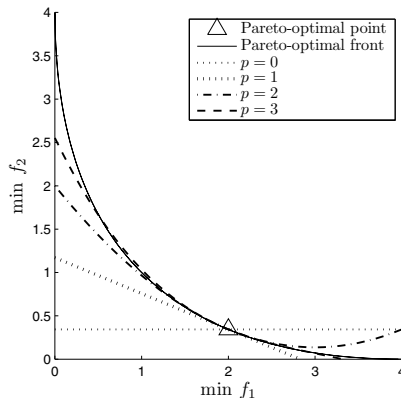


Figure 4.1: Approximations of a Pareto optimal front based on Taylor's polynomial for a multiobjective optimization problem formulated in [127].

If we have derivative information of a high degree p , it is possible to find a Taylor's polynomial approximation to a Pareto optimal front. Nevertheless, in practice (in real world problems), we usually have only first order of derivatives ($p = 1$), and thus the approximation is not accurate globally though it does provide information about local changes. Then, the Taylor's polynomial can be written in the form

$$\mathbf{P}(\mathbf{x} + \mathbf{h}) = \mathbf{f}(\mathbf{x}) + J_f(\mathbf{x})\mathbf{h}, \quad (4.2)$$

where J_f denotes a Jacobian matrix, i.e. $\frac{\partial^1 \mathbf{f}}{\partial \mathbf{x}^1}$. In the following section, it will be assumed that only first order of derivatives are available.

Based on the presented first order linear Taylor's polynomial approximation (4.2), new points (approximating Pareto optimal points) can be generated to the neighborhood of the Pareto optimal point without solving the original problem. *The principle is that a polynomial approximation of the Pareto optimal front can be fitted based on the Pareto optimal points and the approximated Pareto optimal points generated by using the first order linear Taylor's polynomial approximation.* In a bi-objective case, at least two Pareto optimal points and two approximated Pareto optimal points between these points are needed, and, in three dimensions, at least three Pareto optimal points and six approximated points between these points are needed in order to form the polynomial approximation. This approach can be realized as a global algorithm in which the Pareto optimal front is approximated globally, or as a local algorithm in which the Pareto optimal front is approximated

only between Pareto optimal points. In addition, when using this approach, the Pareto optimal front should not be non-connected.

In the algorithms, approximated Pareto optimal points are first calculated by using the Taylor's polynomial, and subsequently, a proper polynomial approximation of a Pareto optimal front is fitted to the Pareto optimal points and the approximated Pareto optimal points. Thus, two algorithms can be written:

Algorithm 4.1.1 (local) *Let PP be a set of Pareto optimal points in objective space and let M be number of these points. Let AP_i for all $i = 1, \dots, M$ be a set of approximated Pareto optimal points generated with the algorithm. Assume that $M \geq k$.*

1. Set $AP_i = \phi$ for all $i = 1, \dots, M$.
2. Let $i = 1$.

Do for $\mathbf{z}_i \in PP$ (\mathbf{x}_i corresponds to \mathbf{z}_i).

- (a) Select $k-1$ nearest points (based on e.g. Euclidean norm) from $PP \setminus \{\mathbf{z}_i\}$ and define a set $\widehat{PP}_i = \{\mathbf{z}_1, \dots, \mathbf{z}_{k-1}, \mathbf{z}_k\}$, where \mathbf{z}_j , $j = 1, \dots, k-1$, are $k-1$ nearest points, and $\mathbf{z}_k = \mathbf{z}_i$.
- (b) Check if there exists another set \widehat{PP}_j such that $\widehat{PP}_i = \widehat{PP}_j$ for some $j = 1, \dots, i-1$, then $\widehat{PP}_i = \phi$ and go to (d).
- (c) Calculate using Taylor's polynomial approximation (4.2) new points as follows:

Do for each $\mathbf{z}_j \in \widehat{PP}_i$ while $j = 1, \dots, k$

Do $l = 1, \dots, k-1$

$$\mathbf{z}_{j,l}^{AP} = \mathbf{P}(\mathbf{x}_j + \mathbf{h}) = \mathbf{f}(\mathbf{x}_j) + J_f(\mathbf{x}_j)\mathbf{h} = \mathbf{z}_j + J_f(\mathbf{x}_j)\mathbf{h},$$

where $\mathbf{h} = \frac{\mathbf{x}_l - \mathbf{x}_j}{\max(C_1, C_2 a)}$, and C_1, C_2 are constants, $a = \|\mathbf{z}_l - \mathbf{z}_j\|$

and \mathbf{z}_l is the l th point in $\widehat{PP}_i \setminus \{\mathbf{z}_j\}$.

End Do

Add the approximated points $\mathbf{z}_{j,l}^{AP}$ into AP_i for all $l = 1, \dots, k-1$.

End Do

- (d) Set $i = i + 1$.

End do

3. For each $i = 1, \dots, M$, fit a proper polynomial approximation for a Pareto optimal front using $AP_i \cup \widehat{PP}_i$.
4. Visualize the approximations obtained to the decision maker. If the decision maker is satisfied with the approximation, then exit.
5. Calculate a new Pareto optimal solution with a multiobjective optimization solver and add it in PP , update $M = M + 1$, $i=1$ and continue from 2.

Algorithm 4.1.2 (global) Let PP be a set of Pareto optimal points in objective space, and let M be number of these points. Let AP_i for all $i = 1, \dots, M$ be a set of approximated Pareto optimal points generated with the algorithm. Assume that $M \geq k$.

1. Set $AP_i = \phi$ for all $i = 1, \dots, M$.

2. Let $i = 1$.

Do for each $\mathbf{z} \in PP$ (\mathbf{x} corresponds to \mathbf{z}).

(a) Select $k - 1$ nearest points (e.g. Euclidean norm) from $PP \setminus \{\mathbf{z}\}$ and define a set $\widehat{PP}_i = \{\mathbf{z}_1, \dots, \mathbf{z}_{k-1}\}$, where \mathbf{z}_j , $j = 1, \dots, k - 1$, are $k - 1$ nearest points.

(b) Calculate using Taylor's polynomial approximation (4.2) new points as follows:

Calculate new point:

Do $l = 1, \dots, k - 1$

$$\mathbf{z}_l^{AP} = \mathbf{P}(\mathbf{x} + \mathbf{h}) = \mathbf{f}(\mathbf{x}) + J_f(\mathbf{x})\mathbf{h} = \mathbf{z} + J_f(\mathbf{x})\mathbf{h},$$

where $\mathbf{h} = \frac{\mathbf{x}_l - \mathbf{x}}{\max(C_1, C_2 a)}$, where \mathbf{x}_l is the l th point in \widehat{PP}_i and

C_1, C_2 are constants, and $a = \|\mathbf{z}_l - \mathbf{z}\|$.

End Do

Add these points $\{\mathbf{z}_1^{AP}, \dots, \mathbf{z}_{k-1}^{AP}\}$ into AP_i .

(c) Set $i = i + 1$

End Do

3. Fit a proper polynomial approximation for a Pareto optimal front using $(\cup_{i=1}^M AP_i) \cup PP$.

4. Visualize the approximations obtained to the decision maker. If the decision maker is satisfied with the approximation, then exit.

5. Calculate a new Pareto optimal solution with a multiobjective optimization solver and add it in PP , update $M = M + 1$, and continue from 2.

Remark Parameter C_1 is needed in such case where $C_2 a \rightarrow 0$. The parameter could be $C_1 = 10^{-6}$, for example. Parameter C_2 can be understood as a case specific weighting factor of parameter a , or it could be 1.

Remark Note that approximated Pareto optimal points \mathbf{z}^{AP} can be dominated by other(s).

Examples of using these algorithms are presented in this thesis. Algorithm 4.1.1 is used in Section 4.1.3 in order to form a local piece-wise polynomial approximation of a Pareto optimal front, and Algorithm 4.1.2 is used in Section 5.4.2 to approximate a Pareto optimal front globally.

For nonlinear problems, the first order Taylor's polynomial is an accurate approximation only in some finite neighborhood of the current solution. In that sense, a fitted approximation of the Pareto optimal front based on only a few Pareto optimal points (and a few approximated points) can even be misleading in some cases; if the Pareto optimal points are not closely-spaced, the approximation between these points may not be accurate. However, a skillful decision maker can obtain more information from the approximation than only from the Pareto optimal points, and naturally the fitted nonlinear approximation of the Pareto optimal front becomes more accurate when the number of Pareto optimal points calculated increases. The next important step in developing this concept is to add an error estimate for the approximated front.

4.1.2 Utilizing trade-off information

DEFINITION OF TRADE-OFF

Definition 4.1.2 The *ratio of change* between points \mathbf{x} and \mathbf{x}^* involving objective functions f_i and f_j is

$$T_{ij}(\mathbf{x}, \mathbf{x}^*) = \frac{f_i(\mathbf{x}) - f_i(\mathbf{x}^*)}{f_j(\mathbf{x}) - f_j(\mathbf{x}^*)}, \quad \mathbf{x}, \mathbf{x}^* \in S,$$

where $f_j(\mathbf{x}) \neq f_j(\mathbf{x}^*)$ [38].

Definition 4.1.3 If $f_l(\mathbf{x}) = f_l(\mathbf{x}^*)$ for all $l \neq i, j$, $l = 1, \dots, k$, then T_{ij} is called *partial trade-off* between vectors \mathbf{x} and \mathbf{x}^* .

If $f_l(\mathbf{x}) \neq f_l(\mathbf{x}^*)$ for at least one $l \neq i, j$, $l = 1, \dots, k$, then T_{ij} is called *total trade-off*.

Using the ratio of change $T_{ij}(\mathbf{x}, \mathbf{x}^*)$ we can define total trade-off rate at the point $\mathbf{x} \in \mathbb{R}^n$ to direction $\mathbf{d} \in \mathbb{R}^n$. Let $\mathbf{x} \in S$ be a decision vector and let $\mathbf{d} \neq 0 \in \mathbb{R}^n$ be a feasible direction emanating from \mathbf{x} .

Definition 4.1.4 The *total trade-off rate* at \mathbf{x} , involving f_i and f_j along the direction \mathbf{d} , is $t_{ij}(\mathbf{x}, \mathbf{d}) = \lim_{\alpha \rightarrow 0^+} T_{ij}(\mathbf{x} + \alpha \mathbf{d}, \mathbf{x})$ [38].

There exists $\alpha_0 > 0$ such that $\mathbf{x} + \alpha \mathbf{d} \in S$ for all $\alpha \in [0, \alpha_0]$. If \mathbf{d} is a feasible direction such that there exists $\bar{\alpha} > 0$ satisfying $f_l(\mathbf{x} + \alpha \mathbf{d}) = f_l(\mathbf{x})$ for all $l \neq i, j$, $l = 1, \dots, k$, and for all $0 \leq \alpha \leq \bar{\alpha}$, then the corresponding t_{ij} is called a *partial trade-off rate*.

In a continuously differentiable case, the total trade-off rate and the partial trade-off rate can be formulated as follows [95]

Definition 4.1.5 The total trade-off rate can be formulated as (in a continuously differentiable case)

$$t_{ij}(\mathbf{x}, \mathbf{d}) = \frac{\nabla f_i(\mathbf{x})^T \mathbf{d}}{\nabla f_j(\mathbf{x})^T \mathbf{d}},$$

where $\nabla f_j(\mathbf{x})^T \mathbf{d} \neq 0$.

Definition 4.1.6 The partial trade-off rate can be formulated as (in a continuously differentiable case)

$$t_{ij}(\mathbf{x}) = \frac{\partial f_i(\mathbf{x})}{\partial f_j},$$

where $\partial f_j \neq 0$.

Figure 4.2 shows the concept of trade-off in the bi-objective function case in the objective space. In the figure, the set $Z = \mathbf{f}(S)$ denotes the image of the feasible set. The trade-off rate related to the objective vector \mathbf{z}^* is shown by an arrow. This means that if we want to improve the objective f_2 by an amount Δf_2 , we can approximate the impairment of objective f_1 by Δf_1 . As can be seen in Figure 4.2, the trade-off rate in a point is exact, but outside the point in question it is a linear approximation and, thus, can only be used in some finite neighborhood of the point being considered.

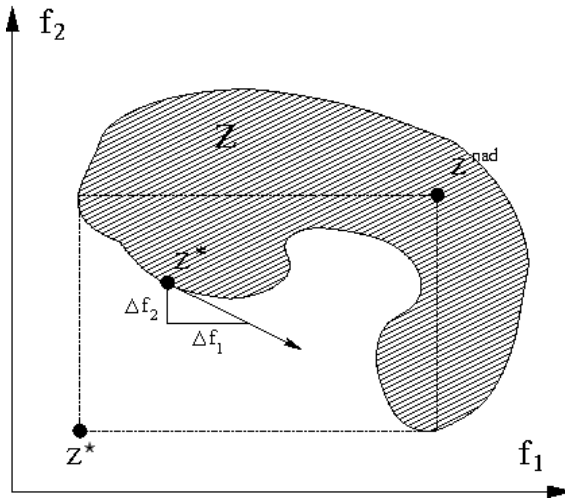


Figure 4.2: An illustrated trade-off for two objectives.

In this thesis, we consider only trade-off rates and by trade-off information we mean trade-off rates. In addition, we are interested in trade-off rates only at Pareto optimal points. Thus, in the above presented trade-off definitions, a feasible set S is replaced by the Pareto optimal set E_{PO} .

Definition 4.1.7 At every point $\mathbf{x} \in E_{PO}$, the total trade-off rate matrix can be formulated as

$$M_{PO}(\mathbf{x}, \mathbf{d}) = \begin{bmatrix} t_{11}(\mathbf{x}, \mathbf{d}) & \dots & t_{k1}(\mathbf{x}, \mathbf{d}) \\ \vdots & \ddots & \vdots \\ t_{1k}(\mathbf{x}, \mathbf{d}) & \dots & t_{kk}(\mathbf{x}, \mathbf{d}) \end{bmatrix}.$$

The trade-off matrix $M_{PO}(\mathbf{x}, \mathbf{d})$ reflects sensitivities between objectives when we are moving in the direction \mathbf{d} from the point \mathbf{x} . A similar matrix $M_{PO}(\mathbf{x})$ can be defined also for partial trade-off rates.

With partial trade-offs, it is possible to study how one objective becomes impaired if we want to improve one other objective by one unit, and other objectives stay unchanged at the same time. In the case of a total trade-off, we can consider how all other objectives change if we improve one objective by one unit. When we have only two objectives, the total and partial trade-off rates are naturally the same. Computing the trade-off rates is presented in [39], for example.

USING TRADE-OFF INFORMATION TO CONTROL THE OPTIMIZATION PROCESS

Trade-off information has been traditionally used as a part of a multiobjective optimization method, see [11], for example. The approach used here concentrates on utilizing the trade-off information as an aid that supports decisions in a similar manner to [32, 34]. In other words, the intention is to produce additional value to the multiobjective optimization method used to ease the decision making. It is possible to use the trade-off information idea in many interactive multiobjective optimization methods such as classification-based methods and reference point methods [39], where the preference information given by the decision maker is needed in specifying a reference point or classifying the objective functions in different classes. The intention is to support the decision maker in the selection of the next reference point or making the next classification. As a consequence, the number of iterations can be reduced. Thus, the whole interactive solution process can be shortened, which saves time of the decision maker and reduces the number of Pareto optimal solutions needed to be calculated.

For nonlinear problems such as those examined in this thesis, the trade-off rate matrix values are often accurate enough approximations only in some finite neighborhood of the current solution. In this sense, it might be misleading to show the trade-off rate matrix to the decision maker who does not appreciate the problem. The proper neighborhood is problem specific and sometimes difficult to characterize. That is why the decision maker has to be a skillful expert in his/her field and to understand the interpretation of the matrix to use the trade-off information.

In this thesis, two different ways to present the trade-off information to the decision maker are proposed. The straightforward approach is to show the numerical trade-off rate information from the trade-off matrix. Another way to present

the trade-off rates to the decision maker is to make some simplifications to the numerical trade-off rate information presented. The reason is because sometimes it might be sufficient for the decision maker simply to appreciate whether the trade-off between the objectives is below, equal or above a neutral rate of change. In such a case, the so-called arrow matrix visualization and visual compromise bars proposed in [39] can be used.

4.1.3 Example

Similar ideas for presenting information and supporting the decision making process have been used with a reference point method [39]. Therefore, we tested these ideas along with the classification based method. In order to demonstrate the ideas, the example presented in [127] will be considered in which there are two conflicting objective functions ($f_1 : \mathbf{R} \rightarrow \mathbf{R}$ and $f_2 : \mathbf{R} \rightarrow \mathbf{R}$) to be minimized at the same time:

$$f_1(x) = x^2 \quad (4.3)$$

and

$$f_2(x) = (x - 2)^2. \quad (4.4)$$

The problem is as follows

$$\begin{aligned} & \text{minimize} && \{f_1(x), f_2(x)\} \\ & \text{subject to} && -10^5 \leq x \leq 10^5. \end{aligned} \quad (4.5)$$

We want to present useful information to the decision maker as much as possible to support the decision-making procedure with a minimal computational effort. Using an interactive classification-based optimization method, after every classification a new Pareto optimal solution is computed, and assuming that gradient information can be utilized, an approximating Pareto optimal front and computing the trade-off rate matrix can be done as follows.

Using the Algorithm 4.1.1 (local), an approximation of a Pareto optimal front is generated during the iterative solution process. First, two Pareto optimal solutions with the interactive multiobjective optimization method are calculated: the decision maker wants to obtain two different kinds of solutions, and thus he has to make two different classifications. Firstly preference may be given to objective function f_1 and secondly to objective function f_2 . Two different kind of solutions are obtained (Figure 4.3 on the upper-left, triangle markers). Using Taylor's polynomial with first order derivatives, a linear approximation of the Pareto optimal front in the neighborhood of the Pareto optimal points is made. With this approximation, two approximating Pareto optimal points are calculated between the real Pareto optimal points (circle markers in Figure 4.3 on the upper-left. Next, the decision maker has four points (two real Pareto optimal points and two approximated), and a nonlinear second order polynomial approximation of the Pareto optimal front can be made to these four points using the least square method (Figure 4.3 on the upper-left). For comparison, there is a linear approximation

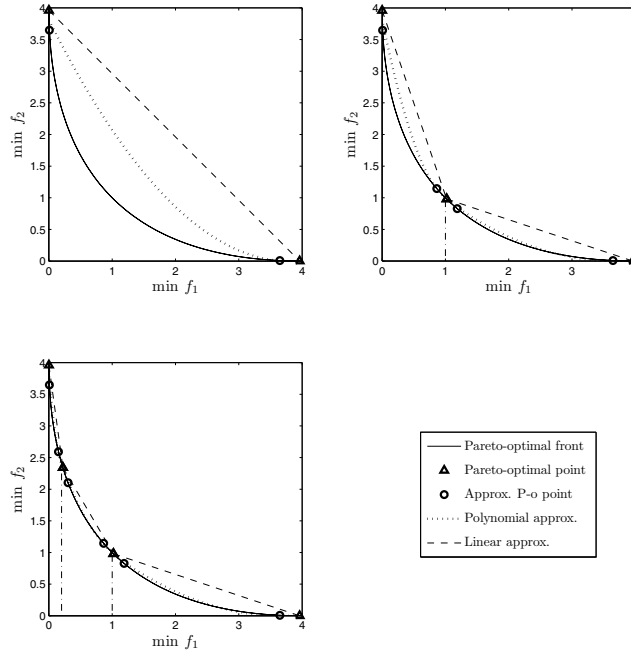


Figure 4.3: A piece-wise nonlinear approximation of a Pareto optimal front based on gradient information for two objectives.

between these two Pareto optimal points presented in the same figure (dash line). The optimization process is iterative: now a new Pareto optimal point between the existing ones can be calculated, and a new Taylor's polynomial approximation of the Pareto optimal front in the neighborhood of this new point can be estimated. Using this Taylor's polynomial approximation, new Pareto optimal points are estimated. Now, the decision maker is able to generate two local separate second order polynomial approximations of the Pareto optimal fronts in both sides of the new Pareto optimal point (Figure 4.3 on the upper-right). In this way, it is possible to obtain a local piece-wise nonlinear approximation of the Pareto optimal front the accuracy of which naturally increases when the number of Pareto optimal points increases (Figure 4.3 on the lower-left, with four Pareto optimal points). In this way, by following the Algorithm 4.1.1, the Pareto optimal points and their gradient information can be utilized in forming an approximation of the Pareto optimal front by computing less Pareto optimal points with the real model (e.g. this can be computationally costly). Even if the approximation gives no error estimate, it

provides more information to the decision maker than if only the Pareto optimal points had been calculated.

In addition, based on the gradients calculated, the trade-off rate matrix is formed. In Table 4.1, there is an example of the trade-off rate information obtained

Table 4.1: Matrix of total trade-off rates in the Pareto optimal point presented in Figure 4.1.

	f_1	f_2
f_1	1	-0.414
f_2	-2.414	1

in the Pareto optimal point presented in Figure 4.1. This information is shown to the decision maker after every iteration (i.e. in each Pareto optimal point). To avoid imposing an information burden on the decision maker, the information presented is reduced by using an arrow matrix visualization as discussed in the previous section. In Figure 4.4, an example of an arrow matrix visualization and

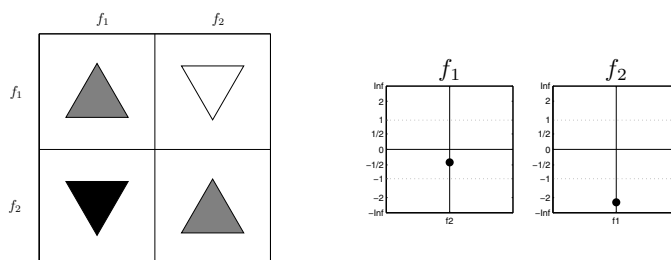


Figure 4.4: Visual rate of change arrows and visual compromise bars for two objectives.

visual compromise bars including the trade-off rates is presented. In this example, threshold values used in the rate of change arrows are as follows: white color represents a small change in objective values (rate of change is from -0.5 to 0.5), and light gray is a neutral change (rate of change is from -2 to -0.5 or from 0.5 to 2). In addition, a significant change is expressed with black color (rate of change less than -2 or more than 2). If the arrow points up, the objective improves, and if the arrow points down, then the objective is impaired. In this particular Pareto optimal point, one can see that if both objectives are equally important to the decision maker, it could be profitable to try to improve f_1 because f_2 impairs only slightly at the same time. Instead, if the decision maker tries to improve f_2 , this will worsen f_1 significantly.

If this information is presented to the decision maker, then the optimization process could be made more efficient and the decision maker could better understand the interrelationships between targets without the numerical burden. Therefore, less Pareto optimal solutions are needed to be computed, and thus solving the optimization problem is shown to be easier and faster.

4.2 Novel visualization technique: virtual reality

As already introduced, the solutions of the multiobjective optimization problem form a Pareto optimal front from where an individual solution can be chosen by the decision maker as the final solution. A Pareto optimal front is often studied with different visualization tools, because in this way comparison between solutions is more illustrative. A Pareto optimal front is easy to visualize when there are only two targets, i.e. objective functions. However, visualizing with more than two objectives has so far been problematic and few attempts have been made to visualize a Pareto optimal front in greater than two dimensions, see [82, 83, 84, 85]. To overcome this shortcoming, we present a new way to support the multiobjective decision making process: visualizing Pareto optimal solutions or a Pareto optimal front with three-dimensional (3D) virtual reality (VR). Our approach utilizes some of Lotov's ideas for presenting objectives in two-dimensional (2D) decision maps [85] (e.g. with colors), but we visualize a Pareto optimal front (decision map) in 3D with VR.

VR is a computer created environment which can be used for visualizing 3D objects (see [29, 130, 148], for example, and references therein). Hence it makes possible to compare solutions which are on a 3D Pareto optimal front. A visualized 3D Pareto optimal front can be examined in many ways: it can be zoomed, rotated, and the decision maker can delve into it. This makes it easier to compare solutions, and learn about the problem and the target's interrelationships, thus, making it easier to identify which solution is the best to choose as the final one. The VR approach has been suggested in multiobjective optimization framework in [148, 149] but in this thesis it is proposed that the VR environment should be used not only to visualize a higher dimensional Pareto optimal front, but also to analyze and understand the nature and relative location of solutions in order to help the decision maker to select the best solution for the particular problem.

Different kinds of 3D visualizations can be done in different cases. First, in evolutionary algorithm-cases, where a large number of solutions form a dense set of non-dominated solutions, the Pareto optimal front obtained can be visualized (see, section 4.2.3). Secondly, if only a few Pareto optimal solutions are obtained, with a reference point approach for example, they can be visualized as 3D points in a virtual reality environment (see, section 5.4.3). In the third case, an approximation of a Pareto optimal front can also be formed with only a few Pareto optimal solutions (see, Appendix B). In this case, after the decision maker has made the final decision about which of the approximated solutions is the most desired, the real model can be used to revise the accuracy of the approximation. In this thesis, examples of these visualizations are presented, and the benefits of employing a

virtual reality as a decision support tool are discussed. In addition, there are some future extensions and ideas considered.

4.2.1 Virtual Reality

VR is often described as a computer-based virtual world [130]. It allows a user to interact with a computer-simulated environment, and produces a physically immersive effect. Most virtual environments give only a visual experience, but more immersive environments can be built by adding sound or haptic elements. Virtual environments can be controlled through a mouse or a 3D pointing device called a wand. Virtual realities have been used since the 1990's, when the first virtual environment called Cave was built in 1992 [18]. The first room-type of environment, the six wall Cave, was built in the Royal Institute of Technology in Stockholm in 1998, and the first one in North America was installed at Iowa State University in 2000 [130].

According to [130], virtual reality consists of four key elements:

- virtual world,
- immersion,
- sensory feedback, and
- interactivity.

A *virtual world* means an imaginary space manifested through a medium and a collection of objects in the space, and the rules and relationships governing those objects. *Immersion* can be defined as the experience of being in an alternative reality, based on mental immersion, i.e. a sense of presence, and physical immersion. To create a good immersion experience, the system must have another key element, *sensory feedback*, based on the user's physical position. Thus, objects in a virtual world alter depending on the user's position giving her/him the most realistic visual experience. In addition to the visual experience, *interactivity* provides other ways in which the environment responds to the user's actions so that the user can affect the computer-based world.

There are many applications that can utilize VR technology: visualizing scientific results, interior design in architecture, and prototype testing in industry [3, 56], for example.

4.2.2 Integration of multiobjective optimization and virtual reality

Integration of multiobjective optimization and VR requires some kind of software for calculating Pareto optimal solutions and hardware for the VR environment as well as software for visualization in stereo [130]. This thesis presents several examples where different optimization methods have been used to calculate a number of Pareto optimal solutions. The virtual reality system in use has been built in the University of Kuopio, Finland, and it is based on OpenDX visualization software. Graphics Computer SGI Prism with 8 CPUs (à 64-bit 1.5 GHz Intel Itanium 2,

24 GB memory, 48 Gflops) was used with SuSe Linux Enterprise Server 9.3 as an operating system. 3D effects were generated through wireless set of liquid crystal shutter eye wear (stereo glasses). The stereo glasses shut alternately left and right eye view with frequency about 45 pictures per eye per second. Visualized 3D objects (in this thesis, Pareto optimal fronts) were controlled through a wand. Polhemus equipment was used to follow the user's movements and to generate an authentic view of the object based on user's location.

Visualization in stereo can be executed also in a modest way with a personal computer. When using a personal computer to visualize the stereo effect, the stereoscopic viewing can be performed on monitors supporting a vertical refresh rate of 100 Hz or more, to avoid noticeable flicker. Stereoscopic viewing with page flipping requires a CRT monitor. Due to the high refresh frequency rate, stereoscopic viewing in a page-flipping mode is not possible with a normal LCD flat panel. In addition, a stereo-ready graphic card with a stereo connector (e.g. 3-pin mini-DIN) is needed. With the stereo ready graphic card, left and right eye views are synchronized (with a frequency of about 45 pictures per eye per second). Visualizing in stereo requires considerable computation power for the graphic card. GPU (graphics processing unit) manufactures provide special graphic cards for this purpose. For example ATI has manufactured FireGL graphic card models and also NVIDIA has a type of Quadro FX graphic card which have been designed to be used in heavy 3D visualizations such as stereoscopic viewing and 3D modeling purposes (e.g. CAD and DCC modeling). Moreover, stereo spectacles and an emitter, which transmits a synchronization signal for the stereo glasses, are required for stereoscopic viewing with a personal computer.

Visualizing in stereo with a personal computer will make it possible for the 3D visualizations of this kind to become more common because there are no major start up costs (no need for a laboratory). Stereoscopic viewing with a personal computer is in use for example in engineering and medicine, but it has unused potential also in computational and decision sciences. However, when using a personal computer in stereoscopic viewing, one has to immerse oneself in the VR and other key elements of VR are not that animated, and furthermore only a few people can examine the visualized object at the same time because of the small display screen.

Figure 4.5 shows users utilizing the VR in order to examine an approximated Pareto optimal front. Here, the users can study the relationships between objectives and then obtain ideas of what kind of compromises between multiple optimization targets can be made, and based on that, the final solution can be selected or new solutions can be computed with better preference information. In Figure 4.5, the front is controlled (zoomed, rotated and scaled) by a user using a wand.

Remark One should note that figures of 3D Pareto optimal fronts visualized in the virtual reality are presented as 2D figures in this thesis. This is because the realistic immersion can only be experienced in laboratory, not by looking at the figures on a flat page.

4.2.3 Example

In this section, we present an example illustrating the new visualizing benefits which a VR facility can offer. In this example, Pareto optimal points of a standard three-objective test problem DTLZ6 [26] having a disconnected set of nonlinear Pareto optimal fronts were produced by MOEA NSGA-II [20], which is capable of finding a large set of trade-off solutions as presented in the example.

In the general form of this problem, there are k objective functions with a complete decision variable vector partitioned in k non-overlapping groups $\mathbf{x} \equiv (\mathbf{x}_1, \dots, \mathbf{x}_k)^T$. We solved a three-objective version of the problem that is written as follows:

$$\begin{aligned} & \text{minimize} && \{f_1(\mathbf{x}), f_2(\mathbf{x}), f_3(\mathbf{x})\} \\ & \text{subject to} && 0 \leq x_i \leq 1 \text{ for } i = 1, \dots, 22, \end{aligned} \quad (4.6)$$

where the objective functions were defined as

$$\begin{aligned} \mathbf{f}_1(\mathbf{x}_1) &= x_1, \\ \mathbf{f}_2(\mathbf{x}_2) &= x_2, \\ \mathbf{f}_3(\mathbf{x}) &= (1 + g(\mathbf{x}_3))h(f_1, f_2, g), \end{aligned}$$

and the functionals were

$$\begin{aligned} g(\mathbf{x}_3) &= 1 + \frac{9}{|\mathbf{x}_3|} \sum_{x_i \in \mathbf{x}_3} x_i, \\ h(f_1, f_2, g) &= 3 - \sum_{i=1}^2 \left[\frac{f_i}{1+g} (1 + \sin(3\pi f_i)) \right]. \end{aligned}$$

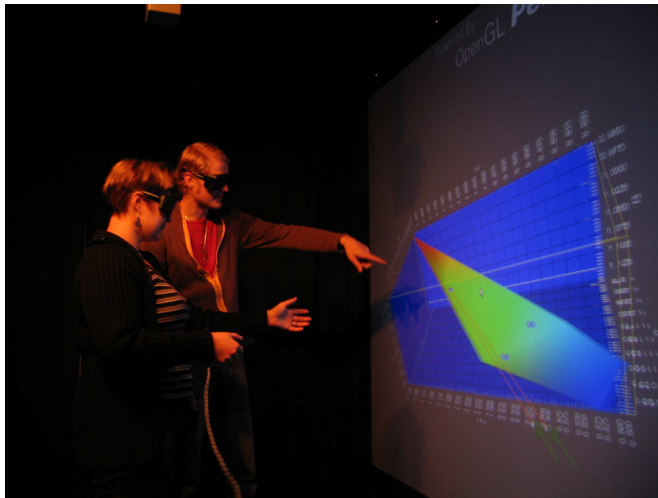


Figure 4.5: Analyzing a Pareto optimal front with the 3D virtual reality.

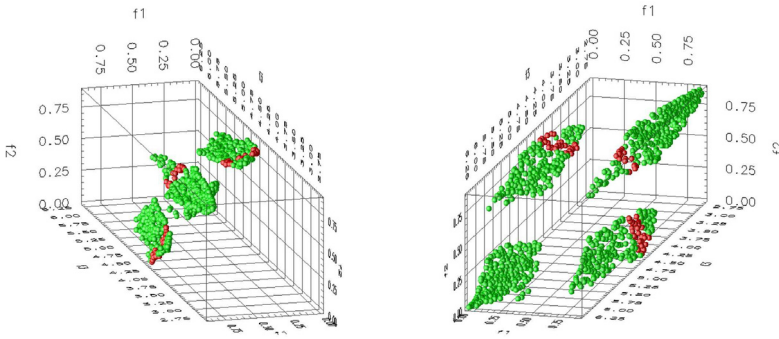


Figure 4.6: Disconnected set of nonlinear Pareto optimal regions (forming the Pareto optimal front) in evolutionary computation example (DTLZ6) in a VR environment. Solutions having $4.2 \leq f_3 \leq 4.4$ are colored red.

The functional $g(\mathbf{x}_3)$ required $|\mathbf{x}_3| = 20$ variables and n was the total number of variables, here $n = 22$. In this test problem, there were $2^2 = 4$ disconnected Pareto optimal regions.

The NSGA-II procedure was run with 1,000 population members. The final solutions were visualized with the proposed VR system and they are shown also in Figure 4.6. With the 3D visualization capabilities, the nonlinear feature of the disconnected Pareto optimal regions was much easier to see in comparison to earlier studies [26]. In this example, the decision maker was first interested in seeing all the solutions in which $4.2 \leq f_3 \leq 4.4$ as presented in Figure 4.6 (in red). As one can see in the figure, this constraint showed that there could be quite different compromises between the other two objectives: the highlighted solutions were located into three separate Pareto optimal regions. Moreover, because of zooming, rotating, and immersion possibilities, the Pareto optimal front was easy to comprehend. Also, the trade-offs between targets were easy to appreciate, and hopping from one Pareto optimal region to another was greatly simplified.

In the concept of *innovization* [24], the task of MOEA optimization is followed by a search of hidden interactions among decision variables and objective functions within obtained solutions. This concept has revealed interesting and important insights about design and optimization problems. Here, we suggest that the proposed VR based visualization tool can be used as an aid to assist in the *innovization* task. Combining these two concepts allows the decision maker to test the validity of different interrelationships among the decision variables and objective functions. For example, the existence of a given relationship, such as $\Phi(\mathbf{f}, \mathbf{x}) = 0$, can be tested by marking all solutions (among the obtained MOEA solutions) which restrict the absolute value of Φ within a threshold, say $\epsilon = 10^{-6}$, in red. The location and trace of these solutions on the Pareto optimal front will provide a plethora of information to the decision maker about the importance of

the above relationship before choosing a particular solution. As an example, we return to the DTLZ6 test problem and investigate the existence of Pareto optimal solutions having the following relationships:

$$\begin{aligned}\Phi_1(\mathbf{f}, \mathbf{x}) &: x_1 = 0 \quad (\text{Red}), \\ \Phi_2(\mathbf{f}, \mathbf{x}) &: x_2 = 0 \quad (\text{Blue}), \\ \Phi_3(\mathbf{f}, \mathbf{x}) &: x_1 = 1 \quad (\text{Brown}), \\ \Phi_4(\mathbf{f}, \mathbf{x}) &: x_2 = 1 \quad (\text{Purple}).\end{aligned}$$

The above conditions check if any Pareto optimal solution made box constraints on variables x_1 and x_2 active. In Figure 4.7, all such solutions are marked with in $\epsilon = 10^{-6}$. It is interesting to note that there were no solutions on the Pareto optimal front close to the upper bounds of these two variables and there were a number of solutions which were close to their lower bounds. Only a few solutions existed where the x_1 value was close to zero, but there are a number of solutions with the x_2 value close to zero. Furthermore, all these solutions seemed to lie on only one of the four Pareto optimal regions. It could be useful to identify solutions close to constraint boundaries and a further investigation and relaxation of active constraints could lead to better solutions. Such information is not only interesting but could be useful if problem-specific relationships were tested.

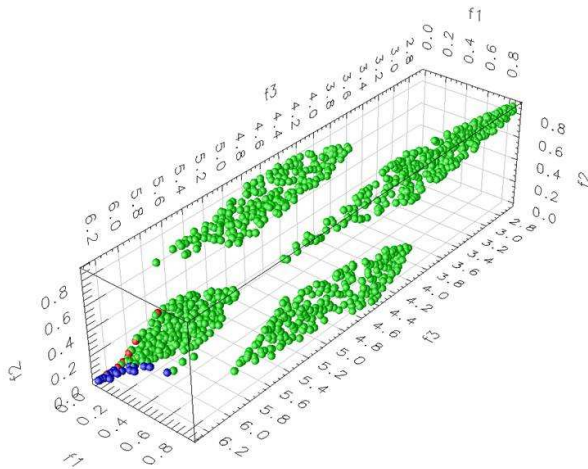


Figure 4.7: Pareto optimal solutions close to the constraint boundaries are highlighted with red and blue colors using the VR environment for DTLZ6 test problem.

4.2.4 Future extensions

In this section, we have revealed a number of advantages of using a VR system in making a better realization of the Pareto optimal fronts and sets of Pareto optimal points in a multiobjective optimization problem. However, the VR system can also be used to pursue a number of other interesting tasks:

1. Navigating through a selected set of Pareto optimal solutions.
2. Navigating through a part of the Pareto optimal front, instead of the complete front.
3. Highlighting Pareto optimal solutions which have special properties.
4. Dealing with more than three (or four) objectives.
5. Comparing different generating methods for multiobjective optimization.

These are only just some examples of how the VR capability can be used to support the decision maker. The purpose of this section is to discuss the power and usefulness of VR in multiobjective optimization and to encourage other researchers to undertake similar research activities. The following paragraphs discuss each of the above issues in greater detail.

NAVIGATING THROUGH A SELECTED SET OF PARETO OPTIMAL SOLUTIONS

First, the idea of combining multiobjective optimization and VR might be useful e.g. when working with Korhonen et al's reference direction concept (the Pareto race concept) [63] or with Eskelinen et al's Pareto navigator for nonlinear multiobjective optimization problems [35]. By specifying a direction (by the decision maker), the corresponding Pareto optimal solutions with the smallest achievement scalarizing function value can be marked on the Pareto optimal front. The visualized 3D Pareto optimal front can then be used to navigate through these Pareto optimal solutions. In this way, the decision maker can see these points by delving into the points or by following them along the Pareto optimal front. The 3D navigation facility offered by a VR system should make the Pareto race or Pareto navigator concepts more lively and interesting for designing a better interactive decision making task.

In addition, other such navigation ideas (e.g. NAUTILUS method [103] or reference-based MOEA [146]) can also be implemented with the VR facility. If the decision maker is not sure that he/she has identified a particular reference direction emanating from the current solution, multiple reference directions can be specified and then the solutions corresponding to each reference direction can be navigated one at a time. The solutions traversed along each path can be qualitatively compared, and a single preferred solution can be chosen for further analysis. A similar concept can also be implemented by suggesting multiple reference points and by navigating from the region obtained by one reference point to another region marked by another reference point. Navigating from one region to another

provides the decision maker with an impression of the relative trade-off regions on the Pareto optimal front, and thereby allows her/him to choose a preferred region for further analysis.

NAVIGATING THROUGH A PART OF THE PARETO OPTIMAL FRONT

So far, we have demonstrated the use of VR facilities in understanding the complete Pareto optimal front. Similar approaches can also be applied to a particular preferred region on the Pareto optimal front, if one has already been identified. This is particularly useful in dealing with a large dimensional Pareto optimal front, since a suitable representation of a higher dimensional Pareto optimal front demands the computation of exponentially large numbers of solutions. Generating multiobjective optimization methods, such as a MOEA, are useful if a part of the Pareto optimal front becomes the target. For this purpose, recent MOEA extensions (the reference point method [25], the light beam method [22]) and other interactive MCDM methods can be implemented with our VR system.

HIGHLIGHTING PARETO OPTIMAL SOLUTIONS WHICH HAVE SPECIAL PROPERTIES

Since the VR facility allows the use of the color, size and shape of points to differentiate different solutions qualitatively, the VR system becomes an ideal tool for highlighting special solutions on the Pareto optimal front. The special points may be chosen using one or more of the following concepts:

- *Utility function*: The optimal solution(s) of one or more utility functions supplied by a decision maker can be highlighted to obtain a better understanding of their location on the Pareto optimal front and their trade-off.
- *Solutions with common properties*: In selecting a preferred solution or understanding the Pareto optimal front better, the decision maker may be interested in visualizing the solutions which have certain relationships among the variables (\mathbf{x}) and/or objectives (\mathbf{f}). The decision maker can try different pre-defined relationships to obtain a better idea of the function-variable interactions present among the Pareto optimal solutions. As stated, one extension of this approach for knowledge discovery is the task of *innovization* [24]. In this task, instead of the decision maker supplying relationships, hidden relationships among the objective and variable values among Pareto optimal solutions are deciphered. Once identified, these properties will indicate relationships inherent to the Pareto optimal solutions and they can act as a 'recipe' for finding the optimal solution. The VR tool suggested here can be used to study the relationships between data supplied by the decision maker and the hidden relationships among all Pareto optimal solutions.
- *Robust solutions*: In many practical problems, decision variables and some problem parameters are uncertain. As a result, their optimum values cannot be estimated with accuracy in practice. For example, if 10 mm is found to

be the optimal diameter of a cylindrical material, the manufacturing process cannot guarantee achieving exactly 10 mm throughout its length. Certain Pareto optimal solutions may be quite sensitive to such uncertainties, whereas some may not [21]. In these kind of scenarios, it may be useful to highlight those Pareto optimal solutions which are less sensitive (within a desired threshold) to parameter and variable uncertainties (called the *robust* solutions). This will also allow the decision maker to obtain a comprehensive idea of the location of the robust part of the Pareto optimal front.

- *Solutions close to constraint boundaries:* In most optimization problems, optimal solutions lie on the intersection of one or more constraint boundaries. These kinds of constraints are critical, and a further investigation and relaxation of such constraints may result in better solutions [161]. If one wishes, Pareto optimal solutions active on different constraints can be highlighted. This will provide a clear picture of the relative importance and effect of each constraint on Pareto optimal solutions, particularly on the region of interest to the decision maker.
- *Special Solutions:* Solutions with special properties, such as exhibiting a knee, a kink, a large trade-off between the objectives, non-convexity, and mathematical Karush-Kuhn-Tucker (KKT) conditions may be of interest to the decision maker and can be highlighted for a better understanding of the nature and shape of the Pareto optimal front.

All these tasks will allow the decision maker to investigate the characteristics of Pareto optimal solutions obtained before making a decision about a region or solution of interest.

DEALING WITH MORE THAN THREE (OR FOUR) OBJECTIVES

In this thesis, there is an example with four objective functions visualized in VR shown in Appendix B. In that example, the fourth objective is presented in color. However, there can be more than four objective functions at the same time. In that case, the visualization of the fifth (and even sixth and seventh) objective function value can be done with a size or shape of the selected solution markers, for example. The navigation facilities associated with the VR system will allow a decision maker to obtain a better understanding of the higher-dimensional surface than 2D or 3D figures.

COMPARING DIFFERENT GENERATING METHODS FOR MULTIOBJECTIVE OPTIMIZATION

A VR tool can also be used to achieve a better qualitative comparison of non-dominated fronts obtained by different generation-based multiobjective optimization algorithms. For example, different fronts can be represented by different colors or markers. An appropriate navigation of both fronts simultaneously should provide a clear idea of the extent of domination of one set of solutions compared to some others, thereby revealing the strengths and weaknesses of each algorithm.

In addition to these concepts, more interactive interfaces are being planned between the VR and multiobjective optimization solution algorithm. It should be straightforward to communicate and transfer data between programs when solving multiobjective optimization problems iteratively in an interactive way. For example, if one has an interactive method then by providing new preference information to the multiobjective solution algorithm, it should be possible to see the outcome with the visualization tool, and new solutions should be calculated automatically.

The following chapters will discuss the applicability of these approaches. Interactive multiobjective optimization and the new decision support ideas are tested for use in IMRT, brachytherapy (only interactive multiobjective optimization), and, in the appendix, in papermaking.

Interactive multiobjective optimization of IMRT

5.1 Introduction to IMRT

This year, millions of people all over the world will be diagnosed with cancer. More than half of these patients will receive radiation at some point during their treatment. Radiation affects the cells' DNA and can kill cancerous cells or prevent them from growing and dividing. Cancerous cells are more susceptible to radiation than healthy ones but radiation affects healthy cells as well. Thus, treatments must be carefully planned so that the effect of radiation is concentrated on cancerous cells while healthy tissue does not receive too much radiation. In this thesis, it will be demonstrated how intelligent interactive multiobjective optimization methods can offer better solutions than the approaches used so far. At the same time, they provide a way to formulate the optimization problem so that the real goals can be considered without overlooking any information about the solution.

In external radiotherapy as in intensity modulated radiotherapy (IMRT), the radiation is delivered via beams fired into the patient's body from an external source. A linear accelerator located in a gantry which can be moved around a patient lying on a couch, allowing the beams to be delivered from a number of different angles, is used to produce the beams. Wedges or a multileaf collimator can be placed in front of the beam across the field to change the shape of the beam. In the so-called step and shoot treatment, the beam is aimed from a number of different angles, a wedge orientation and multileaf collimator shape is chosen for each angle, and the radiation beam is radiated for a certain amount of time. There are two major variants of this approach: conformal radiotherapy, in which the shape of the multileaf collimator at each angle is chosen to match the shape of the tumor as viewed from that angle, and IMRT, in which the beam field is divided for planning purposes into a rectangular array of "beamlets".

Mathematical models describing the behavior of radiation in a patient (needed for radiotherapy treatment planning) have improved over the years, and the dose distribution can be calculated more accurately. Models based on the Boltzmann transport equation (BTE) have been studied extensively for radiotherapy purposes,

and at the moment they are regarded as one of the most promising techniques for dose calculation [137]. Most studies consider the solution of the radiotherapy forward problem, i.e. how to compute the dose within a patient when the treatment settings are decided. Recently, there has been interest in using BTE models in solving the radiotherapy inverse problem, i.e. how to solve the treatment settings when there are some limitations for the dose distribution in the patient [142, 144]. The challenge in using the BTE models is their long computing time and therefore a much faster novel method called parameterization was used in [144] for solving the radiotherapy inverse problem. In this thesis, the BTE model and the parameterization technique have been used in dose calculation.

There has recently been considerable interest in employing multiobjective optimization in radiotherapy treatment planning (see e.g. [14, 37, 42, 51, 64, 74, 118]). This is because the aim of radiotherapy is to destroy the tumor without affecting the healthy tissue, but, naturally, increasing the dose in the tumor also increases the unwanted dose in the surrounding healthy tissue. Thus, when one target is optimized, the other will suffer, and the solution has to be some kind of compromise. This trade-off is complex, and optimization tools capable of handling multiple and conflicting objectives are required. The multiobjective optimization approaches presented in the literature are typically based on using objective weights or penalty coefficients defined beforehand, where the objective function is expressed as a weighted sum of objectives (often penalty functions), see e.g. [30, 65, 66, 72, 93]. Alternatively, evolutionary algorithms (see e.g. [128, 154]) have been used. These methods have their own limitations, e.g. it is typically difficult to predefine the priorities or weights of the optimization targets (for the weighting method) or they are very time consuming, necessitating extensive calculation (evolutionary algorithms). Moreover, sometimes information about the objectives and even the practical relevance of the objective functions can become blurred if the objectives are expressed as a sum. To avoid all these limitations and to overcome the problems related to the computational cost of the BTE modeling in treatment planning optimization, in this thesis work an interactive multiobjective optimization approach was combined with the parameterized BTE radiotherapy dose calculation model.

An interactive multiobjective optimization method was applied for the non-linear BTE model-based radiotherapy treatment planning problem. Typically, optimization problems in treatment planning are often solved without explicitly emphasizing the multiobjective nature of the problem [5]. Here, the multiobjective nature of the problem was exploited in the problem formulation and in the interactive solution process, and demonstrating the advantages of our interactive approach. In this approach, the decision maker's (i.e. radiotherapy expert's) knowledge is used during the iterative solution process in conjunction with the parameterized BTE dose calculation model to direct the search so that it identifies the most preferred plan, that is, the best Pareto optimal solution, between the conflicting criteria. In our earlier research, we have integrated an interactive multiobjective optimization method with a simple pencil beam dose calculation model of IMRT [120], and since the results were promising, we now use the deter-

ministic coupled time-independent linear BTE model, which is an integro-partial differential equation, in the dose calculation. The BTE model enables a more exact and realistic dose calculation. Although the computation of the parameterization is difficult and time-consuming, it has to be done only once before the optimization procedure and thus the BTE model can conveniently be used in an interactive multiobjective optimization procedure with consecutive iterations. In addition, since the decision maker directs the solution process interactively, only feasible and interesting Pareto optimal solutions are generated (according to the preferences of the decision maker). Thus, there is no need for lengthy calculations and a large solution database. With the approach, the desired solution is easily achieved by the decision maker by manipulating the desired values of the objective functions directly. This kind of decision support aid overcomes the drawbacks of trial-and-error planning and defining weights beforehand (which have no direct and fully intuitive meaning for the decision maker), and planning times can be shortened and plan quality can be improved by finding advantageous trade-offs. The idea of supporting the decision making process and comparing solutions has also been presented in [15, 16, 17, 31, 41, 50, 65, 66, 93, 106, 119, 145] but the optimization methods used were either not interactive (as interactive multiobjective optimization is defined e.g. in [95]), or alternatively, they were based on a beforehand calculated database of Pareto optimal plans, and the dose was not calculated with the BTE model. In spite of all research work done so far, it is not well-known how to navigate around in the Pareto set in order to find the final solution.

5.2 Dose calculation using finite element model

Mathematical models describing how radiation behaves have improved continuously, and the dose distribution in a patient can now be calculated quite accurately. Recently, there has been interest in using transport equation models to compute an estimate for the propagation of electrons or photons in tissue instead of the kernel models and the Monte Carlo method [142, 144]. The use of the BTE model is becoming more popular as computer power increases, but it is not yet used in clinics because of computational problems. The BTE model takes a rigorous account of patient inhomogeneity and scattering effects. Apart from the drawback arising from computation time, the advantages of using a BTE model in radiotherapy dose calculation are clear. Thus, new methods must be developed to enable the use of the BTE model for radiotherapy dose calculations. For this reason, in this thesis parameterization [144] was used to shorten the long BTE model dose calculation times in treatment planning optimization. For brevity, the dose calculation model used is presented in Appendix A.

5.3 Objective function formulation

In this section, we specify our goals and objective functions of radiotherapy treatment planning. As stated above, the aim of radiotherapy is to destroy the tumor

without causing damage to healthy tissue. However, these targets are conflicting since increasing the dose in the tumor also increases the unwanted dose in the surrounding healthy tissue. Thus, the final solution is always a compromise and the trade-off is complex. In the literature, guiding the optimization to the solutions most likely to satisfy the radiotherapist has been regarded as a notoriously difficult task, e.g. see [106], and thus some compromises with the objective function formulation (e.g. formulating those as penalties) have been made. This is because it is easier to achieve a solution when simplifications are made to the objective functions, but at the same time information about the actual problem will be lost. In this section, we will formulate alternative objective functions to satisfy the radiotherapy goals without loss of relevant information while aiming at achieving the best possible solution.

5.3.1 Acceptable solution for radiotherapy treatment planning

We define a patient domain $V \subset \mathbf{R}^3$ containing a target region T (which is a tumor), a critical organ region C (which is a very dose-sensitive healthy organ) and a region of normal tissue N (healthy tissue surrounding T and C). Thus, we have the union $V = T \cup C \cup N$, see Figure 5.1. Let us assume that we have fields S_l ($l = 1, \dots, L$) from where the radiation flux u_l is emitted.

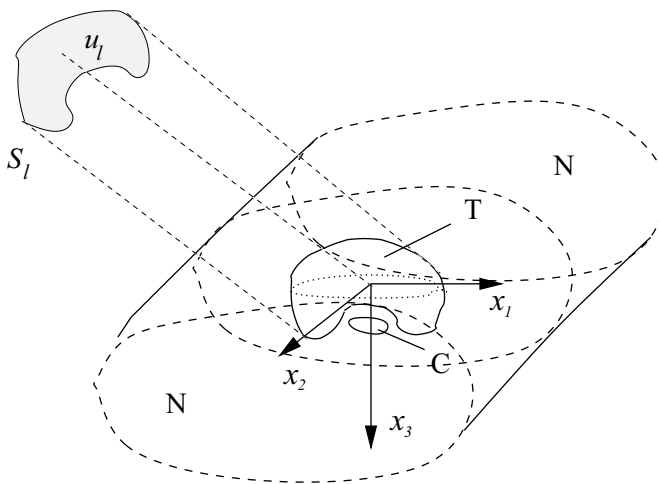


Figure 5.1: In dose calculation, in field S_l there is flux u_l in the treatment space. The flux passes to the patient domain V which includes regions T, C and N.

It is shown in Appendix A that the dose $D(\vec{x})$ can be obtained from the functional (A.23), and an acceptable solution for radiotherapy can now be defined. *Note that \vec{x} is a point in a patient domain, not a decision variable.* It is assumed that D_0 is the prescribed uniform desired dose in tumor T (in practice, it is equally

undesirable to be under or over the prescribed dose in T) and that D_C and D_N are the upper bounds of dose in the critical organ C and in normal tissue N, respectively. The limits D_0 , D_C and D_N are defined by a radiotherapy expert according to commonly used dose limits. Note that the tumor, the critical organ and the normal tissue may be divided into many separate parts, and dose limits may be different in these parts. Now we can write: determine the incoming flux $u \in L_2(\partial V \times I \times S)$ such that

$$\begin{aligned} D(\vec{x}) &= D_0, \quad \vec{x} \in T \\ D(\vec{x}) &\leq D_C, \quad \vec{x} \in C \\ D(\vec{x}) &\leq D_N, \quad \vec{x} \in N \end{aligned} \tag{5.1}$$

and that

$$u \approx S_2\gamma \geq 0, \tag{5.2}$$

where $u \geq 0$ prevents a negative flux, see Appendix A. The dose in (5.1) could be denoted as $D(\vec{x}) = D(\vec{x}, u)$ where the dose's dependence on vector u is also shown. These requirements are commonly used in clinics and in the literature, to guarantee the acceptability of a treatment plan. In other words, these are the minimal requirements that the plan must fulfill. Nevertheless, we should point out that the actual goal is to minimize the unwanted dose in total, not only the dose exceeding the limits D_C and D_N . In order to follow the notation used in Appendix A, we denote $D(\vec{x}) \approx D\gamma(\vec{x})$ in future.

In addition to the requirements (5.1), sometimes dose volume constraints can be used (see e.g. [144]). Dose volume constraints may be necessary for critical organs, for example. Radiobiological or biological objective functions can also be included in some cases (see e.g. [1, 6, 73, 75, 77, 143]), and a large number of other performance measures can be used in conducting the assessment of the treatment plan. Many of these measures are very important in clinical decision making and they can be used as objective functions in optimization, but they will not be used in this work because of the academic nature of our example.

5.3.2 Objective functions

Next, a description and formulation of the objective functions of the multiobjective optimization problem are undertaken in such a way that the treatment planning goals and the principles of an acceptable solution (5.1)-(5.2) are truly taken into account: i.e. these objective functions really minimize the harmful radiation in C and N. These objective functions are not often used without constraints, i.e. setting bounds on the dose to be delivered to the tumor, see e.g. [129]. In addition, with the optimization methods commonly used it is sometimes difficult to guide the solution in the most desired direction if the objectives are not formulated as weighted penalty functions, penalizing only the dose beyond the defined dose limits. However, formulating objectives as penalties, in turn, means that information about the phenomenon can be lost. To avoid this we define three objective functions (instead of only one) according to the wishes of the decision maker as

$$\tilde{f}_1(\gamma) = \|D_0 - D\gamma\|_{L_\infty(T)}, \quad (5.3)$$

$$\tilde{f}_2(\gamma) = \|D\gamma\|_{L_1(C)} \quad (5.4)$$

and

$$\tilde{f}_3(\gamma) = \|D\gamma\|_{L_1(N)}, \quad (5.5)$$

where the decision variables are denoted as γ (not x). For computational needs, functions must be discretized. In a discrete form, these functions are (f_2 and f_3 are scaled) as follows

$$f_1(\gamma) = \max_{\vec{x} \in I_T} (|D_0 - D\gamma(\vec{x})|), \quad (5.6)$$

$$f_2(\gamma) = \frac{1}{|I_C|} \sum_{\vec{x} \in I_C} D\gamma(\vec{x}) \quad (5.7)$$

and

$$f_3(\gamma) = \frac{1}{|I_N|} \sum_{\vec{x} \in I_N} D\gamma(\vec{x}), \quad (5.8)$$

where I_T , I_C and I_N are selected finite sets of nodes in T, C and N, respectively. $|I_C|$ and $|I_N|$ are the numbers of elements of I_C and I_N , respectively, subject to the constraint $u \approx S_2\gamma \geq 0$, where S_2 is a component of a matrix S (see, Appendix A).

Here, the objective function f_1 means the maximum dose deviation from a desired dose D_0 in T, and this is the function which needs to be minimized. The objective functions f_2 and f_3 are the averaged doses in C and N, respectively, which are also to be minimized. These two objective functions really minimize the unwanted (integrated) dose in C and N, i.e. they not only minimize the dose beyond limits D_C and D_N . Another way of looking at these functions is that they realize the actual goals of optimization in radiotherapy treatment planning. The use of such objective functions is recommended because radiotherapy experts have observed that the integral dose can be high when the critical organs and normal tissue are only kept under a predefined dose limit.

Here, a comparison between different optimization approaches is made to demonstrate the convenience of this interactive approach. In the comparison, the objective functions presented in [5, 144] were used, where the penalty function method (also called the weighting method in some cases) is utilized without explicitly emphasizing the multiobjective nature of the problem.

In this case, we can formulate the problem as if we had three objective functions to be minimized as

$$\tilde{f}_4(\gamma) = \|D_0 - D\gamma\|_{L_2(T)}^2, \quad (5.9)$$

$$\tilde{f}_5(\gamma) = \|(D_C - D\gamma)_-\|_{L_2(C)}^2 \quad (5.10)$$

and

$$\tilde{f}_6(\gamma) = \|(D_N - D\gamma)_-\|_{L_2(N)}^2. \quad (5.11)$$

For computational needs, these functions must also be discretized. In a discrete form, the functions are (as scaled)

$$f_4(\gamma) = \frac{1}{|I_T|} \sum_{\vec{x} \in I_T} |D_0 - D\gamma(\vec{x})|^2, \quad (5.12)$$

$$f_5(\gamma) = \frac{1}{|I_C|} \sum_{\vec{x} \in I_C} |(D_C - D\gamma(\vec{x}))_-|^2 \quad (5.13)$$

and

$$f_6(\gamma) = \frac{1}{|I_N|} \sum_{\vec{x} \in I_N} |(D_N - D\gamma(\vec{x}))_-|^2. \quad (5.14)$$

The objective function f_4 controls the violation of the requirement $D_0 = D(\vec{x})$ ($\vec{x} \in T$). The minimization of f_5 and f_6 is actually a part of a penalty function method for handling constraints and it takes care of the requirements $D(\vec{x}) \leq D_C$ ($\vec{x} \in C$) and $D(\vec{x}) \leq D_N$ ($\vec{x} \in N$). Note that in functions f_5 and f_6 , the subscript "–" refers to the negative part of the function. In other words, the functions f_5 and f_6 will minimize only the dose which oversteps the preset limits, not all the unwanted doses. With these objective functions, the constraint $u \approx S_2\gamma \geq 0$ must be used.

These objective functions and weighting coefficients has been routinely used in radiotherapy for over 30 years in studies presented in the literature because it is then easy to obtain the final solution, see [5, 7, 150] and references therein, for example. However, it is particularly difficult to set the optimization parameters, e.g. objective weights, to guide the solution process in the direction desired by the decision maker when the objectives are in such a strong conflict as in this case. These functions are used to guarantee that the solution fulfills the minimum requirements of the plan but, at the same time, the harmful dose is not really minimized and information about the solution is lost due to the use of a quadratic form of functions and penalizing only the dose beyond the predefined dose limits.

In [5, 144], no active constraint handling was used for the constraint $u \approx S_2\gamma \geq 0$, which was formulated as one more objective in the penalty function method

$$\tilde{f}_7(\gamma) = \|S_2\gamma_-\|_{L_2(\partial V \times I \times S)}^2, \quad (5.15)$$

which achieves a discrete form (as scaled)

$$f_7(\gamma) = \frac{1}{\max_{\vec{x} \in I_{\partial V \times I \times S}} S_2\gamma(\vec{x})} \sum_{\vec{x} \in I_{\partial V \times I \times S}} ((S_2\gamma)_-)^2(\vec{x}). \quad (5.16)$$

Therefore, the method used in [5, 144] is actually a combination of the ϵ -constraint method (see e.g. [95]) and the penalty function method. The method used in [5, 144] is sometimes called the weighted sum method or weighting method. Here the weights to be adjusted are the penalty coefficients. Note that this is not the same as the multiobjective optimization method known as the weighting method.

5.4 IMRT examples

In this section, we solve two radiotherapy treatment planning optimization problems with an interactive multiobjective optimization method. In these examples, the real multiobjective nature of the treatment planning process is discussed, and the decision maker's knowledge is utilized during the optimization process. Moreover, in the second problem, we compare the results to those obtained with the single-objective optimization penalty function method described in [5].

There is also an example in which gradient information is utilized in supporting the radiotherapy treatment planning decision-making process as suggested in Section 4.1. Subsequently, there is an example where the VR environment is utilized as well in the process of the radiotherapy treatment planning. The VR tool is used to visualize the conflicting targets of radiotherapy as presented in Section 4.2.

5.4.1 Interactive treatment planning optimization

TEST SETTINGS

The radiotherapy dose calculation model presented in Appendix A was solved using finite element method (FEM) and only one BTE was used to describe the path of artificial particles in a 2D plane ($\vec{x} = (\vec{x}_2, \vec{x}_3)$). The photon scattering data was used, but the dose computation was done from the photon flux using artificial stopping powers $\kappa(\vec{x}, E)$. The particles were assumed to scatter in the spatial 2D plane. Thus, the angular variable was $\theta \in [0, 2\pi[$ and $\theta = 0$ toward the x_3 axis. This caused an insignificant inaccuracy in the computations of the forward problem because the out-of-plane scattering was neglected.

The FEM simulations using singular value decomposition (SVD) parameterization was done in a $[-5,5] \times [0,10]$ cm² domain, which consisted of water. The domain was divided into 121 rectangular elements with 144 node points ($N_s=144$). The elements, node points, and the source nodes for the fields are shown in Figure 5.2. The angular domain $\theta \in [0, 2\pi[$ was divided into 8 evenly distributed intervals, and the energy domain $E \in [0.1, 10]$ MeV was divided into 3 evenly distributed intervals with 4 node points. Thus, we had $N_o = 8$, $N_e = 4$ and $N = N_s N_o N_e = 4608$. In the simulations, only inward directions and maximum energy $E=10$ MeV were allowed in the source nodes, thus $M_e = 1$ and $M_o = 3$. The number of source nodes was $M_s = 32$, and $M = M_s M_o M_e = 96$: hence there were 96 continuous decision variables in this case. The computation of matrix \mathbf{S} (Equation (A.18)) took about 3 hours, but when the geometry remains unchanged and the source nodes are the same, there is no need to re-calculate the matrix \mathbf{S} between optimization runs. The different regions of the domain, T (dark gray), C (light gray), and N (white area), are also shown in Figure 5.2. The interactive multiobjective optimization of radiotherapy treatment planning is at its best when T and C are close together, and when targets are strongly conflicting (clinical examples are head-and-neck and prostate cases).

All the simulations were carried out with the mathematical software Matlab[®]. The multiobjective optimization was made with a personal computer (Pentium[®]).

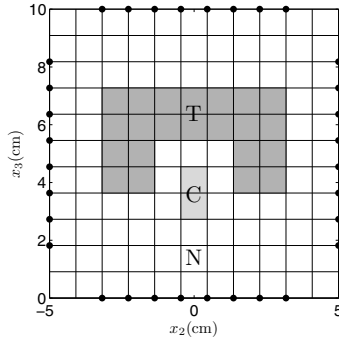


Figure 5.2: Elements, node points, and source nodes.

4 CPU 3.00 GHz with 2 GB central memory). Solving the BTE model, the parameterization and the penalty function method optimization were carried out using a personal computer (Pentium[®] 4 CPU 2.00 GHz with 2 GB central memory). For the multiobjective optimization, an implementation of the NIMBUS method, called IND-NIMBUS[®] [96], was used with a local optimizer based on the proximal bundle method [99], as justified in Section 3.2. In the optimization with the penalty function method, global optimization was done using a simulated annealing algorithm [13] with Matlab[®].

EXAMPLE 1

This example reveals how our interactive approach is capable of handling objective functions which are strongly conflicting. Thus, the multiobjective optimization problem is of the form

$$\begin{aligned} & \text{minimize} && f_1(\gamma), f_2(\gamma), f_3(\gamma) \\ & \text{subject to} && u \geq 0, \end{aligned} \tag{5.17}$$

where γ is a vector of continuous decision variables. In equation (5.6), the dose limit D_0 was set to 10 Gy, and in this example all the objective function values describe dose deviation from the desired dose (f_1) or actual dose (f_2 and f_3) in Grays (Gy). The isodose maps (contour plots) presented are plotted from percentage dose values in which D_0 was scaled to 100%.

Initial solution The interactive multiobjective optimization solution process was guided by preference information obtained from a radiotherapy expert, who was acting as a decision maker. The aim of the planning is to ensure the pre-specified dose D_0 and dose distribution in T and to minimize the unwanted dose in C and N. Initially, the decision maker was given the initial solution, in which the objective functions had the initial values $f_1 = 5.399$, $f_2 = 3.085$ and $f_3 = 3.274$. The initial solution $\mathbf{f}(\gamma^1)$ was produced with typical values of the decision variables and was

projected on the Pareto optimal set by IND-NIMBUS[®]. Figure 5.3 shows the contours describing the dose distribution in the phantom area and a dose volume histogram which were calculated from the initial solution values.

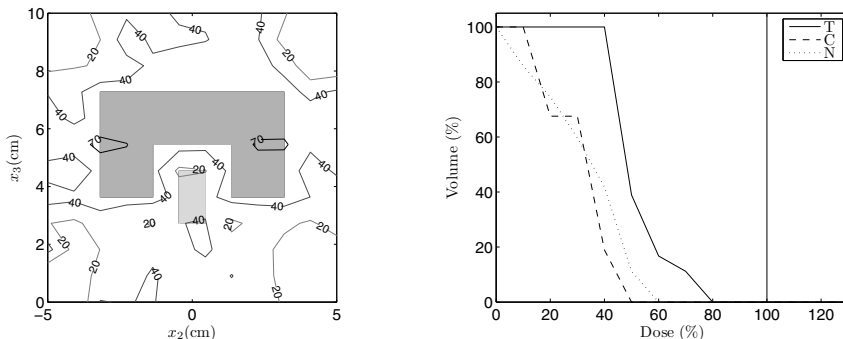


Figure 5.3: Initial solution. Dose distribution with isodoses 20, 40, 70, 90, 100, where 100% is $D_0 = 10$ Gy, and the corresponding dose volume histogram.

In brief, throughout the optimization process, the decision maker had the following aims: he wanted to obtain a solution in which the dose deviation from D_0 in T would be minimized. In addition, he considered it was important that the maximum 10% dose deviation from D_0 should not be overstepped, while the dose in both areas C and N should be as low as possible. As can be seen from the initial objective function values (deviation should be under 10% of D_0 , that is, 1 Gy) and from Figure 5.3, the f_1 value was certainly too high. In the initial solution, the objective functions f_2 and f_3 were nearly at a clinically acceptable level, i.e. the harmful dose in C and N was low but at the same time the deviation from D_0 in T was too high. In other words, the dose in the target was too low and the tumor would not be treated properly. Hence, the decision maker wanted to search for a better solution in an iterative way. The decision maker wanted to obtain four new solutions after every classification. All the solutions obtained during the solution process are collected in Table 5.1.

1st Classification In the first classification, the decision maker wanted to improve the value of f_1 : to decrease the deviation from the desired dose D_0 in T. Simultaneously, he tried to improve f_2 (minimizing the dose in C), but he allowed f_3 (the dose in N) to change freely. This means that he wanted to protect C more efficiently than N. In clinical planning, it is usually more important to save C than N. In brief, the decision maker classified f_1 and f_2 into class $I^<$, and f_3 into class $I^>$ (see classes in Section 3.2.1).

After the classification, the decision maker obtained four new solutions (see Table 5.1). He was able to achieve some improvements and the values of f_1 and f_2

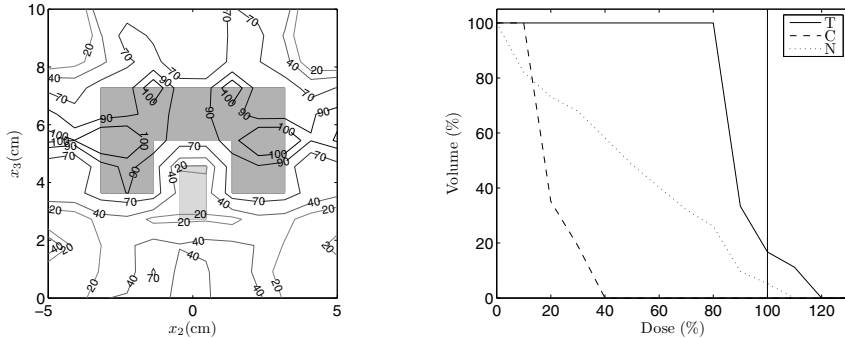


Figure 5.4: 1st classification. Dose distribution with isodoses 20, 40, 70, 90, 100, where 100% is $D_0 = 10$ Gy, and the corresponding dose volume histogram.

in all the new solutions were at a better level than had been obtained in the initial solution. At the same time, the objective function f_3 naturally deteriorated. The best of the solutions according to the preferences of the decision maker is shown in Figure 5.4 ($\mathbf{f}(\gamma^5) = (1.529, 2.170, 4.981)$). As can be seen, the dose in C is low. Nevertheless, the decision maker was not satisfied with the solution because the objective functions f_1 and f_3 were not at acceptable levels; the dose deviation from the desired dose D_0 in T was too high, as was the harmful dose in N. Since the solution was not clinically desirable, the decision maker wanted to classify the objective functions again. Having learnt about the trade-offs in the problem, the decision maker chose to give a new classification, and he used the obtained solution as the starting point of the new classification.

2nd and 3rd Classification In the second classification, the decision maker wanted to guarantee a good level of f_1 (class $I^<$), but now he was ready to impair f_2 up to a bound 3 (Gy). Hence, he classified f_2 into class I^{\geq} . Simultaneously he wanted to improve the objective function f_3 , i.e. he chose classification I^{\leq} and the desired aspiration level was 3 (Gy).

After the second classification, the decision maker obtained two new solutions. He obtained a solution ($\mathbf{f}(\gamma^7) = (0.765, 2.584, 5.608)$) in which the objective function f_1 (which he considered to be very important) was at a clinically acceptable level, but the other objective function values were worse. In the other solution obtained, f_1 was not good enough, but f_3 was good. In other words, if the function f_1 was at a good level, the function f_3 was too poor, and vice versa. The decision maker understood that both the aspiration level and the upper bound he set were too demanding, and he wanted to classify the objective functions again. He used the solution $\mathbf{f}(\gamma^5) = (1.529, 2.170, 4.981)$ again as the starting point of the new classification.

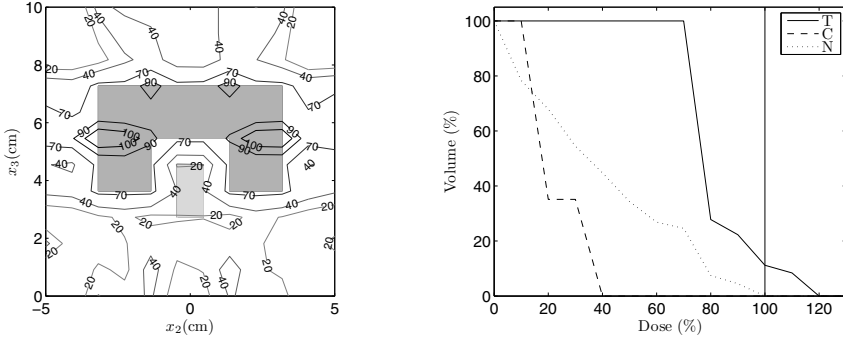


Figure 5.5: 2nd classification. Dose distribution with isodoses 20, 40, 70, 90, 100, where 100% is $D_0 = 10$ Gy, and the corresponding dose volume histogram.

In this classification, the decision maker wanted to moderate his demands. He changed his classification in order to achieve good values of f_1 and f_3 simultaneously. Thus, the third classification was $I^<$, I^{\geq} and I^{\leq} , where the aspiration level and bound was 4 (Gy). After the third classification, some of his goals were fulfilled: now he obtained two solutions which both have excellent f_3 value. However, f_1 was still too poor in both solutions and thus, new solutions were needed to be calculated. The decision maker selected the solution $\mathbf{f}(\gamma^9) = (2.324, 2.525, 3.993)$ as a starting point of a new classification.

4th and 5th Classification and final solution The decision maker knew that if he wanted to improve the value of f_1 , he would have to let f_2 and f_3 deteriorate. The decision maker felt he was close to the most satisfying solution, which is why he set an aspiration level for f_1 and upper bounds for f_2 and f_3 . Firstly, he set that the objective function f_1 should be better than 1.1 (Gy) and the bound for both f_2 and f_3 should be 4 (Gy). In other words, he made the classification f_1 to I^{\leq} (aspiration level 1.1 (Gy)), and f_2 and f_3 to I^{\geq} (bound 4 (Gy)) and obtained two solutions ($f(\gamma^{10})$ and $f(\gamma^{11})$). However, he still wanted to improve the value of f_1 . Thus, he made straight away a new classification which differed from the fourth classification only slightly: he set a new aspiration level 0.999 (Gy) for f_1 and used the solution $\mathbf{f}(\gamma^9)$ as a starting point.

Again, after the fifth classification, the decision maker obtained two new solutions. Another of them ($\mathbf{f}(\gamma^{13}) = (0.985, 2.475, 4.518)$) was an absolutely satisfying compromise and the decision maker felt he was now able to come to the final decision. He was looking for a solution with as uniform a dose in T as possible and where the preferences concerning dose limitations were satisfied. He achieved a solution in which the deviation from the desired dose D_0 in T was satisfactory ($f_1 = 0.985$, which is under 10% of D_0), and simultaneously the unwanted dose in C

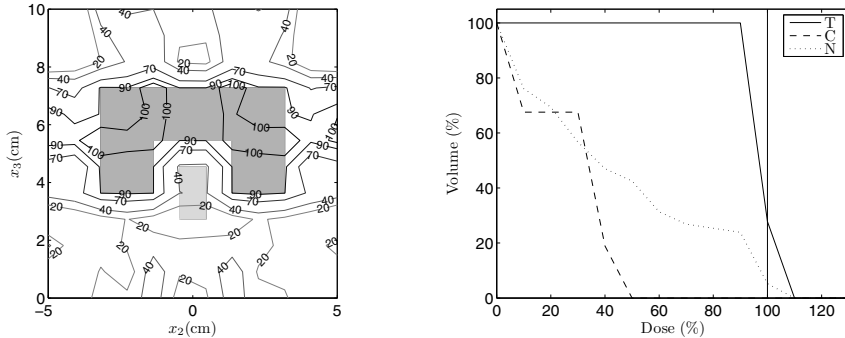


Figure 5.6: Optimal dose distributions with isodoses 20, 40, 70, 90, 100, where 100% is $D_0 = 10$ Gy, and the corresponding dose volume histograms.

($f_2=2.475$) and in N ($f_3=4.518$) was as small as could reasonably be achieved. This can also be seen in Figure 5.6. This solution $\mathbf{f}(\gamma^{13})$ was the most preferred outcome and was considered as the final solution according to the decision maker's expertise in radiotherapy. A summary of the solution process and trade-offs is presented in Table 5.1, including the steps taken by the decision maker and the solutions selected at each iteration (denoted in bold face). Table 5.1 also shows information about the approximate objective function ranges in the Pareto optimal set as discussed in Section 3.1.2. Information of this kind can be easily obtained with this approach and this enables the decision maker to learn and to analyze the interrelationships between the objectives and to compare solutions.

Discussion In this example, our interactive approach was demonstrated to be able to handle the strongly conflicting objective functions in a radiotherapy case. In general terms, it is said that strongly conflicting objective functions are notoriously difficult to guide to the solutions most likely to satisfy the decision maker (the radiotherapist). This is because the objective functions have typically been expressed as a sum where practical information about the functions may have been lost, or it may be hard to define objective weights beforehand because they are not so intuitive. In our approach, practical information about every objective function was maintained, e.g. the objective function values described understandably averaged doses, not uninformative quadratic sums of doses. As can be seen in this example, the objective functions really illustrated how the dose behaved. The function f_1 described the maximum dose deviation from the desired dose and the goodness of the objective function value was easy to understand. In addition, the functions f_2 and f_3 were the averaged doses in C and N, respectively. In this way, the dose could really be minimized in C and N. As can be seen in Table 5.1, with our approach with the objective functions $f_1 \dots f_3$, it was not hard to identify the

Table 5.1: Example 1: Summary of interactive solution process. Aspiration levels and bounds used are denoted as superscripts in the classification notation.

Solution	$f_1(\text{Gy})$	$f_2(\text{Gy})$	$f_3(\text{Gy})$
Ideal	0.274	0.001	0.008
Nadir	10.398	7.349	6.475
Initial solution			
$\mathbf{f}(\gamma^1)$	5.399	3.085	3.274
1st classification	$I^<$	$I^<$	$I^>$
$\mathbf{f}(\gamma^2)$	2.990	1.847	4.668
$\mathbf{f}(\gamma^3)$	3.060	2.013	4.621
$\mathbf{f}(\gamma^4)$	1.533	1.182	5.150
$\mathbf{f}(\gamma^5)$	1.529	2.170	4.981
2nd classification	$I^<$	$I^{\geq 3}$	$I^{\leq 3}$
$\mathbf{f}(\gamma^6)$	2.463	2.462	4.329
$\mathbf{f}(\gamma^7)$	0.765	2.584	5.608
3rd classification	$I^<$	$I^{\geq 4}$	$I^{\leq 4}$
$\mathbf{f}(\gamma^8)$	3.061	2.092	3.923
$\mathbf{f}(\gamma^9)$	2.324	2.525	3.993
4th classification	$I^{\leq 1.1}$	$I^{\geq 4}$	$I^{\geq 4}$
$\mathbf{f}(\gamma^{10})$	1.483	4.223	4.309
$\mathbf{f}(\gamma^{11})$	1.078	4.285	4.483
5th classification	$I^{\leq 0.999}$	$I^{\geq 4}$	$I^{\geq 4}$
$\mathbf{f}(\gamma^{12})$	1.548	4.071	4.148
$\mathbf{f}(\gamma^{13})$	0.985	2.475	4.518

most satisfying solution by manipulating the desired values of objective functions directly (not the weights). Thus, only a few iterations and calculations of Pareto optimal solutions were needed.

In treatment planning, the interactive multiobjective optimization approach made it possible for the decision maker to learn about the conflicting dose distribution targets and their interrelationships. Moreover, a thorough decision maker can see what happens when he/she directs the solution process in different ways. Good and unique solutions, which are hard to obtain without a decision support aid of this kind, can be found to satisfy the therapy plan.

Note also that computing times were short: only about one to two minutes per classification (with a PC). The most time-consuming part was solving the BTE forward problem which was performed before involving the decision maker in the solution process. In the parameterization procedure, the matrix \mathbf{S} is calculated with SVD, which took approximately three hours. Since the matrix \mathbf{S} is solved only once, there is no need to re-solve it if the geometry remains unchanged. Once the matrix \mathbf{S} has been found, the optimization method does not represent a bottleneck

for more complicated simulation models.

EXAMPLE 2

As a comparison, an optimization problem presented in [5] was solved with our interactive multiobjective optimization approach, and here we compare the results with those presented in [5]. In [5], the penalty function method was used without emphasizing the problem's multiobjective nature, and the optimization problem was given as

$$\text{minimize } f_{wm} = \sum_{i=4}^7 w_i f_i(\gamma), \quad (5.18)$$

where w_i ($i = 4, \dots, 7$) were positive weights set as $w_4 = 3$, $w_5 = 1.5$, $w_6 = 0.5$, $w_7 = 100$ (obtained as the final weights after several trials), and the threshold values used in (5.12)-(5.14) were $D_0 = 10$ (Gy) (in T), $D_N = 5$ (Gy) (in N) and $D_C = 2$ (Gy) (in C) [5]. A global single objective solver had to be used to solve the weighted problem (5.18) and this took about 20 minutes [5].

The aim of the planning was to ensure the pre-specified dose D_0 and dose distribution in T. In addition, in C and N, the dose was penalized if the threshold values of 20% (2 Gy) and 50% (5 Gy) of the D_0 , respectively, were overstepped.

On the other hand, the decision maker solved the problem

$$\begin{aligned} &\text{minimize } f_4(\gamma), f_5(\gamma), f_6(\gamma) \\ &\text{subject to } u \geq 0 \end{aligned} \quad (5.19)$$

with our NIMBUS approach in an iterative and interactive way, as in Example 1. Those objective functions are used in order to compare the results to those presented in [5]. During the solution process, the decision maker used three classifications until he obtained a satisfactory solution. All the solutions generated are shown in Table 5.2, and the solutions used as a starting point for the next new classification are denoted in bold face. Note that the objective function values are quadratic sums of dose differences, thus the physical meaning of the value becomes blurred. The final solution $\mathbf{f}(\gamma^9) = (0.985, 0.512, 6.028)$ obtained with the interactive approach is presented in Figure 5.7, on the left. For comparison, the final solution obtained with the penalty function method in [5] is presented in Figure 5.7, on the right. One should notice that the solution obtained in [5] covers the corners of T clearly less well than the solution obtained with the interactive method. The objective function values of these two solution processes are shown in Table 5.3.

Discussion In this example, the results of our interactive approach and those of the penalty function method can be compared (Figure 5.7 and Table 5.3). One can see that the final treatment plan of our approach is better than the plan obtained in [5], but the advantages of our approach are even clearer when the efficiency of the optimization process is considered. As can be seen from the results, with our approach we could see in an understandable manner how the solution process

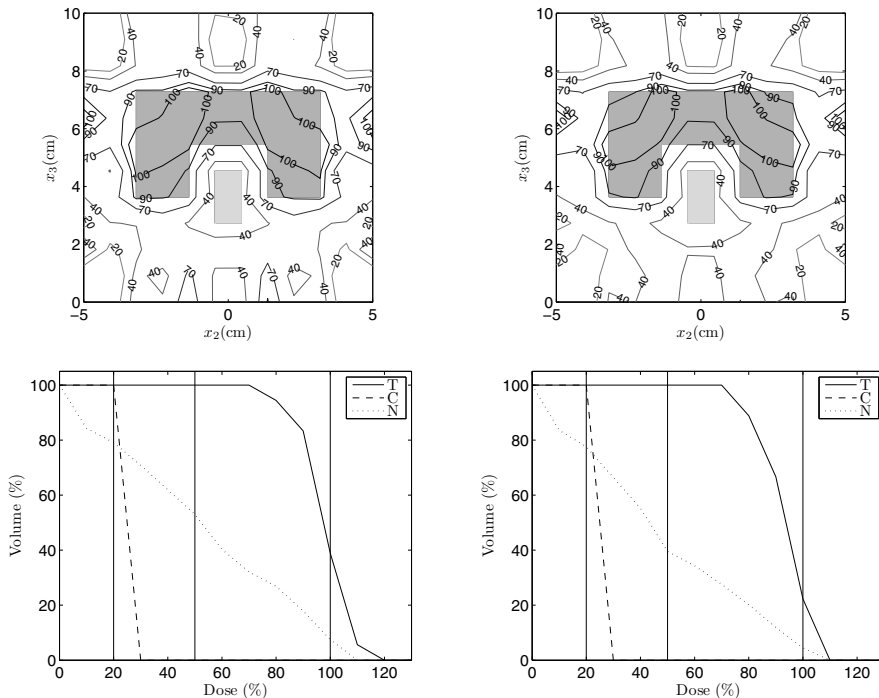


Figure 5.7: On the left, the solution using our interactive approach and, on the right, the solution using the penalty function method [5]. Optimal dose distributions with isodoses 20, 40, 70, 90, 100, where 100% is $D_0 = 10$ Gy, and corresponding dose volume histograms where the predefined dose limits (vertical lines) are plotted.

progressed and how the new radiotherapy treatment plan was fulfilling the decision maker's requirements after every iteration concerning the requirements of the radiotherapy process. In this way, we could avoid the time-consuming trial-and-error planning and re-optimization which happens in the penalty function method if the plan is not satisfactory or the weighting coefficients are not optimally chosen. For example, Figure 5.7 depicts the solution obtained with the penalty function method where all the corners of T are outside the 90% isodose, which is not desirable at all. For comparison, with the interactive multiobjective optimization, only the corners of T nearest to C were outside the 90% isodose. It seems that the solution obtained with the penalty function method was not the most satisfying for the decision maker, and new weighting coefficients would need to be discovered, and the time-consuming optimization procedure repeated if the decision maker wanted to improve the solution. On the other hand, in the interactive multiob-

Table 5.2: Example 2: Summary of interactive solution process. Bound used is denoted as superscripts in the classification notation.

Solution	$f_4(\text{Gy})$	$f_5(\text{Gy})$	$f_6(\text{Gy})$
Ideal	0.001	0	0
Nadir	75.156	32.559	19.175
Initial solution			
$\mathbf{f}(\gamma^1)$	7.188	3.121	1.014
1st classification	$I^<$	$I^>$	$I^>$
$\mathbf{f}(\gamma^2)$	0.067	22.568	7.505
$\mathbf{f}(\gamma^3)$	0.001	31.831	8.825
$\mathbf{f}(\gamma^4)$	0.090	21.299	7.336
2nd classification	$I^<$	$I^<$	$I^>$
$\mathbf{f}(\gamma^5)$	1.173	5.000	3.395
$\mathbf{f}(\gamma^6)$	1.363	5.590	3.346
$\mathbf{f}(\gamma^7)$	0.004	19.569	9.853
$\mathbf{f}(\gamma^8)$	1.429	5.523	3.309
3rd classification	$I^<$	$I^<$	$I^{\geq 7}$
$\mathbf{f}(\gamma^9)$	0.985	0.512	6.028
$\mathbf{f}(\gamma^{10})$	0.098*	9.764	7.595
$\mathbf{f}(\gamma^{11})$	0.001	25.795	9.009
$\mathbf{f}(\gamma^{12})$	0.098*	9.760	7.594

* Pareto optimality is hidden due to the rounding up the decimals

jective optimization, since the decision maker himself was actively involved in the solution process, only interesting Pareto optimal solutions needed to be generated.

Table 5.3: Interactive multiobjective optimization vs. penalty function method.

	Interactive MOO	Penalty function method
$f_4(\text{Gy})$	0.985	1.287
$f_5(\text{Gy})$	0.512	0.368
$f_6(\text{Gy})$	6.028	4.834
Neg. flux	0	0.001

Furthermore, it was observed that the physical feasibility of the solutions obtained was an issue. With the penalty function method, the constraint $u \geq 0$ was included as a penalty term in the objective function. This constraint guarantees that there is no radiation coming outward from the phantom, because only radiation flux inward is physically feasible. Nevertheless, in the solution obtained, there

was a negative flux (0.001 units), as can be seen in Table 5.3, and this affects the solution significantly. It eliminates the dose in the edges of the phantom, and this affects the value of the objective function f_6 . Consequently, the solution of the penalty function method was not physically feasible. In Table 5.3, since the objective function f_6 describes the dose in N, the solution obtained with the penalty function method (or the value describing the dose in N) is unrealistically good. However, this has remained unnoticed previously e.g. in [5] and this phenomenon can occur with the penalty function method if the feasibility of the solutions is not specifically checked.

In our interactive multiobjective optimization approach, $u \geq 0$ could be treated as a constraint, which meant that there was no negative flux in the solution. Thus, in addition to the fact that the solution was somewhat better at handling the dose in the target, the solution obtained with our approach was automatically physically feasible, unlike the other outcome. Without this interactive multiobjective optimization, the infeasibility of the solution would not have been observed because, in the penalty function method, the objectives are expressed as a sum that hides the negative flux value.

When comparing the dose volume histogram obtained in Example 1 with that obtained in Example 2, we see that with the functions f_1, f_2, f_3 , T obtained a steeper curve towards the zero than with the objective functions f_4, f_5, f_6 . In addition, a similar trend can be seen at the beginning of the C and N curve. This is due to the better choice of objective functions: harmful doses in C and N are really minimized, not only penalizing beyond the predefined dose limits (2 Gy and 5 Gy, respectively). Thus, it can be said that formulating the problem as a genuine multiobjective optimization problem and solving it with an interactive method confers many advantages. In addition to the factors discussed so far, it is important to point out that our objective function formulation produced a convex problem that could be solved with a computationally efficient local optimization method (and optimality for that reason could be guaranteed), whereas the formulation in [5] necessitated the use of a computationally costly global optimization method.

5.4.2 Utilizing gradient information

In this section, it will be demonstrated that the use of gradient information can support the radiotherapy treatment planning decision making. The same objective functions as in Example 1 (5.3-5.5) are used. The treatment planning problem is similar to that problem (5.17), but the geometries of the target and critical organ are different, see Figure 5.10. Also in this case $D_0 = 10$ Gy.

In this example, Algorithm 4.1.2 was used to generate a global approximation of a Pareto optimal front. By following the algorithm, Pareto optimal points and their gradient information (calculated by using finite differences) were utilized to form a nonlinear approximation of the global Pareto optimal front. The basic idea is to compute less Pareto optimal points with the computationally costly real model and thus make the treatment planning process more efficient. In this example, there are three Pareto optimal solutions and a total number of six solutions approximating

to Pareto optimal solutions calculated, and the approximation of Pareto optimal front is based on those nine points.

By studying the approximation (Figure 5.8), the decision maker could obtain

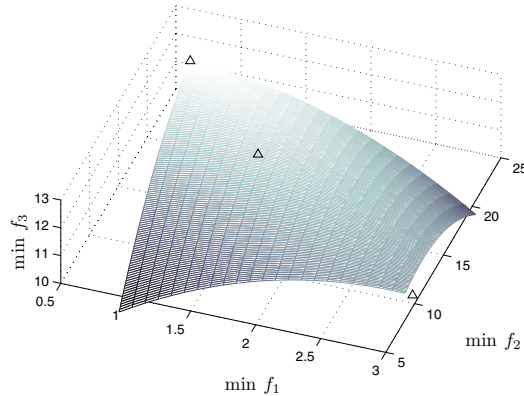


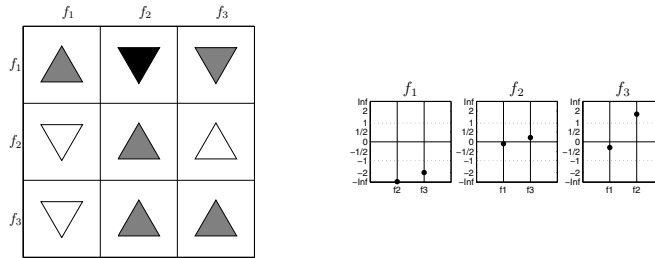
Figure 5.8: A nonlinear approximation of the Pareto optimal front based on gradient information. Three Pareto optimal points calculated are marked with triangles.

a picture in his mind about how the conflicting objectives would behave, and it was possible to identify the interesting regions of the Pareto optimal front. Based on this information, the decision maker is better prepared to guide the planning process in order to find the most satisfying Pareto optimal solution. This approximation of the Pareto optimal front is computationally much less complex than approximating the Pareto optimal solutions e.g. with MOEA, and the approximation gives some more information to the decision maker compared to the numerical values only. However, in Figure 5.8, one can see that the approximation is accurate only in some finite neighborhood of the Pareto optimal solutions: the farthest parts of the approximated Pareto optimal front represent unrealistically good solutions (in lower-left corner, for example). Thus, the decision maker should be a skillful expert in his/her own field in order to interpret the approximated Pareto optimal front.

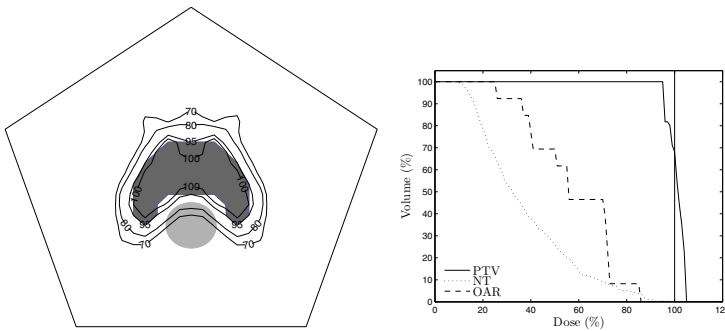
In addition to the approximated Pareto optimal front, trade-off information was shown to the decision maker during the interactive multiobjective optimization process after every iteration. For example, Figure 5.9 (and in Table 5.4) presents the total trade-off information after one iteration. The total trade-off was used because the decision maker felt that it described better his preferences than the partial trade-off: he wanted to see what would happen to the other objectives if he improved one of the objectives by one unit. As can be seen in the figure, it would be profitable to try to improve objective f_3 . For example, if objective f_3 was improved

Table 5.4: Matrix of total trade-off rates.

	f_1	f_2	f_3
f_1	1	-5.161	-1.999
f_2	-0.093	1	0.211
f_3	-0.286	1.673	1

**Figure 5.9:** Visual rate of change arrows and visual compromise bars for three conflicting objectives.

by one unit, the objective f_2 would also improve and the objective f_1 would be impaired only marginally, for example. As a comparison, if he wanted to improve the objective f_1 by one unit, both f_2 and f_3 would be impaired significantly at the same time.

**Figure 5.10:** Optimized radiotherapy treatment plan. Left, isodose map (where light gray is C and dark gray is T) and right, dose volume histogram.

With this additional information presented to the decision maker during the

iterative solution process, he was able to guide the solution process in an efficient way and better treatment plans were created by finding advantageous trade-offs. In addition, fewer Pareto optimal solutions were needed to be computed because after a couple of iterations the decision maker had a clear picture in his mind of the conflicting targets and their behavior and trade-offs. This explains why solving the optimization problem became easier and faster. Figure 5.10 shows the final solution (treatment plan).

5.4.3 Utilizing virtual reality

In this section we visualize the Pareto optimal solutions obtained in Example 1 by using the VR environment. In this way, the decision maker can obtain a confirmation of his impressions and the interrelationships between the Pareto optimal points could be easily seen. All the 13 Pareto optimal points computed (presented in Table 5.1) are visualized in Figure 5.11.

As seen in Figure 5.11, the values of f_1 , f_2 and f_3 were visualized as points in 3D space (they are illustrated in a 2D figure in this thesis), where each axis corresponded to one objective. In the visualization in the VR environment, the conflict between the objectives can be seen in an animated manner, since when one value improves, at least one other is impaired. For example, when the first objective was minimized, the second and third objectives obtained large values which were not desired. However, there were good compromise solutions between the objectives especially when the value of f_1 was around 1. After analyzing and studying the visualized Pareto optimal solutions, the decision maker was convinced that the chosen compromise solution $\mathbf{f}(\gamma^{13}) = (0.985, 2.475, 4.518)$ was the most optimal outcome. In this solution, the first objective was at the good level, which was one of the main criteria. In addition, the second and the third objective had achieved acceptable values at the same time.

Here, using the virtual reality for visualizing the Pareto optimal solutions conferred confidence on the decision maker in that he was actually choosing the final solution in radiotherapy treatment planning because the interrelationships between the objectives could be visualized more clearly. In addition, the plan quality could be improved by finding advantageous trade-offs by analyzing and navigating among the Pareto optimal solutions.

5.5 Concluding comments

New treatment machines provide an opportunity to treat cancer patients in more effective ways but, at the same time, they complicate the radiotherapy modeling and optimization in treatment planning. This chapter had two aims, i.e. not only to obtain an optimal radiotherapy treatment plan, but also to reveal the advantages of interactive multiobjective optimization in radiotherapy treatment planning and to encourage further research in this direction.

We combined the interactive multiobjective optimization approach NIMBUS with the novel parameterized BTE radiotherapy dose calculation model since we wanted to avoid the limitations of the optimization techniques widely used, and

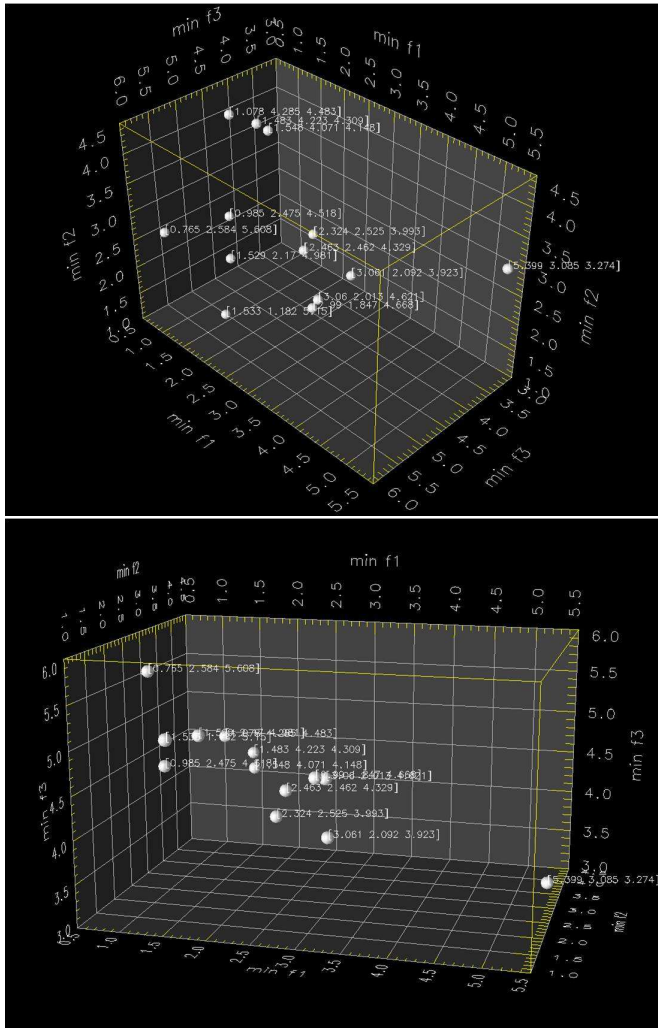


Figure 5.11: Visualized 3D Pareto optimal points of a radiotherapy treatment planning problem.

the advantages of using the BTE model in dose calculations are well recognized. By using parameterization, the BTE dose calculation model is so fast that it can be used in an interactive multiobjective optimization.

In an interactive multiobjective optimization approach, the decision maker’s knowledge is used during the iterative solution process to direct the optimization in order to find the most preferred plan, i.e. the best Pareto optimal solution, between the conflicting radiotherapy targets. A decision support aid of this kind overcomes

the drawbacks of trial-and-error planning, and planning times can be shortened and plan quality improved by finding advantageous trade-offs and finding only feasible solutions by manipulating the desired values of the objective functions directly (e.g. not by using weightings). Our interactive approach is capable of handling radiotherapy objectives which are strongly conflicting. Thus, we are able to describe the objective functions in a way that truly minimized the unwanted dose, i.e. there is no need for penalty functions. Some of these benefits can be obtained by using some other multiobjective optimization approach also, or an interactive treatment planning software in general.

Our BTE model is 3D spatially. Nevertheless, we were able to use it in two-dimensional planning only because of the long computing time of matrix \mathbf{S} . Further, the computing time can be a difficulty in maintaining the interactivity of the planning process in 3D cases. Applicability of the interactive approach to real 3D clinical problems is untested and, thus, it cannot be concluded. However, although the research documented in this paper is academic, the results are promising. In the future, these kinds of computational problems will be overcome, and this approach is worthy of further study in clinical cases.

In addition, presenting an approximation of a Pareto optimal front and the trade-off information to the decision maker makes the optimization process more intuitive. Since decision makers are able to predict how the solutions may behave, directing the solution process becomes more efficient and he/she can learn about the interrelationships between the objectives. Thus, there will be a decrease in the number of uninteresting solutions being computed. The support provided by gradient information is welcome especially when the evaluation of the objectives requires the solution of computationally costly mathematical simulation models.

Moreover, Pareto optimal fronts (i.e. different treatment plans) are often visualized when possible because in this way a comparison between solutions becomes easier. In this thesis, multiobjective optimization have been integrated with the 3D VR tool to supplement the Pareto optimal solutions in order to help the decision maker when choosing the final solution. The 3D VR tool makes it easier to compare solutions, navigate from one solution to another by zooming and rotating the front. Thus, it allows a better comprehension of those solutions with the desired properties. In addition, the use of sophisticated visualization tools means that fewer solutions need to be computed in order to learn and understand the interrelationships of the conflicting objectives.

The following chapter will illustrate how this interactive multiobjective optimization approach can be applied to brachytherapy treatment planning with clinical examples. Brachytherapy treatment planning suffers from similar problems to those needing to be solved in IMRT.

Interactive multiobjective optimization of b-therapy

6.1 Introduction to brachytherapy

The delivery of radiation in high-dose-rate (HDR) intracavitary brachytherapy using an afterloading unit is realized by using temporarily implanted catheters: a programmable remote unit moves a single radioactive source along the catheters. This system produces a high-dose region centered on the target while sparing the adjacent sensitive organs such as bladder and bowel. The flexibility of this system allows it to be tailored to a variety of different patient anatomy and cancer types because a wide variety of dose distributions can be generated from a given implant simply by adjusting the length of time (dwell time) that the source dwells at any location within a catheter (dwell position). In the clinics, this flexibility allows the full benefit of the use of a three-dimensional (3D) planning system based on computer tomography (CT) or magnetic resonance imaging (MRI).

However, the increased flexibility in treatment applications and imaging increases also the complexity in the treatment planning. As in Chapter 5, a patient domain can be divided into three different parts based on the patient's anatomy: a target volume (T), dose sensitive critical organs at risk (C) and healthy normal tissue (N). C and N are typically near T, and thus, they may be unnecessarily overdosed. To maintain a complete coverage of T and simultaneously to reduce the dose to N and C, the dose distribution should conform as well as possible to the relevant anatomy. One way to achieve this goal is to manually adjust the dwell time values until an acceptable solution is found (a computer is used to calculate the dose distribution). This is called forward planning. Nevertheless, this approach is time consuming and, thus, some kind of optimization method could be used. When using an optimization method, a computer is used to determine treatment settings (i.e. dwell times) such that the aims of the treatment planning are met (this is called inverse planning), see e.g. [2, 10, 27, 54, 61, 79, 80, 107, 113, 131, 136, 157].

In addition to the inverse planning, there has been interest in using multiobjective optimization in brachytherapy treatment planning (see, e.g. [69, 78, 159, 160]) similarly to IMRT. This is because the aim of brachytherapy is to treat the tu-

mor without affecting the healthy tissue but, naturally, increasing the dose in the tumor also increases the unwanted dose in surrounding healthy tissue as also in IMRT. Thus, when one target is optimized, the other will suffer, and the solution is a compromise between these goals. This trade-off is complex, and optimization tools capable of handling multiple and conflicting objectives are naturally required also in brachytherapy. Similar trends can be seen in the brachytherapy literature as encountered in IMRT: the multiobjective optimization approaches are based on using objective weights defined beforehand, where the final objective function is expressed as a weighted sum of the conflicting objectives (e.g. [68, 105]). In these cases, objectives are often formulated as using penalties where values exceeding predefined upper limits for doses are penalized (e.g. [70]), and the approach is often the same as in used in inverse planning. Unfortunately, it is typically difficult to predefine the priorities or weights of the optimization targets. Moreover, sometimes information about objectives and even the practical relevance of the objective functions can become blurred if the objectives are expressed as a sum. Furthermore, penalizing only the overdose should not be the actual goal as emphasized in this work. Alternatively, evolutionary algorithms (e.g. [71, 104]) have also been used. These methods have their own difficulties because they are time consuming requiring a considerable amount of calculations when computing a large set of approximating solutions.

In order to overcome some of the shortcomings of the currently used approaches, in this thesis an interactive multiobjective optimization method was utilized for 3D HDR brachytherapy optimization. Surprisingly, interactive multiobjective optimization methods have not been studied previously in the field of brachytherapy optimization. As mentioned, the studies where brachytherapy treatment plan has been optimized are usually based on a priori methods (weighting method, e.g. [105]) or a posteriori methods (evolutionary algorithms, e.g. [70]). The greatest difference between these approaches and our approach is that the decision maker's (i.e. treatment planner's) knowledge and preferences should be used during the iterative optimization process to direct the search in order to find the most preferred plan. In other words, this is the best way to identify the best Pareto optimal solution between the conflicting treatment planning targets. This makes treatment planning times shorter (because there is no need for computing a database of Pareto optimal solutions beforehand which can take two to three hours, for example [145]), and a good trade-offs between the targets can be found to improve the quality of the treatment plan. Furthermore, the interactive approach improves the decision maker's control over treatment: with this system, the treatment planner plays directly with the compromises between target coverage and protection of critical organs instead of with dwell positions, dwell times, and objective weights as shown in Figure 6.1 (as a comparison, see similar illustration in [31]). In the figure, the procedures of forward planning, inverse planning and interactive planning are presented and compared.

Because of this reasoning and experiences from IMRT treatment planning optimization, it seemed reasonable to propose that an interactive multiobjective optimization method would be ideal for brachytherapy optimization, and the ad-

vantages of this interactive approach are demonstrated by providing examples of a treatment plan of cervical cancer. In these examples, the real multiobjective nature of the problem is taken into account in the problem formulation and in the interactive solution process as discussed also in the previous chapter. It is realized that there is not so much scope for improvement of the final treatment plan but the strength of our approach is its interactivity. Our approach brings the planning process near to the real clinical issues avoiding artificial simplifications, and when compared to the occasionally used trial-and-error planning (i.e. treatment planner manually adjusts dwell times and positions), our approach (as also inverse planning algorithms in general) guarantees the mathematical optimality of the final solution, i.e. treatment plan. It is important to emphasize that these kinds of tools are designed to assist human treatment planners in their work, not to replace them.

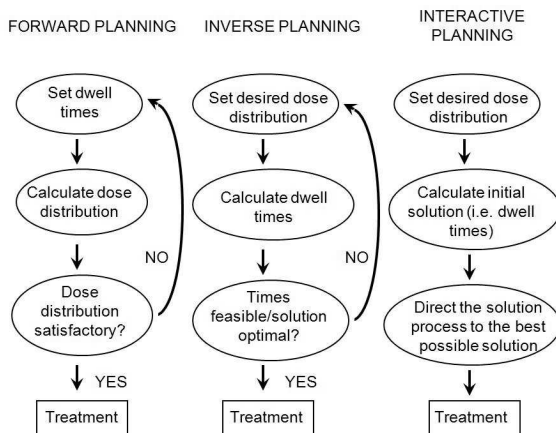


Figure 6.1: Philosophies underpinning forward planning, inverse planning, and interactive planning (see also [31]).

6.2 Dose calculation

Before optimization, the dose distribution in a patient needs to be calculated. The dose $D(\vec{x})$ at the i th sampling (dose calculation) point \vec{x} is calculated by

$$D(\vec{x}) = \sum_{j=1}^p t_j d_{ij}, \quad (6.1)$$

where p is the number of sources, t_j is the dwell time of the j th source dwell position and d_{ij} is the kernel value, i.e. dose value, for the i th sampling point and j th source dwell position. The dose rate matrix d_{ij} can be calculated using the

following equation according to TG43 [110, 116]:

$$d_{ij} = S_k \Lambda \Phi_{an}(\theta, r_{ij}) g(r_{ij}) / r_{ij}^2, \quad (6.2)$$

where S_k is the air kerma strength, Λ is the dose-rate constant, $\Phi_{an}(\theta, r_{ij})$ is the anisotropy function, $g(r_{ij})$ is the radial dose functions, and r_{ij} the distance between the dwell position j and the dose calculation point i (point source). In this section, we use equation (6.1) for dose calculations with a simplification made to the kernel d_{ij} : anisotropy of the patient is neglected. In the interactive multiobjective optimization, the dwell times t_j are the decision variables, not the variable x .

6.3 Objective function formulation

The aim of brachytherapy treatment planning is to obtain a plan which covers T with some specified dose value D_T , which will be case-specific depending on the type of the tumor. In addition, there is an upper bound (ESTRO's guideline) for the dose in N and C which should not be exceeded. We denote these bounds by D_N and D_C . Traditionally in the optimization process, dwell times t ($t:=t_j$) are sought so that the above-mentioned requirements are fulfilled, that is

$$\begin{aligned} D(\vec{x}) &\geq D_T, & x \in T, \\ D(\vec{x}) &\leq D_N, & x \in N, \\ D(\vec{x}) &\leq D_C, & x \in C. \end{aligned} \quad (6.3)$$

In the literature, several different objective functions have been used to fulfill these requirements; variance based objective functions (e.g. [68]) or dose volume histogram based objective functions (e.g. [70]). In addition, the formulation used in [79, 80] is well known. However, it is important to note that even though (6.3) describes an acceptable solution, it is important to carefully consider what actually needs to be optimized: the goal is that the dose in N and C should be as low as possible (minimized), not only under the predefined bounds (as also in IMRT).

Now, based on the fact that it is required to minimize the dose in N and C (i.e. not only the dose exceeding limits D_N and D_C), objective functions can be formulated (in a discrete form) as

$$f_1(t) = \frac{|I_{\bar{T}}|}{|I_T|}, \quad (6.4)$$

$$f_2(t) = \frac{1}{|I_N|} \sum_{\vec{x} \in N} D(\vec{x}), \quad (6.5)$$

$$f_3(t) = \frac{1}{|I_C|} \sum_{\vec{x} \in C} D(\vec{x}) \quad (6.6)$$

and

$$f_4(t) = \max_{\vec{x} \in T} D(\vec{x}), \quad (6.7)$$

where $|I_T|$, $|I_N|$ and $|I_C|$ denote numbers of sampling points in region T, C and N, respectively. For computational reasons, all the sampling points are situated on the surface of the region, and thus a maximum dose inside the T is not an objective but it is controlled later. Here, $|I_T^-|$ represents the number of sampling points in T that have a dose value equal to or larger than the dose limit D_T . Thus, the function f_1 represents a percentual volume where the dose is higher or equally high to the prescribed dose D_T in T, and it is maximized. The functions f_2 and f_3 are the averaged doses on the surface of N and C, respectively, to be minimized. If there are multiple critical organs C (as also here in the examples), there are as many objective functions, each similar to f_3 . The objective function f_4 describes the maximum dose on the surface between T and N. With these objective functions, the unwanted dose in N and C is truly minimized, not only penalized if it exceeds predefined upper limits for doses as it is often presented in the literature, see [70], for example.

In addition to objective functions f_1 , f_2 , f_3 and f_4 , the decision maker (treatment planner) may want to control the dose in T with a continuous objective function. In addition to the functions f_1, \dots, f_4 , one more objective function can be formulated as:

$$f_5(t) = \max_{\vec{x} \in T} |D_T - D(\vec{x})|. \quad (6.8)$$

The objective f_5 represents the maximum dose deviation from a desired dose D_T in T (to be minimized).

The use of the objective function f_1 makes the optimization problem non-convex [19]. There are several ways to convert non-convex objectives into convex forms [118], and this feature has been utilized e.g. in IMRT optimization [16, 17, 41, 117]. The reason for modifying the objective functions into linear convex objectives in optimization is clear: many optimization approaches are capable of solving those optimization problems quickly and exactly, and non-convex objectives cause problems in finding all Pareto optimal solutions when using objective weights [95, 118]. However, here we use an optimization method (NIMBUS, see Section 3.2.1) which is designed to solve non-linear multiobjective optimization problems. Thus, there are no enforcing needs for using linear convex functions in optimization. In addition, the optimization method in use is able to identify any Pareto optimal solutions.

In the following section, some clinical examples of interactive multiobjective optimization of brachytherapy treatment planning will be considered.

6.4 Brachytherapy examples

6.4.1 Problem settings

Here, two clinical examples of seeking dwell time values of a source in a gynecologic cervix cancer treatment are presented. In the examples, Fletcher-Suit and Ring intracavitary applicators were used to deliver the radiation. In Example 1, there were 17 possible dwell positions (resolution of 5 mm in three applicators, Fletcher-Suit intracavitary applicator system). Thus, the number of continuous decision

variables was 17. In addition, the number of sampling points was 508. In the second example, the number of possible dwell positions was 21 (resolution of 5 mm in two applicators, Ring intracavitary applicator system), and the number of sampling points was 473. The problems contained box constraints for the decision variables (i.e. dwell times). In the first example, there were two critical organs C (bladder and rectum, sigmoid colon (abbreviated in future to sigma) was not adjacent to the tumor), and thus, there were two objective functions similar to f_3 ($f_3^{bladder}$ and f_3^{rectum}). In the second example, there were three critical organs C (bladder, rectum, and sigma) and three objective functions similar to f_3 ($f_3^{bladder}$, f_3^{rectum} and f_3^{sigma}).

In these examples, all the simulations were carried out with the mathematical software Matlab[®] R2006b after the patient geometries (anatomy and sampling points) had been generated with a treatment planning software (BrachyVision[®], Varian Medical Systems, software version 7.3.10) at the Kuopio University Hospital. The optimization was conducted with a personal computer (Pentium[®] 4 CPU 3.00 GHz with 2 GB central memory). As in Chapter 5 for interactive multiobjective optimization, an implementation of the NIMBUS method, called IND-NIMBUS[®] was used [96].

In the first example (non-convex optimization problem), a heuristic optimization method approximating global Pareto optimal solutions (a genetic algorithm, computation time was minutes per classification with the presented PC) was used to solve the subproblems devised by NIMBUS. This optimization method does not require continuity of the objective functions. The rapid (computation time was only a few seconds per classification) local optimizer based on the proximal bundle method, which utilizes the continuity of the objective functions, was used in the second example (convex optimization problem). Since the optimization methods used were capable of handling nonlinear objectives and computation times were so short, there was no need for converting objectives into linear objectives in order to enable utilization of linear programming.

6.4.2 Example 1: Fletcher-Suit applicator

The first optimization problem used for the demonstration of the proposed interactive multiobjective optimization approach has the form

$$\begin{aligned} & \text{optimize} && \{f_1(t), f_2(t), f_3^{bladder}(t), f_3^{rectum}(t), f_4(t)\} \\ & \text{subject to} && t \in S, \end{aligned} \tag{6.9}$$

where t is a vector of continuous decision variables, and $S = [0, 100] \times [0, 100] \times \dots \times [0, 100] \subset \mathbf{R}^{17}$. Objective functions $f_1 - f_4$ are defined in Section 6.3: the value of f_1 represents the percentual value of sampling points in T which has a dose value equal to or larger than the dose limit D_T (7 Gy), and values f_2 , $f_3^{bladder}$, f_3^{rectum} represent averaged dose values in N, bladder, and rectum, respectively (in Gy). Finally, f_4 is the maximum dose on the surface between T and N (in Gy).

INTERACTIVE SOLUTION PROCESS

In this optimization problem, the interactive solution process (i.e. moving from one Pareto optimal solution to another) was guided by preference information of a treatment planner, who was acting as the decision maker. Before the solution process, the decision maker expressed the following desires: the percentual value of sampling points in T that have a dose value equally high or higher than the dose limit D_T should be maximized (f_1). At the same time, the averaged doses in N and both critical organs C should be minimized ($f_2, f_3^{bladder}, f_3^{rectum}$). Since the objective function f_4 shows the maximum dose on the surface between T and N, the decision maker also wanted to minimize this value. At the very beginning, the objective functions had the initial values (generated by IND-NIMBUS) $f_1 = 0.58, f_2 = 9.89, f_3^{bladder} = 1.96, f_3^{rectum} = 3.13$ and $f_4 = 96.80$ (initial solution $\mathbf{f}(t^1)$). As can be seen from the initial objective function values $\mathbf{f}(t^1)$, the f_1 value was certainly too low ($f_1 = 0.58$, i.e. 58% of T received a higher dose than D_T which was 7 Gy). Nevertheless, the objective functions $f_2, f_3^{bladder}$ and f_3^{rectum} were at a good level and, thus, the dose in N and critical organs C was low but, as stated, at the same time the dose in T was too low and the tumor would not be treated properly. Thus, the decision maker wanted to search for a better solution in an iterative way. He started to classify the functions and generated new solutions (see classes introduced in Section 3.2.1), and in this way declared his preferences and steered the solution process interactively and iteratively towards the most satisfying Pareto optimal solutions.

In the *1st classification*, as stated, he wanted to obtain a better value to f_1 (aspiration level 0.70) and simultaneously maintain the good values of f_3 and f_4 (save Cs). Thus, he set a bound to $f_3^{bladder}$, and an aspiration level to f_3^{rectum} . The bound and aspiration level both were 2.00. At the same time, he had to allow some other targets (f_2 and f_4) to deteriorate. In other words, the classification was $f_1 : I^{\leq 0.70}, f_2 : I^>, f_3^{bladder} : I^{\geq 2.00}, f_3^{rectum} : I^{\leq 2.00}$ and $f_4 : I^>$, and he wanted to generate one new solution (solutions are collected in Table 6.1). After the first classification, the decision maker obtained a better solution ($\mathbf{f}(t^2)$) because the rectum ($f_3^{rectum}=2.74$), which he considered as very important, obtained a smaller dose value than in solution $\mathbf{f}(t^1)$, but f_1 was still too low according to his preferences. For this reason, he decided to do the *2nd classification* using the solution $\mathbf{f}(t^2)$ as a starting point of the classification. In this classification, the decision maker wanted to improve f_1 as much as possible, and again, he set a bound to $f_3^{bladder}$, and an aspiration level to f_3^{rectum} to achieve the best levels of these objectives. In addition, the decision maker allowed f_2 and f_4 to change freely. Therefore, the classification was $f_1 : I^<, f_2 : I^>, f_3^{bladder} : I^{\geq 2.00}, f_3^{rectum} : I^{\leq 2.00}$ and $f_4 : I^>$. After the second classification, the decision maker asked for three new solutions and they all had excellent f_1 values, but, at the same time, values of other objectives were not so good (Table 6.1). This is the reason why he wanted to generate five *intermediate solutions* between the solutions $\mathbf{f}(t^2)$ and $\mathbf{f}(t^3)$, which had good values of objectives $f_3^{bladder}$ and f_3^{rectum} , and f_1 , respectively. Intermediate solutions represent compromise solutions between the conflicting treatment

planning targets, and the decision maker was able to choose the best Pareto optimal solution according to his knowledge of what he considered the final solution, i.e. the final treatment plan. That solution was $\mathbf{f}(t^9)$, in which the objective values were $f_1 = 0.73$, $f_2 = 10.50$, $f_3^{bladder} = 2.35$, $f_3^{rectum} = 3.15$ and $f_4 = 52.23$. As can be seen in Figure 6.2 (left) and Figure 6.3, all the requirements of the treatment plan were taken into account as much as possible: the harmful dose in rectum and bladder was minimized and the prescribed dose in T was delivered. Thus, the treatment plan was clinically acceptable.

All the solutions obtained and steps taken by the decision maker during the solution process are collected in Table 6.1. In this table, the starting point of a new classification and the final solution are given in bold face. Furthermore, a more thorough description of a typical process of classifying objective functions in a radiotherapy case and steering the optimization process was presented in Chapter 5 (IMRT example).

Table 6.1: Summary of interactive solution process. Bounds and aspiration levels used are denoted as superscripts in the classification notation.

Solution	$f_1(-)$	$f_2(\text{Gy})$	$f_3^{bladder}(\text{Gy})$	$f_3^{rectum}(\text{Gy})$	$f_4(\text{Gy})$
Ideal	1	0	0	0	0
Nadir	0	25.82	4.64	7.72	744.33
Initial solution					
$\mathbf{f}(t^1)$	0.58	9.89	1.96	3.13	96.80
1st classification	$I^{\leq 0.70}$	$I^>$	$I^{\geq 2.00}$	$I^{\leq 2.00}$	$I^>$
$\mathbf{f}(t^2)$	0.58	9.55	1.98	2.74	135.89
2nd classification	$I^<$	$I^>$	$I^{\geq 2.00}$	$I^{\leq 2.00}$	$I^>$
$\mathbf{f}(t^3)$	0.83	11.18	2.67	3.29	55.18
$\mathbf{f}(t^4)$	1.00	15.86	3.34	4.05	109.89
$\mathbf{f}(t^5)$	0.79	11.57	2.55	3.24	76.85
Intermediate sol. ^a					
$\mathbf{f}(t^6)$	0.64	9.87	2.12	2.86	64.23
$\mathbf{f}(t^7)$	0.69	10.02	2.24	2.90	62.11
$\mathbf{f}(t^8)$	0.71	10.44	2.36	3.04	52.23
$\mathbf{f}(t^9)$	0.73	10.50	2.35	3.15	52.23
$\mathbf{f}(t^{10})$	0.76	10.87	2.45	3.22	54.00

^a Intermediate solutions between $\mathbf{f}(t^2)$ and $\mathbf{f}(t^3)$.

COMPARISON AND DISCUSSION

In this example, we have shown how the interactive approach can handle the strongly conflicting objective functions in a case of cervix cancer. As can be seen in Figure 6.4 (a display of IND-NIMBUS software), the solutions obtained can be compared and carefully studied during the interactive solution process.

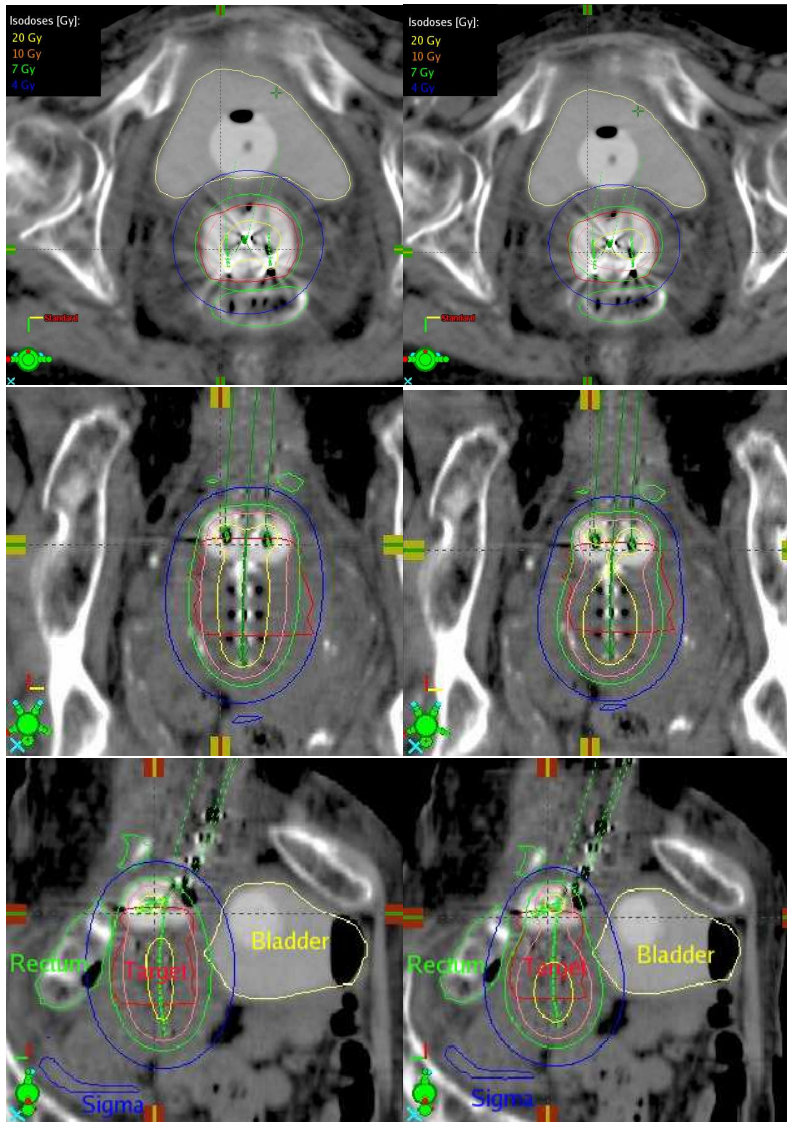


Figure 6.2: Left, the final dose distribution with IND-NIMBUS (solution $f(t^9)$) from different point of views (x, y, and z-direction), and right, for comparison, the solution obtained with BrachyVision[®] optimization. Target is red, rectum green, bladder yellow, and sigma is blue. Isodose of 7 Gy (prescribed dose in target) is colored green.

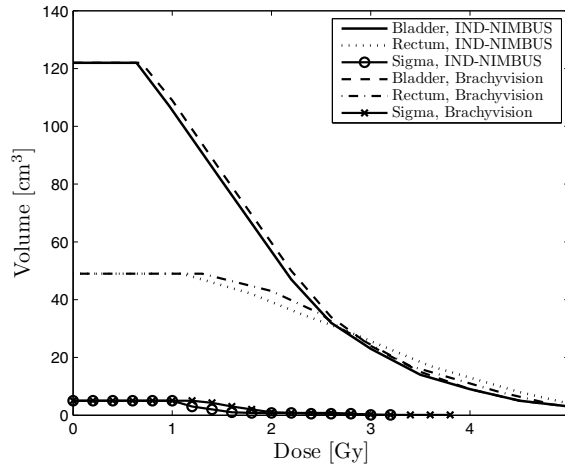


Figure 6.3: For comparison, dose volume histograms of critical organs C. Dose volume histogram values start to decline faster in IND-NIMBUS solution than in the solution obtained with BrachyVision[®].

Thus, the decision maker is better prepared to come to the final decision, i.e. choose the final treatment plan, after analyzing the isodose maps (Figure 6.2), dose volume histograms (Figure 6.3), graphical information (Figure 6.4), and numerical information (Table 6.1 and Figure 6.4). A good example of comparing the trade-offs between the objectives can be seen in Table 6.1: when comparing solutions $\mathbf{f}(t^1)$ and $\mathbf{f}(t^2)$, the dose in the rectum could be decreased without losing the target coverage, for example. With our approach, good trade-offs between the objectives could be found to improve the treatment plan's quality. Similar ideas for presenting information for the decision maker have been presented also in [17, 31, 66, 106, 145].

For comparison, a treatment plan with the BrachyVision[®] optimization tool was made (Figures 6.2 (right) and 6.3) with the objectives being formulated as weighted penalties if the dose exceeded the following limits: bladder 6.2 Gy, rectum 4.9 Gy, and sigma 4.5 Gy. In addition, the dose in T should be at least 7.2 Gy. These limits were based on ESTRO's guideline. The same decision maker executed also the treatment planning optimization using the BrachyVision[®] optimization tool. The time required for this procedure was about half an hour (IND-NIMBUS took about 20 minutes) because the decision maker had to vary the weighting factors many times, and he was not able to say how they should be changed. As stated, the weighting factors are not intuitive and thus it took such a long time to obtain an acceptable solution. For that reason, the BrachyVision[®] optimization tool is not in use in this hospital considered but the treatment planners prefer to

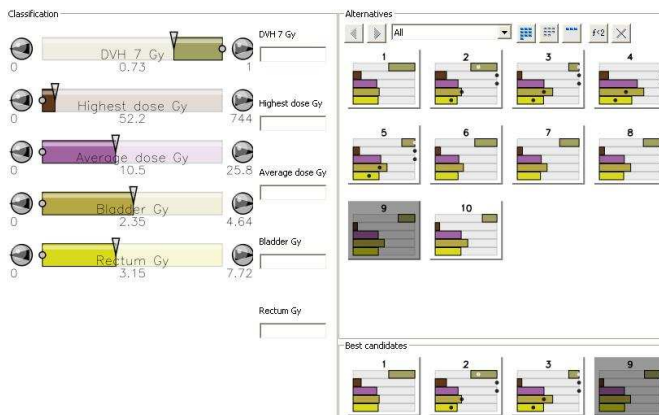


Figure 6.4: All the solutions obtained during the optimization process can be compared also with a graphical tool in IND-NIMBUS. On the left, the final solution $f(t^9)$ presented with bars describing objective function values, and, on the right, all 10 solutions generated. On the lower-right, best candidates, that is, solutions used in classifications and generating intermediate solutions. Solutions can also be visualized in many ways e.g. with value paths, whisker plots, petal diagrams, or spider webs, see for example [99].

rely on the ineffective trial-and-error manipulation of dwell times and positions for treatment planning.

When comparing the results, it can be seen from Figure 6.3 that dose volume histogram values start to decline faster in the IND-NIMBUS solution than in the BrachyVision[®] solution, which is good. In addition, Table 6.2 presents T 90% dose volume value, C 2 cm³ dose volume values, and N's volume where 50% of D_T is exceeded. Here, N includes also Cs but not T. The threshold value 50% of D_T was selected because that dose can cause secondary effects to N. When comparing the values in Table 6.2, we can see that T (90%) is covered with radiation better and the doses in sigma (2 cm³) and N are smaller in the IND-NIMBUS solution than with BrachyVision[®] solution. Since there are conflicting targets, at the same time we can observe that the dose (2 cm³) in bladder and rectum is smaller in the solution obtained with BrachyVision[®] than in IND-NIMBUS solution. This is a good example of a trade-off.

When T exceeds the prescribed dose (here, 7 Gy) it is not because a higher value is better (especially not in an IMRT case). However in brachytherapy in which a radiation source is located in T this is not so critical, and this can be arranged in order to obtain as conformal dose distribution as possible to T.

As can be seen, the results obtained are one further piece of evidence showing that the radiotherapy objectives are in conflict, and new tools capable of help-

ing the decision maker (treatment planner) in navigating among different optimal treatment plans are needed. This is because the optimization tools currently used by treatment planners are not easy to use, they are not intuitive since they are based on setting dose limits and weights, and they are time consuming because the unintuitive weights must be varied. These drawbacks explain why the decision makers prefer to use the trial-and-error approach. However, an interactive approach has been demonstrated to be easy to use and intuitive because the decision maker manipulates directly the balance between target coverage and healthy tissue protection (instead of objective weights). Moreover, with an interactive approach such as NIMBUS, the decision makers can learn about the conflicting targets and their interrelationships during the iterative solution process. Finally, the treatment plan obtained with our approach is really a mathematically optimal plan, which is not the case when one relies on trial-and-error planning.

Table 6.2: Comparison of T 90% values, C 2 cm³ values, and volume of N exceeding 50% of D_T .

	Interactive method (Gy)	BrachyVision [®] (Gy)
Target 90%	7.32	7.23
Bladder 2 cm ³	5.24	5.06
Rectum 2 cm ³	5.64	5.01
Sigma 2 cm ³	1.38	1.61
N 3.5 Gy	177.9 cm ³	200.4 cm ³

6.4.3 Example 2: Ring applicator

In Example 2, the optimization problem has the form

$$\begin{aligned} &\text{optimize} && \{f_2(t), f_3^{bladder}(t), f_3^{rectum}(t), f_3^{sigma}(t), f_4(t), f_5(t)\} \\ &\text{subject to} && t \in S. \end{aligned} \quad (6.10)$$

Functions $f_2 - f_4$ are the same as in the previous example except for f_5 representing the maximum dose deviation from a desired dose D_T (7 Gy) in T (to be minimized). Thus, the dose in T is controlled with f_5 .

The decision maker solved the problem in an interactive way using the IND-NIMBUS software as in Example 1, and the final solution (obtained after four classifications which took about ten minutes) had objective function values $f_2 = 6.70$, $f_3^{bladder} = 1.68$, $f_3^{rectum} = 1.64$, $f_3^{sigma} = 1.87$, $f_4 = 18.83$ and $f_5 = 2.88$ (in Gy). Here, for brevity, the results are only briefly compared with those obtained with the BrachyVision[®] optimization (Figure 6.5 and 6.6). In Table 6.3, T 90% dose volume value, C 2 cm³ dose values, and N volume, where 50% of D_T is exceeded, are presented.

In the comparison of the solutions, it can be seen that the treatment plan devised with the interactive approach is better than the plan obtained with the

BrachyVision[®] optimization. In addition, the treatment plan is intuitive and quick to obtain with an interactive method (no need for varying the objective function weights, which is time consuming and difficult), the target coverage (90%) is better and doses in rectum (2 cm^3) and N are lower in the solution obtained with IND-NIMBUS. In addition, the dose in sigma (2 cm^3) is the same with both solutions. However, bladder receives a lower dose (2 cm^3) in the plan given by BrachyVision[®] optimization. Moreover when studying the dose volume histograms (Figure 6.6), it seems that Cs is radiated with lower doses in the treatment plan obtained with the interactive method than with BrachyVision[®] optimization. Thus, the treatment plan obtained with IND-NIMBUS is clearly superior to the plan obtained with BrachyVision[®] optimization. Further, when comparing the planning processes, the advantages of using an interactive method are obvious: as stated, the treatment planner manipulates directly the desired values of the objective functions, not the objective weights, dwell positions, or dwell times, and thus one can obtain good trade-offs between the solutions and the drawbacks of currently used methods could be overcome.

Table 6.3: Comparison of T 90% values, C 2 cm^3 values, and volume of N exceeding 50% of D_T .

	IND-NIMBUS (Gy)	BrachyVision [®] (Gy)
Target 90%	7.20	7.15
Bladder 2 cm^3	4.53	4.36
Rectum 2 cm^3	3.60	4.17
Sigma 2 cm^3	4.71	4.71
N 3.5 Gy	106.4 cm^3	122.8 cm^3

6.5 Concluding comments

In this chapter, we have presented a new approach utilizing interactive multiobjective optimization for anatomy based 3D HDR brachytherapy optimization, and the advantages of a classification-based interactive approach are demonstrated by two examples of a clinical gynecologic cancer.

In this study, an interactive approach has been used to determine the dwell time values needed to fulfill the prescribed dose to the tumor and to minimize dose in each critical organ. In our approach, the decision maker's (i.e. treatment planner's) knowledge and preferences are used during the iterative optimization process to direct the search in order to find the most preferred treatment plan. This can make treatment planning times shorter and improve the quality of the plans. In addition, one must emphasize that our interactive approach is capable of handling multiple and strongly conflicting objectives in a convenient way, and thus, it offers the possibility to navigate among the obtained Pareto optimal solutions, i.e. different treatment plans. As seen, there is not so much space for improvement

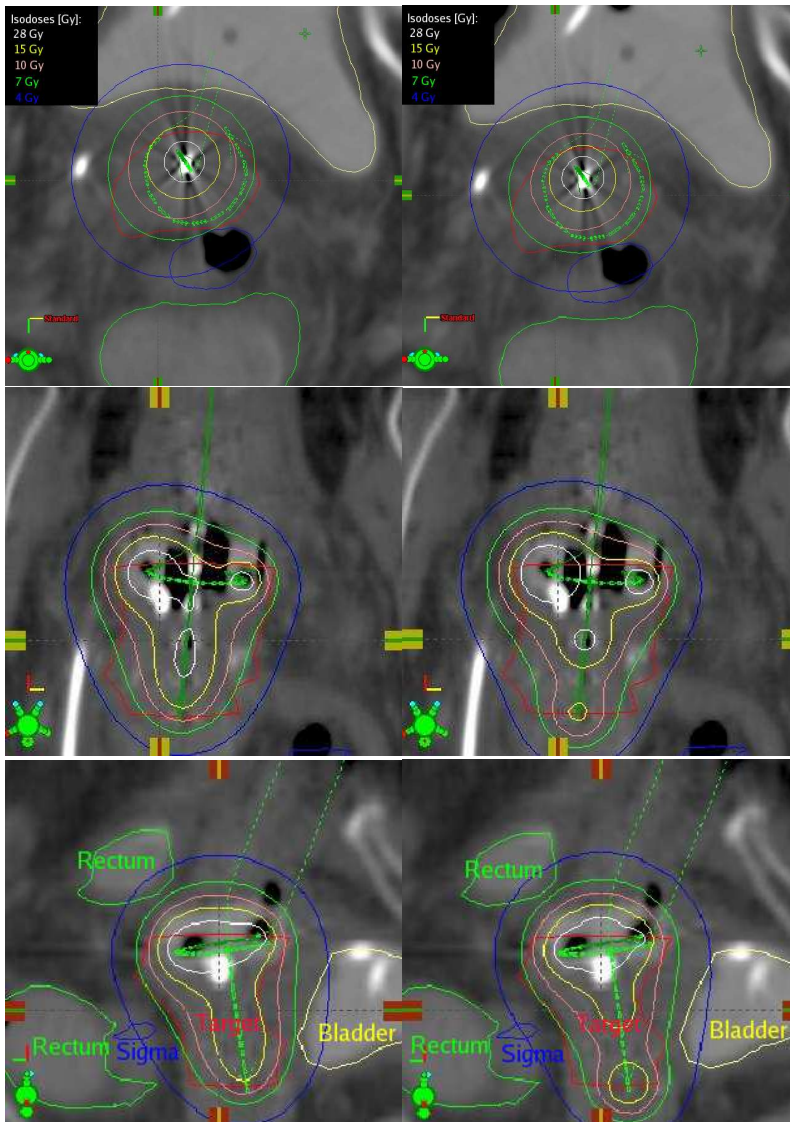


Figure 6.5: Left, the final dose distribution with IND-NIMBUS from different point of views (x, y, and z-direction), and right, for comparison, the solution obtained with BrachyVision[®] optimization. Target is red, rectum green, bladder yellow and sigma is blue. Isodose of 7 Gy is colored green.

of the final treatment plan compared to the other methods but the strength of our

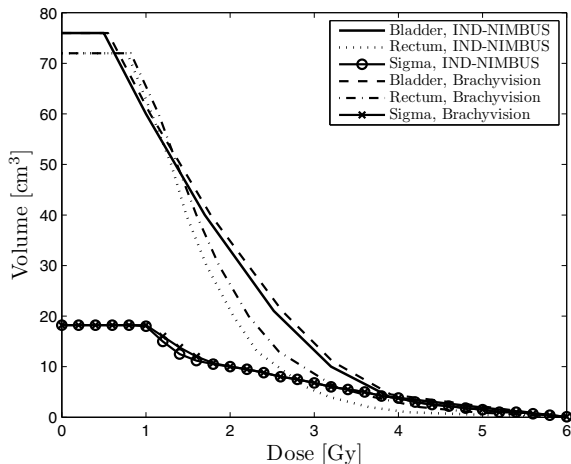


Figure 6.6: For comparison, dose volume histograms of critical organs C. Dose volume histogram values start to decline faster in the IND-NIMBUS solution than in the solution obtained with BrachyVision[®].

approach is its interactivity during the planning process, and thus the drawbacks (e.g. defining weights) of currently used methods can be avoided.

In the presented examples, there were 17 and 21 continuous decision variables and 508 and 473 sampling points, respectively. The amount of variables and sampling points can increase dramatically in more complex cases which are not studied here. Thus, it remains unclear and cannot be concluded how efficient our approach is in such cases. In addition, there were only box constraints for variables. However, it is easy to add any other constraints to our interactive multiobjective optimization approach if needed. Moreover, the idea of classifying objective functions is practical and their computation is fast also with different numbers of objective functions. The number of objective functions can be increased, but naturally this will increase the cognitive load imposed on the decision maker.

Finally, one must state that this approach brings the planning process near to the real clinical issues. With this system, the treatment planner considers directly the compromises to be made between target coverage and protection of critical organs instead of manipulating planning parameters such as dwell positions, dwell times, and objective weights. Whenever a trial-and-error planning is used, there are no guarantees for the *optimality* of the final solution. In contrast, our approach avoids these shortcomings and the treatment planner can be convinced that the final solution is the best compromise that can be achieved. As stated, these kinds of tools are not intended to replace human treatment planners, but to support them in their work.

Conclusions and topics for further research

In this thesis, MCDM and, in particular, multiobjective optimization were studied and developed. The goal was to improve interactive multiobjective optimization methods which could be implemented in real world applications: IMRT and brachytherapy (as well as in papermaking in the appendix). At the time when this research started, in the literature there were no interactive multiobjective optimization methods being applied to planning radiotherapy treatment and the material in this thesis was the first attempt to extend research into that area. There are investigations which are using some other multiobjective optimization method or some other interactive approach (even in the clinics). However, as far as is known, this is still the only approach which tackles the treatment planning process in an interactive and multiobjective way.

The application areas considered in this thesis contain very complex processes which have been developed during the years with the emphasis on modeling and optimization. However, these research areas are still novel, and the problematic is not very well known. These are the reasons why this thesis has focused on studying and developing new ideas for MCDM and multiobjective optimization to be applied to these real world problems. There is still a need for improving the MCDM tools, and the increased computational power has made it possible to use more precise simulation models mimicking the processes in optimization and supporting MCDM.

In this thesis, new ideas developed for supporting MCDM and multiobjective optimization were implemented. These included efficient use of trade-off information, and making approximations of Pareto optimal solutions and fronts in order to reduce the number of solutions needed to be computed. In this thesis, gradient information was used to support the navigation through a Pareto optimal front in interactive multiobjective optimization in different ways. First, we developed an idea on how to produce an approximation of a Pareto optimal front utilizing the gradient information. With this model, the behavior of the Pareto optimal front could be predicted. Second, gradient information could be used to generate trade-off information. In this part of the study the emphasis was that the deci-

sion maker could utilize the trade-off information to predict the most profitable direction where to guide the optimization process between the conflicting targets.

Presenting the gradient information to the decision maker in different ways could make the optimization process more intuitive, and decrease the number of irrelevant solutions needing to be computed. Since decision makers are able to predict how the solutions may behave and thus, identify solution process more efficiently and learn about the interrelationships between the objectives. This kind of assistance is welcome especially when these kinds of simulation models can be computationally costly.

In addition, a new way of visualizing the Pareto optimal solutions obtained as a part of decision making process was introduced in this thesis. In multiobjective decision making, Pareto optimal fronts are often visualized because in this way a comparison between solutions becomes easier. A Pareto optimal front is easy to visualize when there are only two to three objective functions, but visualizing more than three objective functions is challenging. Therefore, we have integrated multiobjective optimization with the 3D VR tool in order to study higher dimensional Pareto optimal solutions and approximated Pareto optimal fronts. The 3D VR tool made it easier to compare solutions, and to navigate from one solution to another by zooming and rotating the front. Moreover, it allowed a better comprehension of those solutions with the desired properties through highlighting. In addition, the use of sophisticated visualization tools meant that fewer solutions were needed to be computed in order to learn and understand the interrelationships of the conflicting objectives, and analyzing the solutions obtained became easier and more easily visualized and animated. This is also important especially if a problem is computationally expensive (e.g. in real-world industrial cases).

The ability to integrate VR with multiobjective optimization opened up a number of challenging research issues, such as handling a large number of objective functions, and simultaneous visualization of objective and solution spaces, as discussed in this thesis. The purpose was to reveal the power and usefulness of the VR environment in multiobjective optimization, and to introduce this technique as a new and promising means of visualizing and understanding complex interactions among objectives and solutions. All these kinds of innovative tools are designed to make it easier to obtain a deeper understanding of the MCDM problem.

In addition to the methodological ideas, in this thesis interactive multiobjective optimization was applied to real-world applications. These applications were IMRT and brachytherapy (and papermaking presented in the appendix). In a nutshell, we can say that based on the research conducted in this thesis, these interactive methods are now ready for implementation in radiotherapy treatment planning in the clinics.

IMRT

In this thesis, we presented an interactive multiobjective optimization approach using a classification-based method NIMBUS combined with the novel parameterized BTE radiotherapy dose calculation model in order to optimize treatment

plans interactively. This was done to avoid the limitations of the widely used optimization techniques, and because of the obvious advantages of using the BTE model in dose calculations. By using parameterization, the BTE dose calculation model is so fast that it can be used in an interactive multiobjective optimization.

In this approach, the decision maker's (i.e. treatment planner's) knowledge was accessed during the iterative solution process to direct the optimization using intuitive preference information in order to find the most preferred plan, that is, the best Pareto optimal solution, finding the correct balance between conflicting radiotherapy targets. This kind of decision support aid overcomes the drawbacks of trial-and-error planning, and planning times can be shortened and the plan quality improved by finding advantageous trade-offs and finding only feasible solutions by manipulating the desired values of the objective functions directly (not having to rely on weights or penalties). Our interactive approach is capable of handling radiotherapy objectives which are in conflict. Thus, we were able to describe the objective functions in a way that truly minimized the unwanted dose. Although this thesis studied academic examples only, we are interested to see how capable this approach is to be used also in clinical IMRT treatment planning problems.

Brachytherapy

Furthermore, an interactive multiobjective optimization method NIMBUS was applied for anatomy based 3D HDR brachytherapy optimization. In this research, the multiobjective nature of the problem was also genuinely taken into account in the problem formulation and in the interactive solution process which was directed by a treatment planner. The advantages of this kind of interactive approach were demonstrated by clinical examples.

The interactive approach was used to determine the dwell time values needed to deliver the desired dose to the tumor and to minimize the dose in each organ at risk in these clinical cases. When using the classification-based NIMBUS method, the decision maker's knowledge and preferences could be used during the iterative optimization process to direct the search in order to find the most preferred treatment plan. This information exchange was intuitive and understandable for treatment planners. In this way, treatment planning times can be made shorter and the quality of the treatment plans can be improved. Furthermore, the interactive approach offers a possibility to navigate among the obtained Pareto optimal solutions (i.e. different treatment plans). Therefore, the strength of our approach is its interactivity during the planning process. This approach brings the planning process near to the real clinical issues: with this system, the treatment planner plays directly with the compromises between target coverage and protection of organs at risk instead of manipulating dwell positions, dwell times, and objective weights. These kinds of tools are not intended to replace human treatment planners, but to support them in their work.

As a comment given by the radiotherapy experts, they conclude that there is a real need for having this kind of decision support tool in clinical use. Treatment planner who acted as a decision maker in this thesis was convinced of the poten-

tial of interactive methods, i.e. he felt that steering the optimization process in an interactive way is a good manner to execute the optimization of a treatment plan. However, he gave also some critical comments concerning the usability and comfortability of the decision making process. In other words, in addition to founding Pareto optimal solutions (treatment plans), the comfortability and smoothness of the treatment planning process must be really taken into account when designing the decision support tools.

In this study, the interaction between treatment planning software (including e.g. patient geometry) and the interactive optimization method was executed using text-files, and this is one reason why the decision making process was not so enjoyable and handy. However, the results presented in this thesis have proved that the approach is ready and easy to be integrated with a treatment planning software when also the usability problems can be fixed. Then, the approach could be taken into fully clinical use.

Topics for further research

Model-based decision support systems will become increasingly common in the near future, and one can predict that they will enter everyday use in the real world applications such as radiotherapy and industry. All the examples presented here are from radiotherapy (from papermaking in the appendix) but, nevertheless, irrespective of the industrial sector in question (e.g. motor, or aircraft industries), modeling related optimization problems need to solve the same challenges everywhere: selection of optimization methods, needs for modeling work, and handling conflicting multiple criteria. Evidence of this is that in this thesis the same optimization approaches were tested with two very different problems – radiotherapy and papermaking. Thus, the approaches presented can be applied to many more areas than considered here.

There are many further potential research topics in the field of MCDM. Ideas developed in this thesis for supporting the decision maker should be developed much more and further. For example, utilizing the gradient information in decision making process is only a beginning of the research. One can envisage more sophisticated ways to approximate Pareto optimal fronts and present the trade-off information to the decision maker. However, hopefully these ideas introduced will inspire further research and other researchers in this direction.

The VR environment also holds massive potential for visualization in the field of MCDM. Some of the developing ideas were discussed in Section 4.2 where the tool was introduced. The power of VR lies in its visualization potential and versatility. It can be used in visualizing not only objects but also scientific results, designs, etc. Thus, the human imagination is truly the only limit when devising the targets where VR technology can be utilized.

One further research topic in the field of model-based decision support systems and model-based multiobjective optimization could be dynamic process modeling and, as a result one could achieve dynamic multiobjective process optimization, for example. Preliminary studies in this area have been already made, see e.g.

[81].

Another potential research interest in the future could be pushing a Pareto optimal front toward an ideal point by reformulating the optimization problem during the optimization process similarly to the ideas presented in [24, 161]. This new optimization procedure differs from earlier approaches since first a multiobjective optimization problem is solved, and subsequently new parameters are explored and set for decision variables to be used in the second multiobjective optimization problem. The hypothesis is that in this way, a Pareto optimal front formed in the first step can be moved toward an ideal point. This would represent a very innovative way of seeking new and innovative variables to be used as decision variables in the optimization procedure. This approach could be useful in the redesigning of process equipment, for example, in which some of the process parameters are fixed but some other could be used as new variables in the process design. This may help to cut costs by simplifying the manufacturing process and providing new design parameters for remodeling and redeveloping processes.

If one wishes to draw a conclusion about future research actions to be done in the field of IMRT and brachytherapy, one can state that the research should be directed strongly in the clinical direction. In other words, the emphasis should be on integrating the interactive multiobjective optimization approach presented here with a clinical treatment planning software and then the developed approach would be ready to be adopted into clinical use on the hospital wards.

- [1] Alber M and Reemtsen R. Intensity modulated radiotherapy treatment planning by use of a barrier-penalty multiplier method. *Optimization Methods and Software*, 22:391–411, 2007.
- [2] Alterovitz R, Lessard E, Pouliot J, Hsu I, O’Brien JF, and Goldberg K. Optimization of HDR brachytherapy dose distributions using linear programming with penalty costs. *International Journal of Radiation Oncology*Biography*Physics*, 33:4012–4019, 2006.
- [3] Antonya C and Talaba D. Design evaluation and modification of mechanical systems in virtual environments. *Virtual Reality*, 11(4):275–285, 2007.
- [4] Belton V and Stewart T. *Multiple Criteria Decision Analysis, an Integration Approach*. Kluwer Academic Publishers, Norwell, MA, 2002.
- [5] Boman E. *Radiotherapy Forward and Inverse Problem Applying Boltzmann Transport Equation*. University of Kuopio, Kuopio, Finland, 2007. Doctoral thesis.
- [6] Brahme A. Treatment optimization using physical and radiobiological objective functions. In Smith AE, editor, *Radiation Therapy Physics*, pages 209–245. Springer, 1995.
- [7] Brahme A. Development of radiation therapy optimization. *Acta Oncologica*, 39:579–595, 2000.
- [8] Buchanan JT. A naïve approach for solving MCDM problems: the GUESS method. *Journal of the Operational Research Society*, 48:202–206, 1997.
- [9] Carlsson C and Fullér R. Multiple criteria decision making: the case for interdependence. *Computers & Operations Research*, 22:251–260, 1995.

- [10] Chajon E, Dumas I, Touleimat M, Magné N, Coulot J, Verstraet R, Lefkopoulos D, and Haie-Meder C. Inverse planning approach for 3-D MRI-based pulse-dose rate intracavitary brachytherapy in cervix cancer. *International Journal of Radiation Oncology*Biology*Physics*, 69:955–961, 2007.
- [11] Chankong V and Haimes YY. *Multiobjective Decision Making: Theory and Methodology*. Elsevier Science Publishing Co., Inc., New York, 1983.
- [12] Coello Coello CA, Van Veldhuizen DA, and Lamont GB. *Evolutionary Algorithms for Solving Multi-objective Problems*. Springer, 2nd edition, 2007.
- [13] Corana A, Marchesi M, Martini C, and Ridella S. Minimizing multimodal functions of continuous variables with the "simulated annealing" algorithm. *ACM Transactions on Mathematical Software*, 13:262–280, 1987.
- [14] Cotrutz C, Lahanas M, Kappas C, and Baltas D. A multiobjective gradient-based dose optimization algorithm for external beam conformal radiotherapy. *Physics in Medicine and Biology*, 46:2161–2175, 2001.
- [15] Craft D and Bortfeld T. How many plans are needed in an IMRT multi-objective plan database? *Physics in Medicine and Biology*, 53:2785–2796, 2008.
- [16] Craft D, Halabi T, and Bortfeld T. Exploration of tradeoffs in intensity-modulated radiotherapy. *Physics in Medicine and Biology*, 50:5857–5868, 2005.
- [17] Craft D, Halabi T, Shih HA, and Bortfeld T. An approach for practical multiobjective IMRT treatment planning. *International Journal of Radiation Oncology*Biology*Physics*, 69:1600–1607, 2007.
- [18] Cruz-Neira C, Sandin D, DeFanti T, Kenyon R, and Hart J. The CAVE: audio visual experience automatic virtual environment. *Communications of the ACM*, 35(6):64 – 72, 1992.
- [19] Deasy JO. Multiple local minima in radiotherapy optimization problems with dose-volume constraints. *Medical Physics*, 24:1157–1161, 1997.
- [20] Deb K. *Multi-Objective Optimization using Evolutionary Algorithms*. John Wiley & Sons, Chichester, 2nd edition, 2001.
- [21] Deb K and Gupta H. Searching for robust Pareto-optimal solutions in multi-objective optimization. In *Proceedings of the Third Evolutionary Multi-Criteria Optimization (EMO-05) Conference (Also Lecture Notes on Computer Science 3410)*, pages 150–164, 2005.
- [22] Deb K and Kumar A. Light beam search based multi-objective optimization using evolutionary algorithms. In *Proceedings of the Congress on Evolutionary Computation (CEC-07)*, pages 2125–2132, 2007.

- [23] Deb K and Miettinen K. Nadir Point Estimation Using Evolutionary Approaches: Better Accuracy and Computational Speed Through Focused Search. In Ehr Gott M, Naujoks B, Stewart T, and Wallenius J, editors, *Proceedings of the 19th International Conference on Multiple Criteria Decision Making*, Berlin, Heidelberg, to appear. Springer-Verlag.
- [24] Deb K and Srinivasan A. Innovization: innovating design principles through optimization. In *Proceedings of the Genetic and Evolutionary Computation Conference (GECCO-2006)*, pages 1629–1636, New York: The Association of Computing Machinery (ACM), 2006.
- [25] Deb K, Sundar J, Uday N, and Chaudhuri S. Reference point based multi-objective optimization using evolutionary algorithms. *International Journal of Computational Intelligence Research (IJCIR)*, 2(6):273–286, 2006.
- [26] Deb K, Thiele L, Laumanns M, and Zitzler E. Scalable Test Problems for Evolutionary Multi-Objective Optimization. In Abraham A, Jain R, and Goldberg R, editors, *Evolutionary Multiobjective Optimization: Theoretical Advances and Applications*, chapter 6, pages 105–145. Springer, 2005.
- [27] DeWitt KD, Hsu I, Speight J, Weinberg VK, Lessard E, and Pouliot J. 3D inverse treatment planning for the tandem and ovoid applicator in cervical cancer. *International Journal of Radiation Oncology*Biophysics**, 63:1270–1274, 2005.
- [28] Dyer JS, Fishburn PC, Steuer RE, Wallenius J, and Zionts S. Multiple criteria decision making, multiattribute utility theory: the next ten years. *Management science*, 38:645–654, 1992.
- [29] Eddy J and Lewis KE. Visualization of multidimensional design and optimization data using cloud visualization. In *Proceedings of DETC'02, ASME 2002 Design Engineering Technical Conferences and Computers and Information in Engineering Conference*, Montreal, Canada, 2002.
- [30] Ehr Gott M and Johnston R. Optimization of beam directions in intensity modulated radiation therapy planning. *OR Spectrum*, 25:251–264, 2003.
- [31] Ehr Gott M and Winz I. Interactive decision support in radiotherapy treatment planning. *OR Spectrum*, 30:311–329, 2008.
- [32] Eskelinen P. Objective trade-off rate information in interactive multi-objective optimization methods – a survey of theory and applications. *Helsinki School of Economics, Working Papers*, W-445, 2008. Available at <http://hsepubl.lib.hse.fi/pdf/wp/w445.pdf>.
- [33] Eskelinen P. *Reference Point Based Decision Support Tools for Interactive Multiobjective Optimization*. Helsinki School of Economics, Helsinki, Finland, 2008. Doctoral thesis.

- [34] Eskelinen P and Miettinen K. Trade-off analysis tool with applicability study for interactive nonlinear multiobjective optimization. *Helsinki School of Economics, Working Papers*, W-453, 2008. Available at <http://hsepubl.lib.hse.fi/pdf/wp/w453.pdf>.
- [35] Eskelinen P, Miettinen K, Klamroth K, and Hakanen J. Pareto navigator for interactive nonlinear multiobjective optimization. *OR Spectrum*, in press.
- [36] ESTECO. www.esteco.com.
- [37] Haas OCL, Burnham KJ, and Mills JA. Optimization of beam orientation in radiotherapy using planar geometry. *Physics in Medicine and Biology*, 43:2179–2193, 1998.
- [38] Haimes YY and Chankong V. Kuhn-Tucker multipliers as trade-offs in multiobjective decision-making analysis. *Automatica*, 15:59–72, 1979.
- [39] Hakanen J and Eskelinen P. Ideas of using trade-off information in supporting the decision maker in reference point based interactive multiobjective optimization. *Helsinki School of Economics, Working Papers*, W-405, 2006. Available at <http://hsepubl.lib.hse.fi/pdf/wp/w405.pdf>.
- [40] Hakanen J, Miettinen K, Mäkelä MM, and Manninen J. On interactive multiobjective optimization with NIMBUS in chemical process design. *Journal of Multicriteria Decision Analysis*, 13:125–134, 2005.
- [41] Halabi T, Craft D, and Bortfeld T. Dose-volume objectives in multi-criteria optimization. *Physics in Medicine and Biology*, 51:3809–3818, 2006.
- [42] Hamacher HW and Küfer KH. Inverse radiation therapy planning - a multiple objective optimization approach. *Discrete Applied Mathematics*, 118:145–161, 2002.
- [43] Hämäläinen J. *Mathematical Modelling and Simulation of Fluid Flows in the Headbox of a Paper Machine*. University of Jyväskylä, Jyväskylä, Finland, 1993. Doctoral thesis.
- [44] Hämäläinen J, Hämäläinen T, Madetoja E, and Ruotsalainen H. CFD-based optimization for a complete industrial process: papermaking. In Thévenin D and Janiga G, editors, *Optimization and Computational Fluid Dynamics*, pages 267–289. Springer, 2008.
- [45] Hämäläinen J, Madetoja E, and Ruotsalainen H. Simulation-based optimization and decision support for papermaking. In *Proceedings of International Conference on Pulping, Papermaking and Biotechnology*, pages 612–618, Nanjing, China, 2008.

- [46] Hämäläinen J, Miettinen K, Tarvainen P, and Toivanen J. Interactive solution approach to a multiobjective optimization problem in a paper machine headbox design. *Journal of Optimization Theory and Applications*, 116:265–281, 2003.
- [47] Heikkola E, Miettinen K, and Nieminen P. Multiobjective optimization of an ultrasonic transducer using NIMBUS. *Ultrasonics*, 44:368–380, 2006.
- [48] Henig MI and Buchanan JT. Tradeoff directions in multiobjective optimization problems. *Mathematical Programming*, 78:357–374, 1997.
- [49] Hiltunen K. *Mathematical and Numerical Modeling of Consolidation Processes in Paper Machines*. University of Jyväskylä, Jyväskylä, Finland, 1995. Doctoral thesis.
- [50] Hoffmann AL, Siem AYD, den Hertog D, Kaanders JHAM, and Huizenga H. Derivate-free generation and interpolation of convex Pareto optimal IMRT plans. *Physics in Medicine and Biology*, 51:6349–6369, 2006.
- [51] Holder A. Partitioning multiple objective optimal solutions with applications in radiotherapy design. *Optimization and Engineering*, 7:501–526, 2006.
- [52] Holm R. *Fluid Mechanics of Fibre Suspensions Related to Papermaking*. KTH The Royal Institute of Technology, Stockholm, Sweden, 2005. Doctoral thesis.
- [53] Horn J. Multicriteria decision making. In Bäck T, Fogel DB, and Michalewicz Z, editors, *Handbook of evolutionary computation*, Bristol, UK, 1997. Institute of Physics Publishing.
- [54] Hsu I, Lessard E, Weinberg V, and Pouliot J. Comparison of inverse planning simulated annealing and geometrical optimization for prostate high-dose-rate brachytherapy. *Brachytherapy*, 3:147–152, 2004.
- [55] Hwang CL and Masud ASM. *Multiple objective decision making - methods and applications*. Lecture Notes in Economics and Mathematical Systems. Springer-Verlag, Berlin, Germany, 2000.
- [56] Jayaram S, Jayaram U, Kim Y, DeChenne C, Lyons K, Palmer C, and Mitsui T. Industry case studies in the use of immersive virtual assembly. *Virtual Reality*, 11(4):217–228, 2007.
- [57] Kaliszewski I and Michalowski W. Generation of outcomes with selectively bounded trade-offs. *Foundations of Computing and Decision Sciences*, 20:113–122, 1995.
- [58] Kaliszewski I and Michalowski W. Efficient solutions and bounds on trade-offs. *Journal of Optimization Theory and Applications*, 94:381–394, 1997.

- [59] Karlsson M. *On-line Study and Mathematical Modeling of a Paper Dryer Section*. University of Turku, Turku, Finland, 1984. Doctoral thesis.
- [60] Klamroth K and Miettinen K. Integrating approximation and interactive decision making in multicriteria optimization. *Operations Research*, 56:222–234, 2008.
- [61] Kneschaurek P, Schiessl W, and Wehrmann R. Volume-based dose optimization in brachytherapy. *International Journal of Radiation Oncology*Biophysics*Physics*, 45:811–815, 1999.
- [62] Korhonen P and Wallenius J. *Visualization in the Multiple Objective Decision-Making Framework*. Lecture Notes in Economics and Mathematical Systems. Springer, 2008.
- [63] Korhonen P and Yu G. Quadratic Pareto race. In Shi Y and Zeleny M, editors, *New frontiers of decision making for the information technology era*. World Scientific Publishing Company, Singapore, 1st edition, May 2000.
- [64] Küfer KH, Hamacher HW, and Bortfeld TR. A multicriteria optimization approach for inverse radiotherapy planning. In Bortfeld TR and Schlegel W, editors, *Proceedings of the XIIIth ICCR*, pages 26–29. Springer, Berlin, 2000.
- [65] Küfer KH, Monz M, Scherrer A, Süß P, Alonso F, Sultan ASA, Bortfeld T, Craft D, and Thieke C. Multicriteria optimization in intensity modulated radiotherapy planning. *Berichte des Fraunhofer ITWM*, 2005.
- [66] Küfer KH, Scherrer A, Monz M, Alonso F, Trinkaus H, Bortfeld T, and Thieke C. Intensity-modulated radiotherapy - a large scale multi-criteria programming problem. *OR Spectrum*, 25:223–249, 2003.
- [67] Kuk H, Tanino T, and Tanaka M. Trade-off analysis for vector optimization problems via scalarization. *Journal of Information & Optimization Sciences*, 18:75–87, 1997.
- [68] Lahanas M and Baltas D. Are dose calculations during dose optimization in brachytherapy necessary? *Medical Physics*, 30(9):2368–2375, 2003.
- [69] Lahanas M, Baltas D, and Zamboglou N. Anatomy-based three-dimensional dose optimization in brachytherapy using multiobjective genetic algorithms. *Medical Physics*, 26:1904–1918, 1999.
- [70] Lahanas M, Baltas D, and Zamboglou N. A hybrid evolutionary algorithm for multiobjective anatomy based dose optimization in HDR brachytherapy. *Physics in Medicine and Biology*, 48:399–415, 2003.
- [71] Lahanas M, Milickovic N, Papagiannopoulou M, Baltas D, Zamboglou N, and Karouzakis K. Application of a hybrid version of NSGA-II for multiobjective dose optimization in brachytherapy. In Giannakoglou KC, Tsahalis DT, Périaux J, Papailiou KD, and Fogarty T, editors, *Evolutionary*

- Methods for Design, Optimization and Control with Applications to Industrial Problems*, pages 299–304, Athens, Greece, 2001. International Center for Numerical Methods in Engineering (CIMNE).
- [72] Lahanas M, Schreibmann E, and Baltas D. Multiobjective inverse planning for intensity modulated radiotherapy with constraint-free gradient-based optimization algorithms. *Physics in Medicine and Biology*, 48:2843–2871, 2003.
- [73] Langer M, Brown R, Urie M, Leong J, Stracher M, and Shapiro J. Large scale optimization of beam weights under dose-volume restrictions. *International Journal of Radiation Oncology*Biology*Physics*, 18:887–893, 1990.
- [74] Langer M, Lee EK, Deasy JO, Rardin RL, and Deye JA. Operations research applied to radiotherapy, an NCI-NSF-sponsored workshop-February 7-9, 2002. *International Journal of Radiation Oncology*Biology*Physics*, 57:762–768, 2003.
- [75] Langer M, Morrill S, Brown R, Lee O, and Lane R. A comparison of mixed integer programming and fast simulated annealing for optimizing beam weights in radiation therapy. *Medical Physics*, 23:957–964, 1996.
- [76] Larichev O. Cognitive validity in design of decision aiding techniques. *Journal of Multicriteria Decision Analysis*, 1:127–138, 1992.
- [77] Lee EK, Fox T, and Crocker I. Integer programming applied to intensity-modulated radiation treatment planning optimization. *Annals of Operations Research*, 119:165–181, 2003.
- [78] Lessard E, Hsu I, Aubry J, and Pouliot J. SU-FF-T-337: multiobjective inverse planning optimization: adjustment of dose homogeneity and urethra protection in HDR-brachytherapy of the prostate. *Medical Physics*, 33:2124, 2006.
- [79] Lessard E, Hsu I, and Pouliot J. Inverse planning for interstitial gynecologic template brachytherapy: truly anatomy-based planning. *International Journal of Radiation Oncology*Biology*Physics*, 54:1243–1251, 2002.
- [80] Lessard E and Pouliot J. Inverse planning anatomy-based dose optimization for HDR-brachytherapy of the prostate using fast simulated annealing algorithm and dedicated objective function. *Medical Physics*, 28:773–779, 2001.
- [81] Linnala M, Ruotsalainen H, Madetoja E, and Savolainen J. Dynamic multi-objective optimization in papermaking process simulation. In Madetoja E, Niskanen H, and Hämäläinen J, editors, *Proceedings of Papermaking Research Symposium 2009*, Kuopio, Finland, 2009.

- [82] Lotov AV. Computer-based support for planning and negotiation on environmental rehabilitation of water resource systems. In Loucks DP, editor, *Restoration of Degraded Rivers: Challenges, Issues and Experience*. Kluwer Academic publishers, Netherlands, 1998.
- [83] Lotov AV. Approximation and visualization of Pareto frontier in the framework of classical approach to multi-objective optimization. In Branke J, Deb K, Miettinen K, and Steuer RE, editors, *Practical Approaches to Multi-Objective Optimization*, number 04461 in Dagstuhl Seminar Proceedings. Internationales Begegnungs- und Forschungszentrum fuer Informatik (IBFI), Schloss Dagstuhl, Germany, 2005.
- [84] Lotov AV, Bourmistrova LV, Efremov RV, Bushenkov VA, L. BA, and Brainin NA. Experience of model integration and Pareto frontier visualization in the search for preferable water quality strategies. *Environmental modelling and software*, 20(2):243–260, 2005.
- [85] Lotov AV, Bushenkov V, and Kamenev G. *Interactive Decision Maps: Approximation and Visualization of Pareto Frontier*. Springer, 2004.
- [86] Lotov AV and Miettinen K. *Visualizing the Pareto Frontier*. Lecture Notes in Economics and Mathematical Systems. Springer, 2008.
- [87] Madetoja E. *Novel Process Line Approach for Model-based Optimization in Papermaking – Sensitivity and Uncertainty Analysis*. University of Kuopio, Kuopio, Finland, 2007. Doctoral thesis.
- [88] Madetoja E, Miettinen K, and Tarvainen P. Issues related to the computer realization of a multidisciplinary and multiobjective optimization system. *Engineering with Computers*, 22:33–46, 2006.
- [89] Madetoja E, Ruotsalainen H, and Mönkkönen VM. New visualization aspects related to intelligent solution procedure in papermaking optimization. In Herskovits J, Canelas A, Cortes H, and Aroztegui M, editors, *CD Proceedings of Conference on EngOpt 2008 - International Conference on Engineering Optimization*, Rio de Janeiro, Brazil, 2008.
- [90] Madetoja E, Ruotsalainen H, Mönkkönen VM, Hämäläinen J, and Deb K. Visualizing multi-dimensional Pareto-optimal fronts with a 3D virtual reality system. In *Proceeding of IMCSIT 2008 - International Multiconference on Computer Science and Information Technology: Workshop on Computational Optimization (WCO'08)*, pages 907–913, Wisla, Poland, 2008.
- [91] Madetoja E, Ruotsalainen H, Mönkkönen VM, Hämäläinen J, and Deb K. Approach for visualizing multi-dimensional Pareto-optimal fronts using a 3D VR system. *Analele Universitatii de Vest Timisoara, Seria Matematica-Informatica*, in press.

- [92] Madetoja E and Tarvainen P. Multiobjective process line optimization under uncertainty applied to papermaking. *Structural and Multidisciplinary Optimization*, 35:461–472, 2008.
- [93] Meyer J, Phillips MH, Cho PS, Kalet I, and Doctor JN. Application of influence diagrams to prostate intensity-modulated radiation therapy plan selection. *Physics in Medicine and Biology*, 49:1637–1653, 2004.
- [94] Miettinen K. *On the Methodology of Multiobjective Optimization with Applications*. University of Jyväskylä, Jyväskylä, Finland, 1994. Doctoral thesis.
- [95] Miettinen K. *Nonlinear Multiobjective Optimization*. Kluwer, Boston, 1999.
- [96] Miettinen K. IND-NIMBUS for demanding interactive multiobjective optimization. In Trzaskalik T, editor, *Multiple Criteria Decision Making '05*, pages 137–150. The Karol Adamiecki University of Economics, Katowice, 2006.
- [97] Miettinen K and Mäkelä MM. Interactive bundle-based method for non-differentiable multiobjective optimization: NIMBUS. *Optimization*, 34:231–246, 1995.
- [98] Miettinen K and Mäkelä MM. On scalarizing functions in multiobjective optimization. *OR Spectrum*, 24:193–213, 2002.
- [99] Miettinen K and Mäkelä MM. Synchronous approach in interactive multiobjective optimization. *European Journal of Operational Research*, 170:909–922, 2006.
- [100] Miettinen K, Mäkelä MM, and Kaario K. Experiments with classification-based scalarizing functions in interactive multiobjective optimization. *European Journal of Operational Research*, 175:931–947, 2006.
- [101] Miettinen K, Mäkelä MM, and Männikkö T. Optimal control of continuous casting by nondifferentiable multiobjective optimization. *Computational Optimization and Applications*, 11:177–194, 1998.
- [102] Miettinen K and Mäkelä M. Comparing two version of NIMBUS optimization system. *Reports of the department of mathematical information technology, Laboratory of Scientific Computing*, 23, 1996.
- [103] Miettinen K, Ruiz F, Luque M, and Eskelinen P. NAUTILUS method: an interactive technique in multiobjective optimization based on the nadir point. *European Journal of Operational Research*, submitted.
- [104] Milickovic N, Lahanas M, Papagiannopoulou M, Baltas D, Zamboglou N, and Karouzakis K. Application of multiobjective genetic algorithms in anatomy based dose optimization in brachytherapy and its comparison with deterministic algorithms. In Giannakoglou KC, Tsahalis DT, Périaux J,

- Papailiou KD, and Fogarty T, editors, *Evolutionary Methods for Design, Optimization and Control with Applications to Industrial Problems*, pages 293–298, Athens, Greece, 2001. International Center for Numerical Methods in Engineering (CIMNE).
- [105] Milickovic N, Lahanas M, Papagiannopoulou M, Zamboglou N, and Baltas D. Multiobjective anatomy-based dose optimization for HDR-brachytherapy with constraint free deterministic algorithms. *Physics in Medicine and Biology*, 47:2263–2280, 2002.
- [106] Monz M, Küfer KH, Bortfeld TR, and Thieke C. Pareto navigation - algorithmic foundation of interactive multi-criteria IMRT planning. *Physics in Medicine and Biology*, 53:985–998, 2008.
- [107] Morton GC, Sankrecha R, Halina P, and Loblaw A. A comparison of anatomy-based inverse planning with simulated annealing and graphical optimization for high-dose-rate prostate brachytherapy. *Brachytherapy*, 7:12–16, 2008.
- [108] Nakayama H. Trade-off analysis using parametric optimization techniques. *European Journal of Operational Research*, 60:87–98, 1992.
- [109] Nakayama H and Sawaragi Y. Satisficing trade-off method for multiobjective programming. In Grauer M and Wierzbicki AP, editors, *Interactive Decision Analysis*, pages 113–122. Springer Verlag, Berlin, 1984.
- [110] Nath R, Anderson LL, Luxton G, Weaver KA, Williamson JF, and Meigooni AS. Dosimetry of interstitial brachytherapy sources: recommendations of the AAPM Radiation Therapy Committee Task Group No. 43. *Medical Physics*, 22:209–234, 1995.
- [111] Pareto V. *Cours d'Economie Politique*. Librairie Droz, Genève, 1964. The first edition in 1896.
- [112] Pareto V. *Manual of Political Economy*. The MacMillan Press Ltd, 1971. The original edition in French in 1927.
- [113] Pouliot J, Kim Y, Lessard E, Hsu I, Vigneron DB, and Kurhanewicz J. Inverse planning for HDR prostate brachytherapy used to boost dominant intraprostatic lesion defined by magnetic resonance spectroscopy imaging. *International Journal of Radiation Oncology*Biophysics*, 59:1196–1207, 2004.
- [114] Power D. *Decision Support Systems: Concepts and Resources for Managers*. Quorum Books, Westport, Conn., 2002.
- [115] Riestra JA. *A Generalized Taylor's Formula for Functions of Several Variables and Certain of Its Applications*. John Wiley & Sons Inc., New York, NY, 1995.

- [116] Rivard MJ, Coursey BM, DeWerd LA, Hanson WF, Saiful Huq M, Ibbott GS, Mitch MG, Nath R, and Williamson JF. Update of AAPM Task Group No. 43 report: a revised AAPM protocol for brachytherapy dose calculations. *Medical Physics*, 31:633–674, 2004.
- [117] Romeijn HE, Ahuja RK, Dempsey JF, Kumar A, and Li JG. A novel linear programming approach to fluence map optimization for intensity modulated radiation therapy treatment planning. *Physics in Medicine and Biology*, 48:3521–3542, 2003.
- [118] Romeijn HE, Dempsey JF, and Li JG. A unifying framework for multi-criteria fluence map optimization models. *Physics in Medicine and Biology*, 49:1991–2013, 2004.
- [119] Rosen I, Liu HH, Childress N, and Liao Z. Interactively exploring optimized treatment plans. *International Journal of Radiation Oncology*Biophysics*, 61(2):570–582, 2005.
- [120] Ruotsalainen H, Boman E, Miettinen K, and Hämäläinen J. Interactive multiobjective optimization for IMRT. *Helsinki School of Economics, Working Papers*, W-409, 2006. Available at <http://hsepubl.lib.hse.fi/pdf/wp/w409.pdf>.
- [121] Ruotsalainen H, Boman E, Miettinen K, and Tervo J. Nonlinear interactive multiobjective optimization method for radiotherapy treatment planning with Boltzmann transport equation. *Contemporary Engineering Sciences*, 2:391–422, 2009.
- [122] Ruotsalainen H, Madetoja E, and Hämäläinen J. Navigation on a Pareto-optimal front utilizing gradient information in interactive multiobjective optimization. In Herskovits J, Canelas A, Cortes H, and Aroztegui M, editors, *CD Proceedings of Conference on EngOpt 2008 - International Conference on Engineering Optimization*, Rio de Janeiro, Brazil, 2008.
- [123] Ruotsalainen H, Madetoja E, Mönkkönen VM, and Deb K. Supporting multiobjective decision making with 3D virtual reality: preliminary results and future extensions. *International Journal of Information Technology and Decision Making*, submitted.
- [124] Ruotsalainen H, Miettinen K, and Palmgren JE. Interactive multiobjective optimization for 3D HDR brachytherapy applying IND-NIMBUS. In Jones D, Tamiz M, and Ries J, editors, *New Developments in Multiple Objective and Goal Programming*. Springer, 2010.
- [125] Ruotsalainen H, Miettinen K, Palmgren JE, and Lahtinen T. Interactive multiobjective optimization for HDR brachytherapy. *Reports of the department of mathematical information technology, Series B. Scientific Computing*, B 14, 2008.

- [126] Sawaragi Y, Nakayama H, and Tanino T. *Theory of Multiobjective Optimization*. Academic Press Inc., Orlando, FL, 1985.
- [127] Schaffer J. Multiple objective optimization with vector evaluated genetic algorithms. In Grefensttete J, editor, *Proceedings of the First International Conference on Genetic Algorithms (ICGA)*, pages 93–100. Hillsdale, NJ, 1987.
- [128] Schreibmann E, Lahanas M, Xing L, and Baltas D. Multiobjective evolutionary optimization of the number of beams, their orientations and weights for intensity-modulated radiation therapy. *Physics in Medicine and Biology*, 49:747–770, 2004.
- [129] Shepard DM, Ferris MC, Olivera GH, and Mackie TR. Optimization the delivery of radiation therapy to cancer patients. *SIAM Review*, 41:721–744, 1999.
- [130] Sherman W and Craig A. *Understanding Virtual Reality: Interface, Application, and Design*. Elsevier Science, 2003.
- [131] Sloboda RS. Optimization of brachytherapy dose distributions by simulated annealing. *Medical Physics*, 19:955–964, 1992.
- [132] Starr MK and Zeleny M. *Multiple Criteria Decision Analysis*. North-Holland, 1978.
- [133] Steuer RE. *Multiple Criteria Optimization: Theory, Computation, and Application*. John Wiley & Sons, New York, 1986.
- [134] Steuer RE and Na P. Multiple criteria decision making combined with finance: a categorized bibliographic study. *European Journal of Operational Research*, 150:496–515, 2003.
- [135] Stewart TJ. A critical survey on the status of multiple criteria decision making theory and practise. *OMEGA - The International Journal of Management Science*, 20:569–586, 1992.
- [136] Sumida I, Shiomi H, Yoshioka Y, Inoue T, Lessard E, Hsu I, and Pouliot J. Optimization of dose distribution for HDR brachytherapy of the prostate using attraction-repulsion model. *International Journal of Radiation Oncology*Biography*Physics*, 64:643–649, 2006.
- [137] Tagziria H. Review of Monte Carlo and deterministic codes in radiation protection and dosimetry. In *NLP Report*. Teddington, 2000.
- [138] Tanino T and Kuk H. Nonlinear multiobjective programming. In Ehrgott M and Gandibleux X, editors, *Multiple Criteria Optimization: State of Art Annotated Bibliographic Surveys*, International Series in Operations Research & Management Science, pages 71–128. Springer US, 2008.

- [139] Tappeta RV and Renaud JE. Interactive multiobjective optimization procedure. *American Institute of Aeronautics and Astronautics Journal*, 37:881–889, 1999.
- [140] Tappeta RV, Renaud JE, Messac A, and Sundararaj GJ. Interactive physical programming: tradeoff analysis and decision making in multidisciplinary optimization. *American Institute of Aeronautics and Astronautics Journal*, 38:917–926, 2000.
- [141] Tappeta RV, Renaud JE, and Rodríguez JF. An interactive multiobjective optimization design strategy for decision based multidisciplinary design. *Engineering Optimization*, 34:523–544, 2002.
- [142] Tervo J, Kolmonen P, Vauhkonen M, Heikkinen LM, and Kaipio JP. A finite-element model of electron transport in radiation therapy and a related inverse problem. *Inverse Problems*, 15:1345–1361, 1999.
- [143] Tervo J, Lyyra-Laitinen T, Kolmonen P, and Boman E. An inverse treatment planning model for intensity modulated radiation therapy with dynamic MLC. *Applied Mathematics and Computation*, 135:227–250, 2003.
- [144] Tervo J, Vauhkonen M, and Boman E. Optimal control model for radiation therapy inverse planning applying the Boltzmann transport equation. *Linear Algebra and Its Applications*, 428:1230–1249, 2008.
- [145] Thieke C, Küfer KH, Monz M, Scherrer A, Alonso F, Oelfke U, Huber DJ, P. E., and Bortfeld T. A new concept for interactive radiotherapy planning with multicriteria optimization: first clinical evaluation. *Radiotherapy and Oncology*, 85:292–298, 2007.
- [146] Thieke L, Miettinen K, Korhonen P, and Molina J. A preference-based evolutionary algorithm for multiobjective optimization. *Evolutionary Computation*, in press.
- [147] Tilanus CB, de Gans OB, and Lenstra JK. Postscript: a survey of reasons for failure or success of quantitative methods in management. In Tilanus CB, de Gans OB, and Lenstra JK, editors, *Quantitative Methods in Management: Case Studies of Failures and Successes*, pages 269–273. Wiley, 1983.
- [148] Valdés J and Barton A. Virtual reality spaces for visual data mining with multi-objective evolutionary optimization: implicit and explicit function representations mixing unsupervised and supervised properties. In *Proceedings of IEEE World Congress on Evolutionary Computation*, Vancouver, Canada, 2006.
- [149] Valdés J, Barton A, and Orchard R. Virtual reality high dimensional objective spaces for multi-objective optimization: an improved representation. In *Proceedings of IEEE World Congress on Evolutionary Computation*, Singapore, 2007.

- [150] Webb S. *The Physics of Three-Dimensional Radiation Therapy*. IOP Publishing Ltd, Bristol, UK, 1993.
- [151] Weistroffer HR and Narula SC. The state of multiple criteria decision support software. *Annals of Operations Research*, 72:299–313, 1997.
- [152] Wierzbicki A. A mathematical basis for satisficing decision making. *Mathematical Modelling*, 3:391–405, 1982.
- [153] Wierzbicki A. *Model-based Decision Support Methodology with Environmental Applications*. Kluwer, Dordrecht, Netherlands, 2000.
- [154] Wu X and Zhu Y. An optimization method for importance factors and beam weights based on genetic algorithms for radiotherapy treatment planning. *Physics in Medicine and Biology*, 46:1085–1099, 2001.
- [155] Yang JB and Li D. Normal vector identification and interactive tradeoff analysis using minimax formulation in multiobjective optimization. *IEEE Transactions on Systems, Man, and Cybernetics – Part A: Systems and Humans*, 32:305–319, 2002.
- [156] Yano H and Sakawa M. Trade-off rates in the weighted Tchebycheff norm method. *Large Scale Systems*, 13:167–177, 1987.
- [157] Yasuo Y, Harada H, Murayama S, Kanazawa K, Nishimura T, Kamata M, and Fuji H. Evaluation of anatomy-based dwell position and inverse optimization in high-dose-rate brachytherapy of prostate cancer: a dosimetric comparison to a conventional cylindrical dwell position, geometric optimization, and dose-point optimization. *Radiotherapy and Oncology*, 75:311–317, 2005.
- [158] Yu PL. *Multiple-Criteria Decision Making*. Mathematical concepts and methods in science and engineering. Plenum Press, New York, 1985.
- [159] Yu Y. Multiobjective decision theory for computational optimization in radiation therapy. *Medical Physics*, 24:1445–1454, 1997.
- [160] Yu Y, Zhang JB, Cheng G, Schell MC, and Okunieff P. Multi-objective optimization in radiotherapy: applications to stereotactic radiosurgery and prostate brachytherapy. *Artificial Intelligence in Medicine*, 19:39–51, 2000.
- [161] Zeleny M. A concept of compromise solutions and the method of the displaced ideal. *Computers & Operations Research*, 1:479–496, 1974.
- [162] Zeleny M. The KM-MCDM interface in decision design: tradeoffs-free conflict dissolution. *International Journal of Applied Decision Sciences*, 1:3–23, 2008.
- [163] Zitzler E. *Evolutionary Algorithms for Multiobjective Optimization: Methods and Applications*. Swiss Federal Institute of Technology Zurich, Zürich, Switzerland, 1999. Doctoral thesis.

Dose calculation using finite element model

Boltzmann transport equation model

Here, the BTE model used in this thesis is described briefly: for further information, see [144]. Physically, the BTE model is based on particle equilibrium in infinitesimally small voxels of tissue. In the case of radiotherapy, it is appropriate to use the stationary form of the BTE. In this case, taking into account elastic collision, inelastic collision and deceleration radiation, the model consists of a coupled system of stationary linear integro-partial differential equations

$$\begin{aligned}
 \Omega \cdot \nabla \psi_1 + K_1(\psi_1, \psi_2, \psi_3) &= Q_1(\vec{x}, E, \Omega) \\
 \Omega \cdot \nabla \psi_2 + K_2(\psi_1, \psi_2, \psi_3) &= Q_2(\vec{x}, E, \Omega) \\
 \Omega \cdot \nabla \psi_3 + K_3(\psi_1, \psi_2, \psi_3) &= Q_3(\vec{x}, E, \Omega),
 \end{aligned} \tag{A.1}$$

where $\psi_j = \psi_j(\vec{x}, E, \Omega)$ ($j = 1, 2, 3$) are the phase space densities for photons, electrons and positrons, respectively. The variable $\vec{x} = (\vec{x}_1, \vec{x}_2, \vec{x}_3)$ is a point in the patient domain $V \subset \mathbb{R}^3$. Particle energy is denoted by E . The surface of the unit sphere in \mathbb{R}^3 is denoted by S , and $\Omega = (\cos \varphi \sin \theta, \sin \varphi \sin \theta, \cos \theta) =: h(\varphi, \theta)$ is a point on S , where φ and θ are standard spherical coordinates on surface S .

The functions $K_j(\psi_1, \psi_2, \psi_3)$ ($j = 1, 2, 3$) are collision terms combining attenuation and secondary production resulting from the above-mentioned different kinds of interactions, and K_1, K_2, K_3 are linear operators of $\psi := (\psi_1, \psi_2, \psi_3)$. Finally, $Q_j(\vec{x}, E, \Omega)$ ($j = 1, 2, 3$) are the source terms, which are typically zero in external radiotherapy, as also in this case. In the following section, we denote the system (A.1) in a compact way by

$$(\Omega \cdot \nabla + K)\psi = Q. \tag{A.2}$$

Boundary conditions and variational form

We consider the external photon radiation by setting boundary conditions for the photon inflow [144]. We assume that the boundary of the patient domain ∂V is a

piecewise smooth Lipschitz boundary. Thus, the outward normal $\nu(\vec{x})$ exists and is continuous on ∂V even though there might exist a set with surface measure zero.

A typical photon inflow boundary condition for the solution ψ is of the form

$$\begin{aligned} \psi_2(\vec{x}, E, \Omega) &= \psi_3(\vec{x}, E, \Omega) = 0 \text{ for } (\vec{x}, E, \Omega) \in \partial V \times I \times S \\ &\quad \text{such that } \Omega \cdot \nu(\vec{x}) < 0 \\ \psi_1(\vec{x}, E, \Omega) &= u(\vec{x}, E, \Omega) \text{ for } (\vec{x}, E, \Omega) \in \partial V \times I \times S \\ &\quad \text{such that } \Omega \cdot \nu(\vec{x}) < 0, \end{aligned} \quad (\text{A.3})$$

where I is an energy interval. The symbol u stands for the photon flux density on ∂V and $u \in L_2(\partial V \times I \times S)$. The boundary condition $\psi_1 = u$ for $\Omega \cdot \nu(\vec{x}) < 0$ and $\vec{x} \in \partial V$ means that the flux u is incoming outwardly on the patch ∂V and the boundary condition $\psi_j = 0, (j = 2, 3)$ for $\Omega \cdot \nu(\vec{x}) < 0$ means that no other particles generate outward fluxes. The solution ψ is defined in the six-dimensional state space $G := V \times I \times S$.

The variational form of the equation (A.2) with the stated boundary condition (A.3) is given in [144], and it is of the form

$$B(\psi, v) = F(v), \quad v \in H^3, \quad (\text{A.4})$$

where $B(\cdot, \cdot) : H^3 \times H^3 \mapsto \mathbb{R}$ is the bilinear form, v is a test function, H is an appropriate Hilbert space,

$$\begin{aligned} B(\psi, v) &= -\langle \psi, \Omega \cdot \nabla v \rangle_{L_2(G)^3} \\ &\quad + \sum_{j=1}^3 \int_S \int_I \int_{\partial V} (\Omega \cdot \nu)_+ \psi_j v_j d\sigma dE d\Omega + \langle K\psi, v \rangle_{L_2(G)^3} \end{aligned} \quad (\text{A.5})$$

and

$$F(v) = \langle Q, v \rangle_{L_2(G)^3} + \int_S \int_I \int_{\partial V} (\Omega \cdot \nu)_- uv_1 d\sigma dE d\Omega, \quad (\text{A.6})$$

where σ is the surface measure on ∂V . The subscript “+” refers to the positive part of the function and the subscript “-” refers to the negative part of the function.

Dose computation

We compute the dose in the following way. The incoming flux density of the l^{th} field S_l is u_l . It is assumed that $u_l \in L_2(\Gamma_l \times I \times S)$, where Γ_l is a patch of ∂V where the radiation is entering the domain V . Here $\psi^l = (\psi_1^l, \psi_2^l, \psi_3^l)$ is the flux density corresponding to the field S_l , i.e. ψ^l is the solution of the equation

$$(\Omega \cdot \nabla + K)\psi^l = 0 \quad (\text{A.7})$$

with the boundary condition

$$\begin{aligned}
\psi_2^l(\vec{x}, E, \Omega) &= \psi_3^l(\vec{x}, E, \Omega) = 0 \text{ for } (\vec{x}, E, \Omega) \in \partial V \times I \times S \\
&\quad \text{such that } \Omega \cdot \nu(\vec{x}) < 0 \\
\psi_1^l(\vec{x}, E, \Omega) &= 0, \text{ for } (\vec{x}, E, \Omega) \in (\partial V \setminus \Gamma_l) \times I \times S \\
&\quad \text{such that } \Omega \cdot \nu(\vec{x}) < 0 \\
\psi_1^l(\vec{x}, E, \Omega) &= u_l(\vec{x}, E, \Omega) \text{ for } (\vec{x}, E, \Omega) \in \Gamma_l \times I \times S \\
&\quad \text{such that } \Omega \cdot \nu(\vec{x}) < 0.
\end{aligned} \tag{A.8}$$

We define $u \in L_2(\partial V \times I \times S)$ such that

$$u = \sum_{l=1}^L u_l \chi_l, \tag{A.9}$$

where $\chi_l : \partial V \times I \times S \rightarrow \mathbb{R}$ are the characteristic functions of $\Gamma_l \times I \times S$ ($l = 1, \dots, L$). Let $\psi = (\psi_1, \psi_2, \psi_3)$ be the solution of problem (A.2) with the boundary condition (A.3) where u is defined by (A.9). The solution of problem (A.2)-(A.3) is

$$\psi = \left(\sum_{l=1}^L \psi_1^l, \sum_{l=1}^L \psi_2^l, \sum_{l=1}^L \psi_3^l \right), \tag{A.10}$$

where ψ^l ($l = 1, \dots, L$) are the solutions of (A.7)-(A.8). Now the total dose distribution $D(\vec{x})$ from the incoming fields S_l ($l = 1, \dots, L$) at a point \vec{x} of the patient domain V can be obtained from the measurement integral

$$D(\vec{x}) = \sum_{j=2}^3 \int_S \int_I \kappa_j(\vec{x}, E) \psi_j(\vec{x}, E, \Omega) dE d\Omega, \tag{A.11}$$

where $\kappa_j(\vec{x}, E)$ are known stopping power factors for electrons and positrons and ψ is the solution of (A.4) with $u = \sum_{l=1}^L u_l \chi_l$.

Discrete finite element model for radiotherapy

For computer needs, the model presented has to be discretized, and we use the finite element method (FEM) because the inflow boundary condition is quite easy to handle via variational formulations.

To clarify the u -dependence of variables, we denote $\psi = \psi(u)$ if needed. Let $F : L_2(\partial V \times I \times S) \mapsto (H^3)^*$ (where $*$ refers to the adjoint space, see [144]) be the operator defined by

$$(Fu)(v) = \int_S \int_I \int_{\partial V} (\Omega \cdot \nu)_- u v_1 d\sigma dE d\Omega. \tag{A.12}$$

Note that $F(v) = (Fu)(v)$. Using these notations $\psi = \psi(u)$ satisfies the variational equation

$$B(\psi(u), v) = (Fu)(v), \quad v \in H^3. \tag{A.13}$$

Let X_h be a finite dimensional subspace of H^3 and let Y_h be a finite dimensional subspace of $L_2(\partial V \times I \times S)$. Denote a basis of X_h by $\{v_1, \dots, v_N\}$ and denote a basis of Y_h by $\{w_1, \dots, w_M\}$. Let

$$\psi_h = \sum_{n=1}^N \alpha_n v_n, \quad u_h = \sum_{m=1}^M \beta_m w_m. \quad (\text{A.14})$$

Now the FEM approximation of the variational equation (A.13) is defined as

$$B(\psi_h, v) = (Fu_h)(v), \quad v \in X_h. \quad (\text{A.15})$$

This leads to the system of equations

$$\mathbf{A}\alpha = \mathbf{B}\beta, \quad (\text{A.16})$$

where $\mathbf{A} \in M(N \times N)$, $\mathbf{B} \in M(N \times M)$ such that $\mathbf{A}(k, n) = B(v_n, v_k)$ and $\mathbf{B}(k, m) = (Fw_m)(v_k)$. In addition, we have vectors $\alpha = (\alpha_1, \dots, \alpha_N)^T$ and $\beta = (\beta_1, \dots, \beta_M)^T$. Equation (A.16) can be expressed in the form

$$(\mathbf{A} \quad -\mathbf{B}) \begin{pmatrix} \alpha \\ \beta \end{pmatrix} = 0, \quad (\text{A.17})$$

which is actually the variational equation (A.13) in its discrete form.

Parameterization of the discrete finite element model

We say that the equation (A.17) is parameterized by a matrix $\mathbf{S} \in M(N + M, p)$ if

$$(\mathbf{A} \quad -\mathbf{B}) \begin{pmatrix} \alpha \\ \beta \end{pmatrix} = 0 \Leftrightarrow \begin{pmatrix} \alpha \\ \beta \end{pmatrix} = \mathbf{S}\gamma, \quad \gamma \in \mathbb{R}^p. \quad (\text{A.18})$$

Let p_1, p_2 be the canonical projections

$$p_1 : \mathbb{R}^{N+M} \rightarrow \mathbb{R}^N \quad (\text{A.19})$$

$$p_2 : \mathbb{R}^{N+M} \rightarrow \mathbb{R}^M. \quad (\text{A.20})$$

Denote $\mathbf{S}_j\gamma = p_j(\mathbf{S}\gamma)$ ($j = 1, 2$). Then $\alpha = \mathbf{S}_1\gamma$ and $\beta = \mathbf{S}_2\gamma$. Hence we can denote

$$\psi \approx \psi_h = \sum_{n=1}^N \alpha_n v_n = \sum_{n=1}^N (\mathbf{S}_1\gamma)_n v_n := S_1\gamma \quad (\text{A.21})$$

and

$$u \approx u_h = \sum_{m=1}^M \beta_m w_m = \sum_{m=1}^M (\mathbf{S}_2\gamma)_m w_m := S_2\gamma, \quad (\text{A.22})$$

where $\gamma \in \mathbb{R}^p$. With finite elements, the matrices \mathbf{A} and \mathbf{B} have a full rank and that is why we have here $p = M$.

After the parameterization, the dose can be approximately solved from the equation

$$D(\vec{x}) \approx D\gamma(\vec{x}) = \sum_{j=2}^3 \int_S \int_I \kappa_j(\vec{x}, E) (S_1\gamma)_j(\vec{x}, E, \Omega) dE d\Omega. \quad (\text{A.23})$$

In optimization, γ is the vector of decision variables.

Singular value decomposition (SVD) can be used in the parameterization of the discrete system, that is, in finding the matrix \mathbf{S} . Parameterization makes it possible to optimize large problems based on the finite element model. After parameterization, the number of unknown variables is decreased from $N + M$ to M . Parameterization of the system $(\mathbf{A} \quad -\mathbf{B}) \begin{pmatrix} \alpha \\ \beta \end{pmatrix} = 0$ is considered in more detail in [144].

Case study: papermaking

In this thesis, papermaking is investigated as a case study. The methods developed and applied in this work were tested also in the papermaking example in order to prove their versatility and power. This case study continues the research initiated by Prof. Hämäläinen and Dr. Madetoja et al [44, 45, 46, 87, 92].

Papermaking process is an example of an industrial process that has been studied extensively with modeling, simulation and optimization. The basic papermaking process involves two main stages: forming a pulp (i.e. a suspension of fibres), and forming of paper sheet by spreading this suspension on a porous forming fabric, where it is dried often under pressure. Nowadays there are four main paper machine parts involved in papermaking process: headbox, former, press section and drying. In addition, there can be some finishing parts such as coating or calendering in order to improve paper surface properties. Research in modeling of the papermaking unit-processes has been active through the years, see [43, 49, 52, 59], for examples. Modeling the whole papermaking process requires several modeling techniques as well as combining different unit-process models together into a large simulation model. For this purpose, a process line approach (called also a virtual papermaking line) [87, 92] has been developed. This makes it possible to combine unit-processes and define model-based optimization problems with numerous criteria. Thus, the interactive multiobjective optimization, in which a user can participate in processing the solution by giving preference information, can be used.

Interactive multiobjective optimization of papermaking

As an industrial optimization case, the papermaking optimization problem is naturally multiobjective, i.e. it contains several conflicting objectives. Thus, when handling multiphysical or multidisciplinary problems such as in papermaking, more efficient and intelligent optimization procedures are needed. As stated, the unit-processes of the paper machine have been individually modelled and optimized for more than ten years, but there is an increasing demand to be able to handle larger

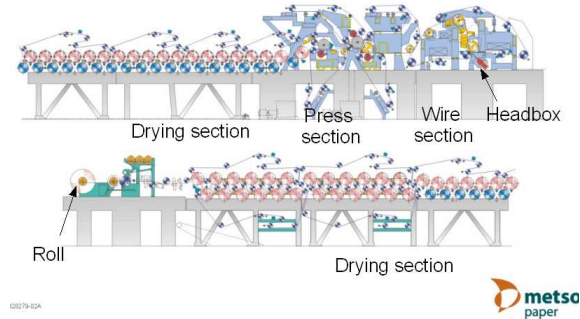


Figure B.1: Layout of a paper machine. Courtesy of Metso Paper, Inc.

ensembles, even the whole papermaking process. This is a real challenge, because the paper machine consists of a number of consecutive sub-ensembles, where the output of one unit-process is an input for the following unit-process. Figure B.1 shows an example of a paper machine construction, where the process starts from the headbox, then continues from right to left terminating as ready paper in a roll.

In the papermaking process, there are always several requirements for the end product that should be simultaneously achieved. These targets are often conflicting; for example, by accelerating the machine speed in order to increase production amount, the probability of web breaks may increase resulting in more downtime, which in turn, decreases the production amount. Better runnability could be achieved by making stronger paper from more expensive raw material, but this affects the costs and profitability. Therefore, numerous criteria need to be taken into account simultaneously.

Although accurate simulation of the whole paper machine is still far in the future, a multiobjective optimisation tool, called a virtual papermaking line, has been developed [87, 92]. It combines dissimilar unit-process models from different disciplines, for example, mathematical formulas ranging from simple algebraic equations to CFD models. It also includes models for moisture and heat transfer, and for paper quality properties. Simplifications of computationally expensive models are used for water removal, for instance. In other words, an accurate multiphase flow model of the dewatering phenomena is replaced with a statistical model based on data produced by the accurate model. These kinds of models are useful especially in optimization when tens, hundreds or even thousands simulation model evaluations are needed.

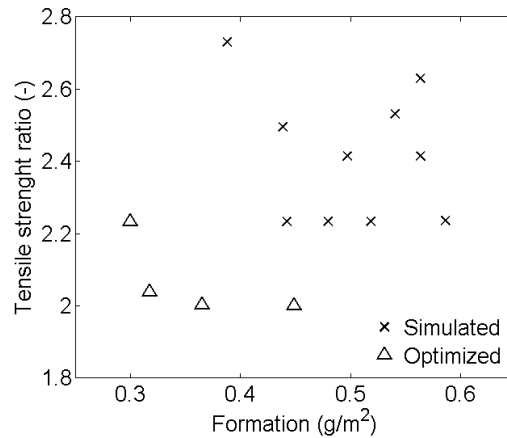


Figure B.2: Simulated and optimized conflicting paper quality properties.

Examples

In the following examples, the introduced interactive multiobjective optimization tools are applied to papermaking problems as a case study. First, there is an example of the conflicting targets of papermaking, and the problem is solved with an interactive multiobjective optimization. After that, the trade-off information is used to support the MCDM process of papermaking. Finally, there is an example in which the VR environment is utilized in visualizing the Pareto optimal fronts obtained in a papermaking study.

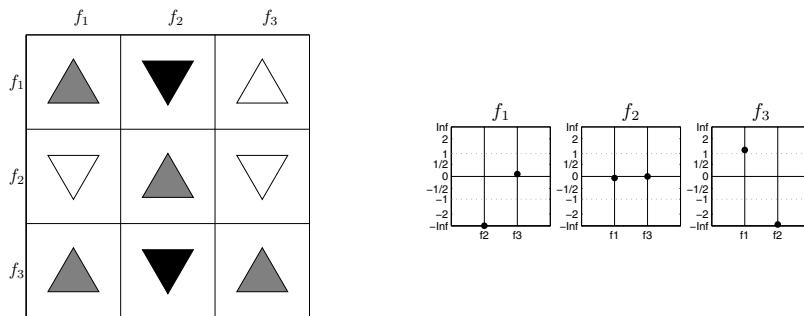
Example 1: Conflicting papermaking targets

The following example illustrates the advantages of multiobjective optimization compared to trial-and-error simulations [44]. It also reveals the conflict between two paper quality properties, formation and tensile strength ratio. Formation is a small scale weight variation and tensile strength ratio is the machine-directional tensile strength divided by the cross-directional strength. Both of them are to be minimized in this example and the calculations are done by using the virtual papermaking line [87, 92]. By doing trial-and-error simulations, a number of solutions are obtained, see Figure B.2. But, by allowing a multiobjective optimization routine to search for the decision variable values, much better solutions can be found as they are located in the left-bottom corner of the graph (Figure B.2). The clear advantage of using multiobjective optimization is that all the solutions it finds are Pareto optimal, i.e. the best possible mathematical compromises.

An example of four papermaking targets is studied next. Table B.1 shows the desired values and six Pareto optimal compromise solutions calculated with the virtual papermaking line. When comparing the values, it can be seen that the

Table B.1: Six Pareto optimal compromise solutions.

Target	Tensile strength (-)	Formation (g/m ²)	Basis weight (g/m ²)	Dry solid (%)
Desired value	3.00	0.30 ... 0.35	54.00	92.00
Compr.1	2.80	0.43	54.03	92.48
Compr.2	3.00	0.40	54.00	92.14
Compr.3	2.34	0.39	54.33	92.30
Compr.4	4.91	0.35	54.35	92.27
Compr.5	3.90	0.38	53.74	92.27
Compr.6	3.38	0.41	53.92	92.12

**Figure B.3:** Trade-off information presented in two ways.

targets chosen are conflicting. For example, tensile strength and basis weight are the best in Compromise 2, but e.g. formation is better in Compromise 4.

Handling even a few conflicting targets at the same time is too complex for human mind [76] and therefore multiobjective optimization routines are needed. Furthermore, the papermaking process can be controlled as a whole and relationships between the targets can be seen.

Example 2: Trade-off information of three conflicting papermaking targets

Here the optimization of three objectives was studied: the content of paper dry solids after pressing, formation and tensile strength ratio. Both of these quality properties as well as dry solids content are created during the papermaking process. Thus, several unit-process models are combined together in a virtual papermaking line as in the previous example.

In this example, the papermaking process is studied by the help of trade-off information [45]. This is performed because even small changes can affect many of the processes and the decision maker wants to predict how the objectives will

Table B.2: Trade-off rates.

	Formation (g/m ²)	Tensile strength (-)	Dry solid (%)
Formation (g/m ²)	0.1	-1.409	0.010
Tensile strength (-)	-0.065	1	-0.002
Dry solid (%)	1.192	-4.265	1

behave in response to these changes. Thus, in addition to the objective function values, also trade-off information is shown to the decision maker during the interactive optimization process. The total trade-off is used because the decision maker considers that it describes better his preferences than partial trade-off: the wish is to see what happens to the other objectives if there is an improvement in one of the objectives by one unit.

In Figure B.3 and in Table B.2 the total trade-off information after obtaining an interesting solution (f_1 : formation 0.487 g/m², f_2 : tensile strength ratio 3.261 and f_3 : dry solids content 50.930 %) is presented. As can be seen in the figure, it would be profitable to try to improve tensile strength. If tensile strength is improved by one unit, the formation and dry solids would be impaired only slightly (-0.0654 and -0.0016, respectively), for example. For comparison, if the wish was to improve the formation by 0.1 unit (scaled, normally one unit), this would impair tensile strength considerably at the same time (-1.4091).

With this information presented to the decision maker, the decision maker is able to steer the solution process in an efficient way and better paper could be obtained by finding advantageous trade-offs. In addition, less Pareto optimal solutions are needed to be computed because the decision maker receives a clear picture of the conflicting targets and their behavior and trade-offs. In brief, the optimization problem is solved more easily and faster by using this kind of decision support aid.

Example 3: Multiple criteria decision making of papermaking using virtual reality

In this example a papermaking optimization problem is studied, and because of the long computational time of the simulation model, the decision maker wants to compute as few solutions as possible. The Pareto optimal solutions computed are visualized as 3D points in the VR, and an approximation of a Pareto optimal front is formed with these few solutions [89].

In this example, there are four papermaking objectives and eight decision variables. The problem is formed as a model-based optimization problem and the virtual papermaking line [87] is used in the computations. The objectives in this example are f_1 which represents paper tensile strength ratio and it is given the desired value 3.4. The objective functions f_2 and f_3 are paper formation and basis weight, which are given the desired values 0.36 g/m² and 50.5 g/m², respectively. The fourth objective function f_4 is evaporated water which was to be maximized.

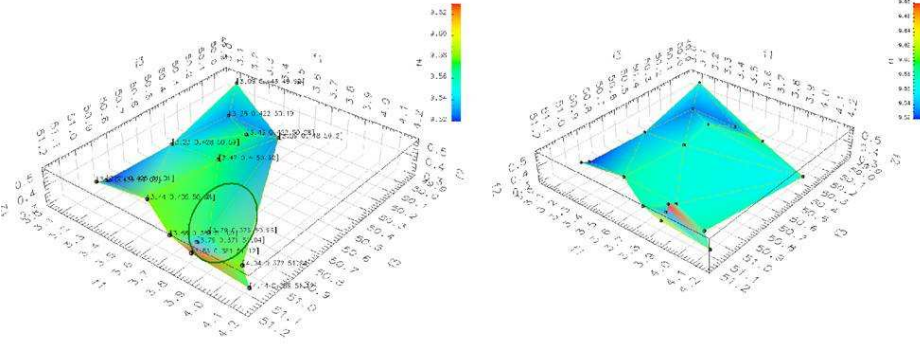


Figure B.4: On the left, solutions after the first step, and on the right, all solutions after the first and the second steps. The objective functions from f_1 to f_3 are presented as a 3D surface and f_4 is presented as a variation in color. Note that 3D fronts visualized in the VR are presented as 2D figures in this thesis.

The optimization process contains two separate steps. *In the first step*, a set of the trade-off solutions are calculated with a genetic algorithm with scalarization by achievement scalarizing function. Then, an approximation of the Pareto optimal front is generated in the VR environment using these solutions. The left plot in Fig. B.4 shows the solutions and the approximated front obtained after the first step. The values of the objective functions f_1 , f_2 and f_3 are presented on the axes and f_4 is presented by different colors in the figure. Here, the proposed VR environment is found to be quite an effective tool to explore the multidimensional Pareto optimal solutions and the approximated front between them. The decision maker observes a conflict between the first two objective functions, i.e. a good tensile strength ratio causes a large formation value which is not desired and vice versa. Thus, there exists a trade-off. Another observation is that a large value of the fourth objective function comes with a large value of the third objective function, thereby producing also a conflict between these two objective functions: the desired value of f_3 cannot be achieved at the same time as a good value of f_4 . However, there are good compromise solutions between the objective functions in the middle and front part of the approximated set. Based on these observations, the region highlighted by an ellipse (shown in the figure, on the left) is chosen and the optimization process is re-directed toward this region in the second step. This preference information is obtained with the help of visualization with the VR tool, where the decision maker could examine the existing solutions in many ways by rotating and zooming the Pareto optimal set.

In the second step, three new solutions are calculated using the reference point method and the gradient-based optimizer. The decision maker's preferences, the circled region in Fig. B.4, is utilized in defining the reference points. Unfortunately, only one of the three new solutions generated is located into the preferred

region and other two are located in that part of the solution space, which had no solutions after the first step. The plot on the right side in Fig. B.4 shows all the solutions, i.e. the solutions produced in the first step complemented by three solutions produced in the second step. Two of the new solutions are interesting from the papermaking point of view: one is located inside the preferred region (circled in Fig. B.4) and another one is located on the right side having values ($\mathbf{f} = (3.78, 0.39, 50.19, 9.59)$), which represents also a good compromise between the objective functions. However, the first-mentioned solution (inside the circled part) has objective function values $\mathbf{f} = (3.79, 0.41, 51.02, 9.68)$ and thus it can be considered to be the most satisfying compromise solution, i.e. to be the final one selected by the decision maker.

The ability to visualize trade-off information among objective functions through the 3D VR system makes it possible to focus on the interesting part of the solution space. This will certainly enhance the decision making ability in computationally demanding real-world optimization problems and reduce the number of irrelevant solutions needed to be calculated. In addition, the better visualization technique allows one to obtain more information about the relationships between the solutions and objective functions than a simple plot of the numerical data. It is concluded that the VR tool will help the decision makers to understand and analyze the Pareto optimal fronts, and thus make it easier to identify the optimal solution.

Conclusion

In papermaking, mathematical modeling and computer simulations can be used to partly replace the expensive trials employed nowadays. Moreover, optimization routines are utilized in order to improve the efficiency of the papermaking processes. In this thesis, multiobjective process-line optimization for papermaking was used to search for the best possible compromise between numerous contradictory objectives as a case study. In addition, the decision making in papermaking can be supported by using trade-off information and utilizing the VR environment to make it easier to visualize the results of the optimization procedure. This kind of simulation-based optimization can be considered as a platform to provide assistance to decision makers in the papermaking industry, and one goal of this thesis was demonstrate how these kinds of techniques utilizing multiobjective optimization can become implemented in the pulp and paper industry in the future.

Kuopio University Publications C. Natural and Environmental Sciences

- C 243. Savolainen, Tuomo.** Modulaarinen, adaptiivinen impedanssitomografialaitteisto.
2008. 188 p. Acad. Diss.
- C 244. Riekkinen, Ossi.** Development and application of ultrasound backscatter methods for the diagnostics of trabecular bone.
2008. 79 p. Acad. Diss.
- C 245. Autio, Elena.** Loose housing of horses in a cold climate: effects on behaviour, nutrition, growth and cold resistance.
2008. 76 p. Acad. Diss.
- C 246. Saramäki, Anna.** Regulation of the p21 (CDKN1A) gene at the chromatin level by 1 α ,25-dihydroxyvitamin D₃.
2008. 100 p. Acad. Diss.
- C 247. Tiiva, Päivi.** Isoprene emission from northern ecosystems under climate change.
2008. 98 p. Acad. Diss.
- C 248. Himanen, Sari J.** Climate change and genetically modified insecticidal plants: plant-herbivore interactions and secondary chemistry of Bt CryI Ac-Toxin producing oilseed rape (*Brassica napus* L.) under elevated CO₂ or O₃.
2008. 42 p. Acad. Diss.
- C 249. Silvennoinen, Hanna.** Nitrogen and greenhouse gas dynamics in rivers and estuaries of the Bothnian Bay (Northern Baltic Sea).
2008. 98 p. Acad. Diss.
- C 250. Degenhardt, Tatjana.** An integrated view of PPAR-dependent transcription.
2009. 120 p. Acad. Diss.
- C 251. Häikiö, Elina.** Clonal differences of aspen (*Populus* spp.) in responses to elevated ozone and soil nitrogen.
2009. 49 p. Acad. Diss.
- C 252. Hassinen, Viivi H.** Search for metal-responsive genes in plants: putative roles in metal tolerance of accumulation.
2009. 84 p. Acad. Diss.
- C 253. Markkanen, Ari.** Effects of electromagnetic fields on cellular responses to agents causing oxidative stress and DNA damage.
2009. 59 p. Acad. Diss.
- C 254. Jokitulppo, Jaana.** Non occupational noise: sources, exposure and effects on hearing.
2009. 111 p. Acad. Diss.
- C 255. Rokhina, Ekaterina V.** Heterogeneous ruthenium-based catalytic systems in wet peroxide oxidation of organic compounds.
2009. 124 p. Acad. Diss.
- C 256. Amstislavsky, Sergei.** Reproductive biology and embryo technology in Mustelidae.
2009. 149 p. Acad. Diss.
- C 257. Sorvari, Joonas.** Modelling methods for viscoelastic constitutive modelling of paper.
2009. 25 p. Acad. Diss.
- C 258. Kempainen, Niina.** Refinement and reduction outcomes of cage furniture and restricted feeding in laboratory rats.
2009. 140 p. Acad. Diss.